Karlsruher Institut für Technologie

Interaction of *Arthrobotrys flagrans* with *Caenorhabditis elegans* involves G-protein dependent signaling

Zur Erlangung des akademischen Grades eines

DOKTORS DER NATURWISSENSCHAFTEN

(Dr. rer. nat.)

von der KIT-Fakultät für Chemie und Biowissenschaften

des Karlsruher Institut für Technologie (KIT)

genehmigte

DISSERTATION

von

MSc. Xiaodi Hu

1. Referent: Prof. Dr. Reinhard Fischer
2. Referent: Prof. Dr. Jörg Kämper
Tag der mündlichen Prüfung: 18.07.22

Statutory declaration

I hereby declare that I did all the work independently. All of samples, methods and sentences that were used or cited from sources were identified by specifying the respective source.
The regulation at the Karlsruhe Institute of Technology (KIT) to ensure appropriate scientific practice was read intensively. Furthermore, the submission and archiving of the primary data complied with the requirements at KIT to ensure good scientific practice.

_____ _____

Ort, den Xiaodi Hu

Publications

Yu, X.[#], **Hu, X.[#]**, Mirza, M., Kirschhöfer, F., Brenner-Weiß, G., Schäfer, J., Bunzel, M. & Fischer, R. (2021). Fatal attraction of *Caenorhabditis elegans* to predatory fungi through 6-methyl salicylic acid. *Nat Commun* **12**, 5462.
[#] These authors contributed equally.

Hu, X., Wang, M., Yu, X. & Fischer, R. (2022). The nematode-trapping fungus *Arthrobotrys flagrans* acquired G-protein coupled receptor proteins from its prey *Caenorhabditis elegans* for sensing *C. elegans* pheromones. *In preparation.*

Contents

Abstract

Nematode-trapping fungi (NTF) are a large group of predatory microorganisms some of which form three-dimensional trapping networks to capture nematodes. When the living environment is deprived of nutrients and in the presence of nematodes, they switch from saprotrophism to a predatory lifestyle. The production of trap cells and the secretion of low molecular compounds are indicators of lifestyle change. I studied the NTF *Arthrobotry flagrans* (formerly *Duddingtonia flagrans*) and used *Caenorhabditis elegans* as prey. The predacious fungi emit attractive olfactory substances to lure their prey and the polyketide arthrosporols to inhibit trap induction. On the other hand, *Caenorhabditis elegans* secretes ascarosides as pheromones which control many developmental processes in *C. elegans*. They are also recognized by *A. flagrans* and induce trap formation by downregulation of the arthrosporol biosynthesis pathway. The question arises of how the predator senses ascarosides derived from nematodes and how the external signals are transmitted to downregulate the fungal arthrosporol biosynthesis.

I assumed that G-protein dependent signaling fulfills this task. Heterotrimeric G-proteins are conserved among all eukaryotes and are critical elements for sensing and transmitting extracellular signals into the cells to induce proper biochemical and physiological responses. G-protein signaling pathways comprise G-protein-coupled receptors (GPCRs) and α, β and γ subunits of a G-protein, and a variety of regulators. When a GPCR binds external cues, it activates the G-α subunit to exchange GDP for GTP which accelerates the dissociation of Gα-GTP from the βγ dimer, inducing downstream cellular responses.

I analyzed the main components of G-protein cascades, G-alpha subunits (Gas). Three encoding genes of Gas proteins were identified in *A. flagrans*, namely *gasA*, *gasB* and *gasC*, and they were deleted individually by homologous recombination. In contrast to wild type the *gasA*-deletion strain did not show the down-regulation of the *artA* cluster in the presence of *C. elegans* or enriched ascarosides, indicating that GasA plays a role in sensing nematode-derived ascarosides. Hence, the strain did not produce traps. A *gasB*-deletion strain produced fewer conidia and aerial hyphae and significantly fewer traps, but more than the *gasA*-mutant. In substrate hyphae, the transcript abundances of the *artA* gene cluster were higher in the *gasB*-mutant strain compared to wild type. No defect was observed in a *gasC*-deletion strain. In short, GasA acts as the switch of trap induction while GasB modulates the trap number. The phenotypes observed in the *gasB*-deletion strain were rescued by adding 8'-Bromo-cAMP (an analog of cAMP), indicating that GasB uses cAMP as second messenger. Additionally, the transcriptional factor Ste12 acts upstream of the *artA* cluster by regulating its expression level.

I also studied the role of G-protein coupled receptor proteins (GPCRs). GPCRs of conserved groups were identified in *A. flagrans*, and one of the receptors of the carbon class, GprC, was essential for the production of traps. Interestingly, normal

trap morphogenesis in a *gprC*-deletion strain was restored by introducing a chimeric protein that is composed of the N-terminal half of the *C. elegans* SRBC-64, SRBC-66 or Daf-38 receptors and the *A. flagrans*-derived C-terminal half of GprC. This could be first evidence for horizontal gene transfer (HGT).

In addition to the G-protein signaling pathway analysis in *A. flagrans*, a putative effector protein (PefD) was characterized in this fungus. The gene *pefD* harbors a signal peptide and a propeptide. The signal peptide was demonstrated to be functional, suggesting that PefD is secreted. The presence of a propeptide suggests further processing to obtain the mature protein. The *pefD* gene was induced in traps as demonstrated by both, quantitative RT-PCR and a reporter assay. Localization analysis tagged with fluorescent proteins revealed that PefD accumulates at the penetration site during nematode capturing. A *pefD* over-expressing *A. flagrans* strain displayed highly nematicidal activity, indicating its involvement in the attack against nematodes.

Taken together, this work contributes to a better understanding of interkingdom communication between a fungus and a nematode and sheds light on the molecular components involved in signaling and in the killing process.

Zusammenfassung

Nematodenfressende Pilze (NFP) sind eine große Gruppe von räuberischen Mikroorganismen, von denen einige dreidimensionale Fangnetze bilden, um Nematoden zu fangen. Bei Nährstoffmangel in ihrem Lebensraum und in Gegenwart von Nematoden gehen sie vom Saprotrophismus zu einer räuberischen Lebensweise über. Die Produktion von Fangzellen und die Sekretion von niedermolekularen Verbindungen sind Indikatoren für die Änderung der Lebensweise. Ich habe den NTF *Arthrobotry flagrans* (früher *Duddingtonia flagrans*) untersucht und *Caenorhabditis elegans* als Beute verwendet. Die räuberischen Pilze geben attraktive Geruchsstoffe ab, um ihre Beute anzulocken, und das Polyketid Arthrosporole, um die Falleninduktion zu hemmen. Andererseits sondert *Caenorhabditis elegans* Ascaroside als Pheromone ab, die viele Entwicklungsprozesse in *C. elegans* steuern. Sie werden auch von *A. flagrans* erkannt und induzieren die Fallenbildung durch Herunterregulieren des Arthrosporol-Biosynthesewegs. Es stellt sich die Frage, wie der Räuber die von den Nematoden stammenden Askaroside wahrnimmt und wie die externen Signale übertragen werden, um die Arthrosporol-Biosynthese des Pilzes herunterzuregulieren.

Ich nahm an, dass diese Aufgabe von G-Protein-abhängigen Signalen erfüllt wird. Heterotrimere G-Proteine sind in allen Eukaryonten konserviert und sind entscheidende Elemente für die Wahrnehmung und Übertragung extrazellulärer Signale in die Zellen, um die richtigen biochemischen und physiologischen Reaktionen auszulösen. G-Protein-Signalwege umfassen G-Protein-gekoppelte Rezeptoren GPCRs (G-protein-coupled receptors) und α-, β- und γ-Untereinheiten eines G-Proteins sowie eine Vielzahl von Regulatoren. Wenn ein GPCR externe Signale bindet, aktiviert er die G-α-Untereinheit, um GDP gegen GTP auszutauschen, was die Dissoziation von Gα-GTP aus dem βγ-Dimer beschleunigt und nachgeschaltete zelluläre Reaktionen auslöst.

Ich analysierte die Hauptkomponenten der G-Protein-Kaskaden, die G-alpha-Untereinheiten (G-alpha subunits, Gas). In *A. flagrans* wurden drei kodierende Gene für Gas-Proteine identifiziert, nämlich *gasA*, *gasB* und *gasC*, und sie wurden einzeln durch homologe Rekombination deletiert. Im Gegensatz zum Wildtyp zeigte der GasA-Deletionsstamm in Anwesenheit von *C. elegans* oder angereicherten Ascarosiden keine Herabregulierung des *artA*-Clusters, was darauf hindeutet, dass GasA eine Rolle bei der Erkennung von Ascarosiden spielt, die von Nematoden stammen. Daher produzierte der Stamm keine Fallen. Ein Stamm mit GasB-Deletion produzierte weniger Konidien und Lufthyphen und deutlich weniger Fallen, jedoch mehr als die GasA-Mutante. In den Substrathyphen waren die Transkriptionshäufigkeiten des *artA*-Genclusters in dem *gasB*-mutanten Stamm höher als im Wildtyp. In einem *gasC*-Deletionsstamm wurde kein Defekt beobachtet. Kurz gesagt, GasA fungiert als Schalter für die Falleninduktion, während GasB die Fallenanzahl moduliert. Die im GasB-Deletionsstamm beobachteten Phänotypen wurden durch Zugabe von 8'-Bromo-cAMP (einem Analogon von cAMP) gerettet, was

darauf hindeutet, dass GasB cAMP als zweiten Botenstoff verwendet. Außerdem wirkt der Transkriptionsfaktor Ste12 stromaufwärts des artA-Clusters, indem er dessen Expressionsniveau reguliert.

Ich habe auch die Rolle von G-Protein-gekoppelten Rezeptorproteinen (GPCRs) untersucht. In *A. flagrans* wurden GPCRs aus konservierten Gruppen identifiziert, und einer der Rezeptoren der Kohlenstoffklasse, GprC, war für die Herstellung von Fallen wesentlich. Interessanterweise konnte die normale Morphogenese der Fallen in einem *gprC*-Deletionsstamm wiederhergestellt werden, indem ein chimäres Protein eingeführt wurde, das aus der N-terminalen Hälfte der *C. elegans*-Rezeptoren SRBC-64, SRBC-66 oder Daf-38 und der von *A. flagrans* stammenden C-terminalen Hälfte von GprC besteht. Dies könnte der erste Beweis für einen horizontalen Gentransfer (horizontal gene transfer, HGT) sein.

Zusätzlich zur Analyse der G-Protein-Signalwege in *A. flagrans* wurde ein mutmaßliches Effektorprotein (putative effector protein, PefD) in diesem Pilz charakterisiert. Das Gen *pefD* beherbergt ein Signalpeptid und ein Propeptid. Das Signalpeptid erwies sich als funktionell, was darauf hindeutet, dass PefD sezerniert wird. Das Vorhandensein eines Propeptids deutet auf eine weitere Verarbeitung hin, um das reife Protein zu erhalten. Das *pefD*-Gen wurde in Fallen induziert, wie sowohl durch quantitative RT-PCR als auch durch einen Reporter-Assay nachgewiesen wurde. Eine mit fluoreszierenden Proteinen markierte Lokalisierungsanalyse ergab, dass sich PefD während des Nematodenfangs an der Penetrationsstelle anreichert. Ein *A. flagrans*-Stamm, der PefD überexprimiert, zeigte eine hohe nematizide Aktivität, was darauf hindeutet, dass PefD an der Bekämpfung von Nematoden beteiligt ist.
Insgesamt trägt diese Arbeit zu einem besseren Verständnis der Kommunikation zwischen einem Pilz und einem Nematoden bei und wirft ein Licht auf die molekularen Komponenten, die an der Signalübertragung und am Abtötungsprozess beteiligt sind.

1 Introduction

1.1 Nematode trapping fungi (NTF)

Fungi are eukaryotes which have evolved about one billion years ago. In nature, they normally play a role as decomposer, and their fruiting bodies are common food sources of animals. However, a particular type of fungi behaves as predator and actively feeds on animals, namely nematophagous fungi. Based on the attacking mechanisms, they are classified into four groups including nematode-trapping fungi (NTF), endoparasitic fungi, egg parasitic fungi and toxin producing fungi (Hyde *et al*., 2014). They handle a variety of weapons including trap-networks, zoospores, appressoria or secreted toxins (Li *et al*., 2015). For example, the genus *Arthrobotrys* is generally known as a kind of NTF that forms traps and predates on nematodes; the genus *Drechmeria* employs adhesive conidia for endoparasitism; the *Pochonia* genus produces appressoria for the egg-parasitic lifestyle; and toxic substances are produced by the edible mushroom *Pleurotus* against nematodes (Jansson, 1994; Escudero *et al*., 2016; Wernet *et al*., 2022; Barron & Thorn, 1987).

Among the four groups mentioned above, NTF have been a popular subject of research which can be traced back to the 19th century. As one genus among NTF, *Arthrobotrys* was discovered first in 1839 and later the species *A. oligospora* was founded in 1852 (Corda, 1839; Fresenius, 1852). Scientists recognized the distinguished cell structure (trap) but did not discover its ability of predate nematodes. Until the year 1888, Zopf described the predatory process in detail (Zopf, 1888). In the last century a new nematode trapping fungus *Trichothecium flagrans* was described. It produces similar traps as *A. oligospora* while conidiophores were more like *Trichothecium* (Duddington, 1949). After subsequent observations, it was found that *T. flagrans* does not harbor catenulate conidia clusters of *Trichothecium* genus and conidia are more like the species described by Duddington. This strain was redefined as *Duddingtonia flagrans* and analyzed of the trapping style (Duddington, 1969). After dozens of years, it is defined again as the species *Arthrobotrys flagrans* (Dudd.) Mekht., Dokl. Akad. Nauk Azerb. SSR 20 (6): 70 (1964). Now it belongs to *Ascomycota*, *Orbiliomycetes*, *Orbiliales*, *Orbiliaceae* and *Arthrobotrys Corda* (GBIF Backbone Taxonomy). In this case, *T. flagrans* and *D. flagrans* are the synonyms of *Arthrobotrys flagrans* which is used now.

The genus *Arthrobotrys* produces various trap devices that were categorized into six classes: constricting rings, adhesive nets, adhesive columns, stalked adhesive knobs, unstalked adhesive knobs and non-constricting rings (Liu *et al*., 2012). For instance, *Arthrobotrys* is characterized by adhesive trap networks, *Dactylellina (Da)* has non-constricting ring and/or adhesive knobs, and *Drechslerella (Dr)* is known by the trapping devices of constricting ring (Wernet *et al*., 2021b; Yu *et al*., 2012; Fan *et al.*,

2021). The process of evolution of these devices was deduced based on genome sequencing of *A. oligospora* (traps), *Monacrosporium haptotylum* and *Dactylellina entomopaga* (adhesive knobs), *Drechslerella brochopaga* and *Dactylellina cionopagum* (adhesive columns) (Ji *et al*., 2019; Yang *et al*., 2011; Meerupati *et al*., 2013; Ji *et al*., 2020). From the perspective of adhesion-related genes, the order of constricting ring, adhesive nets, adhesive column and adhesive knob means less and less complicated devices whereas more and more adhesiveness of the trap surface **(Fig. 1)**. These classifications and descriptions provide broad insights for understanding the differences of NTF species.

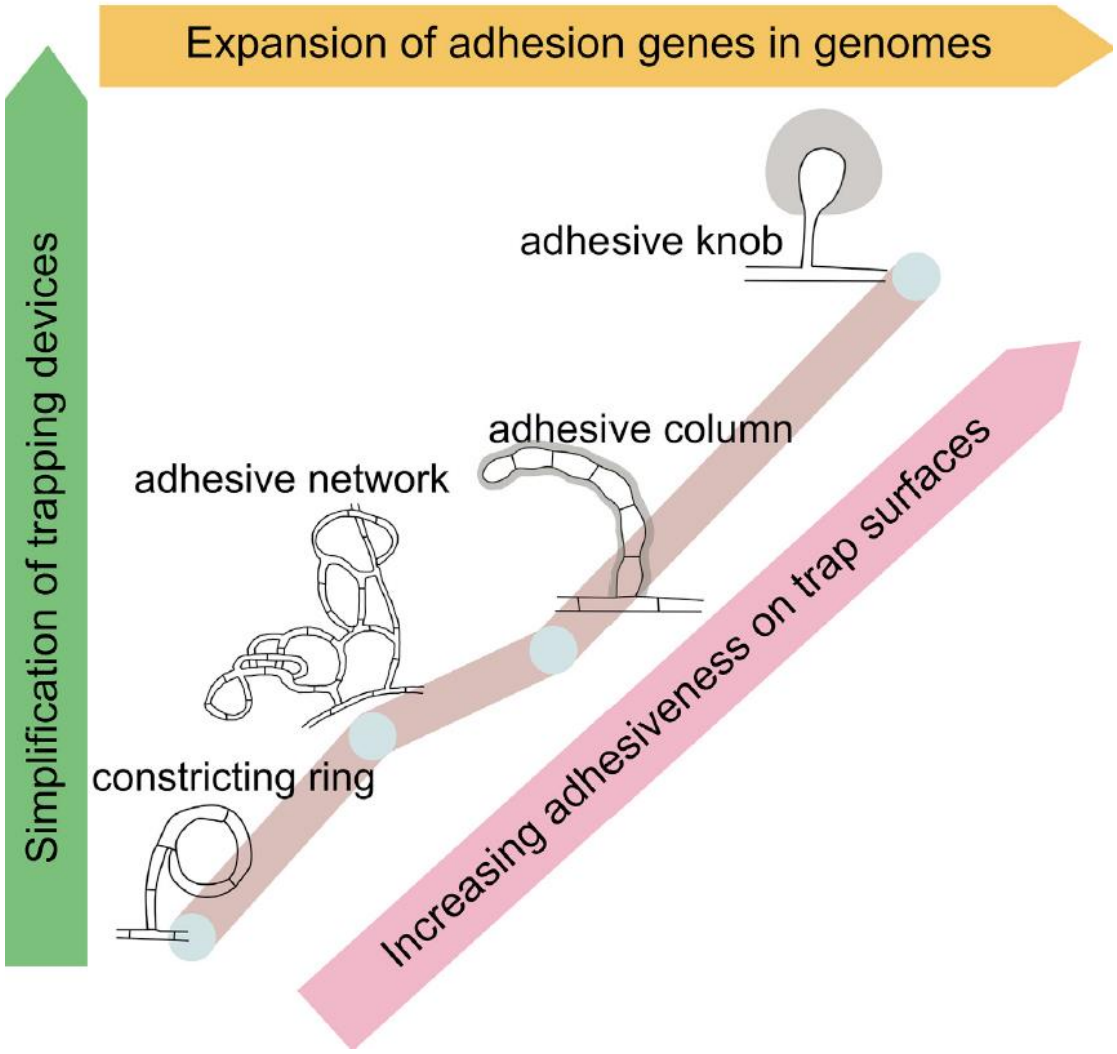

Fig. 1: The evolution of diverse trapping devices. Comparative genomic analysis toward the NTF species of four corresponding trapping structures was performed. An evolutionary development of trapping structure simplification in morphology is displayed by phylogenetic reconstruction of these NTF (Ji *et al*., 2020).

Nematodes are the most abundant animals on earth and found in diverse habitats including soil, water, meadow and living animals including livestock. Its prevalence and propagation lead to tremendous losses to agriculture and animal husbandry. Since the human population is expanding, there is an increasing demand of the

agriculture productivity especially in developing countries and areas. Crops have been always facing challenges from a variety of nematodes, and more than 4,100 species plant-parasitic nematodes have been discovered. Plant-parasitic nematodes cause 5-10 % loss of crop production in developed countries, much more losses in the developing ones (Mitiku, 2018). In addition, the livestock economy is indispensible and irreplaceable for human society. Both national economy and the livelihood of rural communities are in crucial need of the healthy development of animal husbandry. This industry provides meat, milk for the daily life of people, feces and other input for the agriculture, and fur and feather for the other industries which can tremendously improve the living standard of people. Goats and sheep play a crucial role as the major source of livelihood especially in the rural regions of the developing areas (Dugassa *et al*., 2018). However, gastrointestinal nematodes lead to tremendous economic losses by causing reduced production of sheep and goats in both developed and developing countries including but not limited to India, Africa, Sweden, New Zealand and Australia (Ilangopathy *et al*., 2019; Dugassa *et al*., 2018; Waller *et al*., 2006; SKIPP *et al*., 2002; Roeber *et al*., 2013). In order to prevent it from happening, anthelmintics have been world-widely used. However these chemicals subsequently showed unsustainable and led to other problems to human society such as water pollution and parasite resistance. To deal with the problem, biocontrol strategies are another approach to eliminate nematodes without causing drops in production and anthelmintic contaminations (Burke, 2019). Especially the NTF species *A. flagrans* has been widely applied in animal husbandry since it can produce plenty of resistant chlamydospores. This kind of spore has thick walls to enable passage alive through the gas-intestinal system of animals and excreted to the pasture where the fungi grow as predators to trap and consume nematodes on the grassland (SKIPP *et al*., 2002; Burke *et al*., 2005).

1.2 Molecular analyses of NTF

Along with the development of molecular biology, the study in NTF was not only limited to characterization of classification, general morphology and application. There are many reports toward the sequencing of genome, transcriptome, proteome and mitochondrial genome in several species covering *A. oligospora*, *A. flagrans*, *A. musiformis* and *Da. Haptotyla* (Zhang *et al*., 2020; Liang *et al*., 2019; Yang *et al*., 2011; Jiang *et al*., 2018; Yang *et al*., 2022; Liu *et al*., 2020; Zhang *et al*., 2019; Zhou *et al*., 2018; Youssar *et al*., 2019). Scientists explored the genes related to the production of trapping devices, compared the differences between NTF on the molecular level, laying a basis for the deep exploration of trap mechanisms and better application as a biocontrol agent against nematodes.

Apart from the sequencing research, the predatory process has been characterized mostly in the adhesive net-producing genus *Arthrobotrys*. The trapping mechanism is divided into three steps: recognition, predation and digestion. When the nematodes are close by and the environmental nitrogen is limited, the mycelia are induced by

the presence of prey and then set up the generation of trap networks. A trap is formed by an adhesive ring which is closed by fusing with the parental hyphae. The nematodes swim by and drill into the trap cell where they get stuck, and the nematode struggles desperately to escape the ring. At this time, a hypha developing from the trap grows perpendicular towards the cuticle of the nematode. With the help of a variety of hydrolases and effector proteins, the penetration peg forces on the cuticle and subsequently pierces into it. A penetration bulb is formed between the cuticle and the intestinal tract of the nematode. The prey does not struggle at this point. Hyphae and branches originated from the bulb grow into the nematode body and mycelia consume the prey. Once the body is filled with mycelia, hyphae will grow out of the nematode body.

In recent years multiple reports about molecular mechanisms of trapping were published. Most of the research is about trap formation since it is an important indicator of the fungal shift from saprotrophic to the predatory lifestyle. The trap is a circle generated from a bended hypha, and the formation of the trap requires reorganization of the cytoskeleton and the polar growth machinery (Wernet *et al*., 2022). The lack of *crn1p* (the gene encoding a conserved actin-associated protein) results in trap structural defects and nematode-attacking failure (Zhang *et al*., 2017). The sealing of the septal pores also appears to be important, since the absence of Hex1, the main component of Woronin bodies, prevents trap formation (Liang *et al*., 2016). Trap morphogenesis occurred also in a deletion strain of the *velB* gene, a gene encoding a velvet family protein (Zhang *et al*., 2019). The velvet protein complex is involved in the regulation of secondary metabolite formation (Martín JF, 2017) and hence could be involved in arthrosporol or other secondary metabolite formations in *A. flagrans* (Zhang *et al*., 2019). Besides the arthrosporol signaling, a cell-to-cell communication is required for ring closure. If a secondary metabolite serves as a communication molecule remains to be determined **(Fig. 2;** Hammadeh *et al*., 2022**)**. Other components of the cell dialogue system is a MAP kinase and a signalinG-protein called *soft* (Youssar *et al*., 2019; Wernet *et al*., 2021). At the physiological stage, cells in the developing tips in trap formation conduct coordinated, rapid switching, which is a hallmark of the cell dialogue communication process.

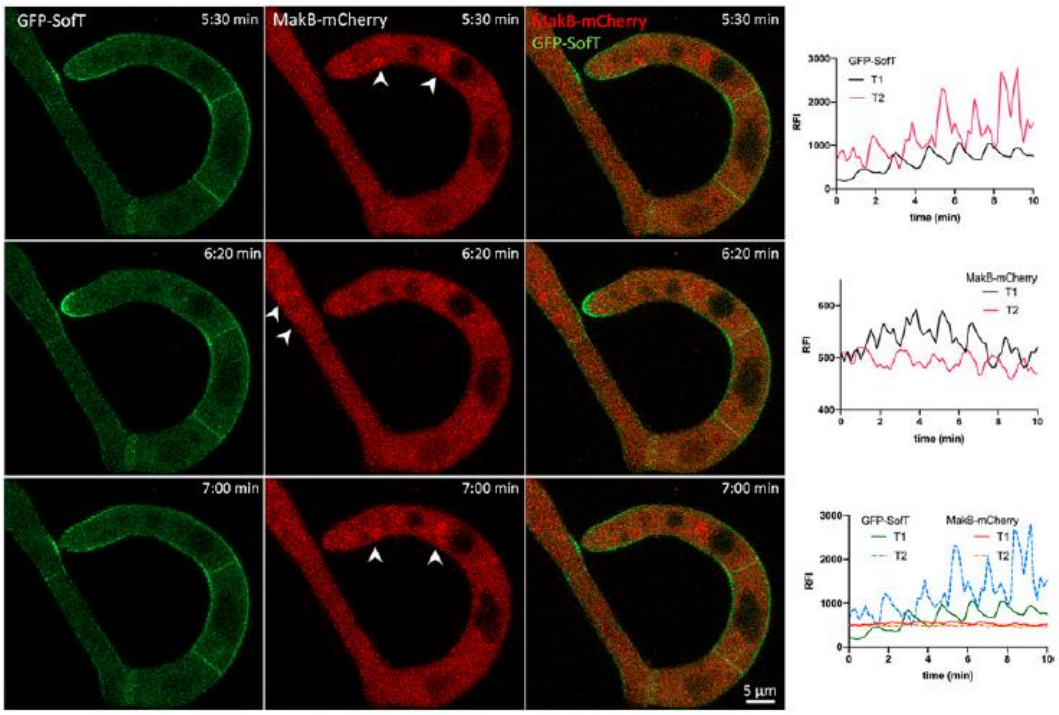

Fig. 2: In *A. flagrans*, trap generation is mediated by a conserved cell communication mechanism. Left: Time course of the oscillation of GFP-SofT at the tip membrane and MakB-mCherry in nuclei during trap production. Right: y axis indicates RFI quantification in the interacting zone and x axis indicates minutes. White arrow heads indicate the localization of the fusion protein MakB-mCherry in nuclei of the interacting cells (Hammadeh *et al*., 2022).

Multiple central signaling pathways and kinases take part in the trap morphology such as the low-affinity calcium uptake system (LACS), an inducer of meiosis 2 Ime2, Ca2+/calmodulin-dependent protein kinases (CaMKs), and the Mitogen-activated protein (MAP) kinase Slt2 and the deletion strains of their encoding genes showed defects in trap generation (Zhang *et al*., 2019; Zhen *et al*., 2019; Xie *et al*., 2020; Zhen *et al*., 2018). The assimilation pathway of nitrogen was also demonstrated to be involved in trap formation because lack of nitrogen is a precondition for trap-formation (Liang *et al*., 2016). Moreover, trap formation is correlated to a variety of genes including *stuA* (encodes a transcriptional factor in the APSES family), *palH* (a putative ambient pH receptor harboring a seven transmembrane domain in the PacC/Rim101 signaling) and the cysteine protease encoding gene *atg4* related to autophagy (Xie *et al*., 2019; Li *et al*., 2019; Zhou *et al*., 2020). The generation of ROS (Reactive oxygen species) is involved in the trap producing process (Li *et al*., 2017). Except the components described above, there is an interesting report that microRNA-like RNAs (milRNAs) are involved in the switch of lifestyles since the deficiency in transition to the predatory lifestyle was found in the deletion strain of the argonaute gene *qde-2* (Ji *et al*., 2020).

In addition, there are several reports about the participation of other microorganisms in the interaction of nematodes and NTF. The involvement of a third

party is reasonable since the soil environment supports a wide variety of organisms, all of which are likely to interact with each other. Bacteria are one of the third parts. Bacteria possess multiple roles including as the food source of nematodes or as parasites of fungi, plants and animals. A defense mechanism was described that bacteria mobilize NTF to catch nematodes. Bacteria-produced urea leads to shift the lifestyle from saprophyism to the predatory lifestyle *A. oligospora*. The formation of urea-induced traps in *A. oligospora* is abolished when genes involved in urea transport and metabolism are disrupted (Wang *et al*., 2014). Additionally, small-molecular compounds secreted by bacterial species such as ammonia are responsible for the production of traps and similar cases are not limited to *A. oligospora* but also in other NTF like *Dr. brochopaga* (Su *et al*., 2016). Correlation of bacteria with two organisms is also reflected in the involvement of bacterial biofilm and specific genera *Stenotrophomonas* and *Rhizobium* (Li *et al*., 2016). These studies broad our horizons and lay the molecular foundation for the application of NTF.

1.3 Interaction between nematodes and NTF involves secondary metabolites

A. oligospora has recently been described to secrete a group of arthrosporol metabolites that are synthesized by a polyketide synthase (PKS; AOL_s00215g283) and some tailoring enzymes. The arthrosporols together with other compounds such as oligosporons and anthrobotrisins are isolated from *A. oligospora* and belong to a distinct class of sesquiterpenyl epoxy-cyclohexenoids (SEC) derived from PK-TP hybrid pathways (Chen *et al*., 2020). The substances control trap morphogenesis since a deletion strain of the PKS encoding gene *pksA* displays increased trap numbers (Xu *et al*., 2015). Subsequent analyses revealed the biosynthesis pathway and the role of the enzymes encoded in the gene cluster **(Fig. 3**, He *et al*., 2021**)**. In a metabolomics approach more secondary metabolites were discovered that act as morphological regulators (Xu *et al*., 2016).

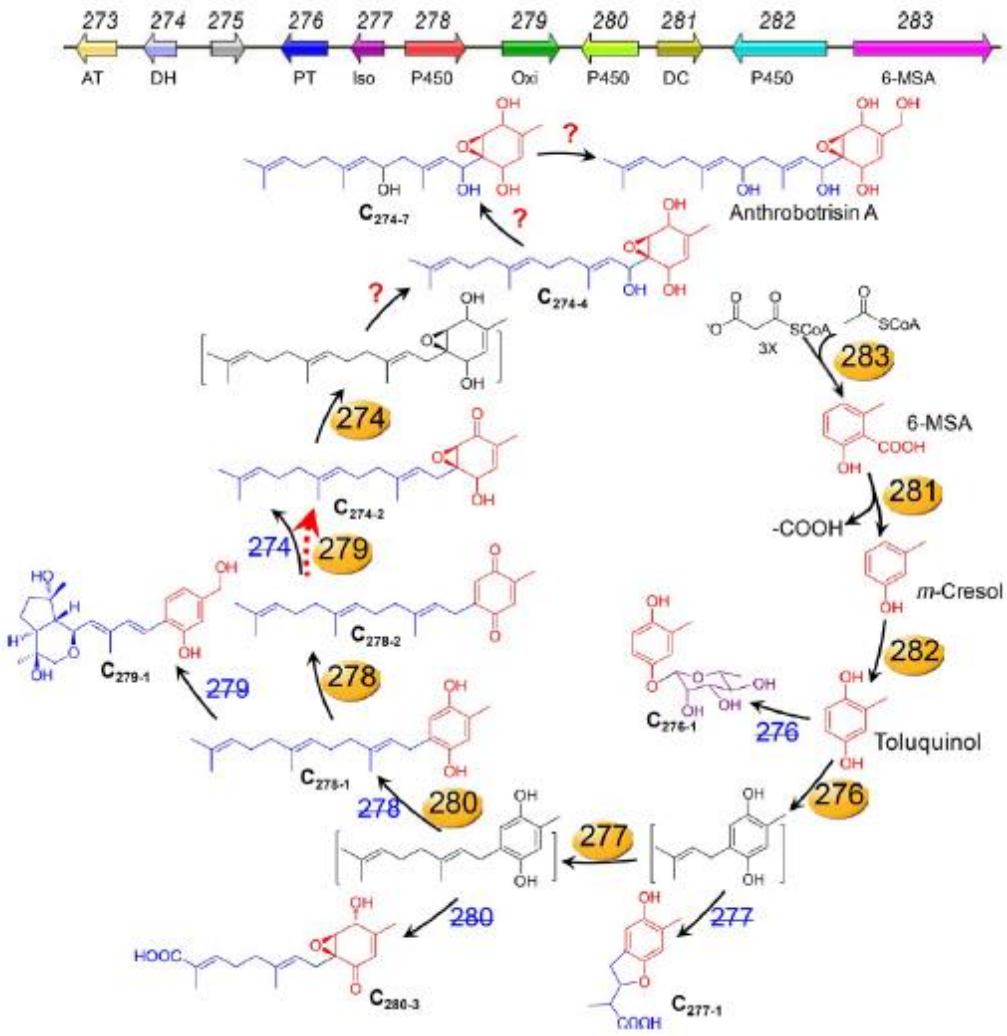

Fig. 3: A complete biosynthesis pathway for anthrobotrinsin A in the nematode-trapping fungus *A. oligospora* was proposed according to intermediates and derivatives (labled in red and blue) from deletion strains of genes in the cluster *AOL_s00215g*. Deleted genes are indicated by crossed-out numbers. The chemical compounds labled in black color indicate putative precursors and intermediates (He *et al*., 2021).

The recognition of the prey by the fungi is always the first step of lifestyle shifting. The nematode-derived pheromones, the ascarosides, take an important role for sensing since traps are not formed constitutively but only in the presence of nematodes and deprivation of nutrient. Ascarosides are glycosides of the dideoxysugar ascarylose harboring a fatty acid-derived lipophilic side chain that can be decorated with additional building elements from various metabolic pathways and they are evolutionarily conserved groups of small compounds (Manohar *et al*., 2020). These glycolipids are isolated from nematodes, including free-living as well as parasitic species to insects, vertebrates and plants. They appear to play a fundamental role in nematode chemical communication, controlling various aspects of the growth and behavior including larval development, dauer stage formation, mating and foraging (Golden *et al*., 1982; Jeong *et al*., 2005; Srinivasan *et al*., 2008; Butcher *et al*., 2007; Schroeder *et al*., 2015). Earlier reports demonstrated that the

broth where nematodes were suspended can induce trap formation and respective compounds were extracted from the nematode culture and named as nemin (Lawton, 1957; Pramer & Stoll, 1959). Many years later, ascarosides were discovered as highly conserved molecules among various nematode species (Srinivasan *et al*., 2008; Butcher *et al*., 2007). Subsequently it was found that ascarosides are acutally the molecules in nematode culture supernatants which affect trap induction under nutrient-deprived conditions (Hsueh *et al*., 2013). Nematodes secrete more than 100 types of ascarosides. The examined ascarosides exhibited a potentially trap-inducing role and substances with 7- and 9-carbon side chains possessed the most potent effect **(Fig. 4A, B)**. A concentration of ascarosides as low as 0.5 nM is sufficient to trigger trap formation. This ascaroside concentration falls within the range of physiological amounts discovered around nematode populations. Similar to the prior report in 1994 (Scholler & Rubner), *A. oligospora* must be deprived for nutrients, particularly nitrogen in order to detect and respond to ascarosides. In rich medium or Low nutrient medium supplemented with nitrogen, trap induction is entirely repressed and with additional carbon sources, it was obviously reduced (Hsueh *et al*., 2013).

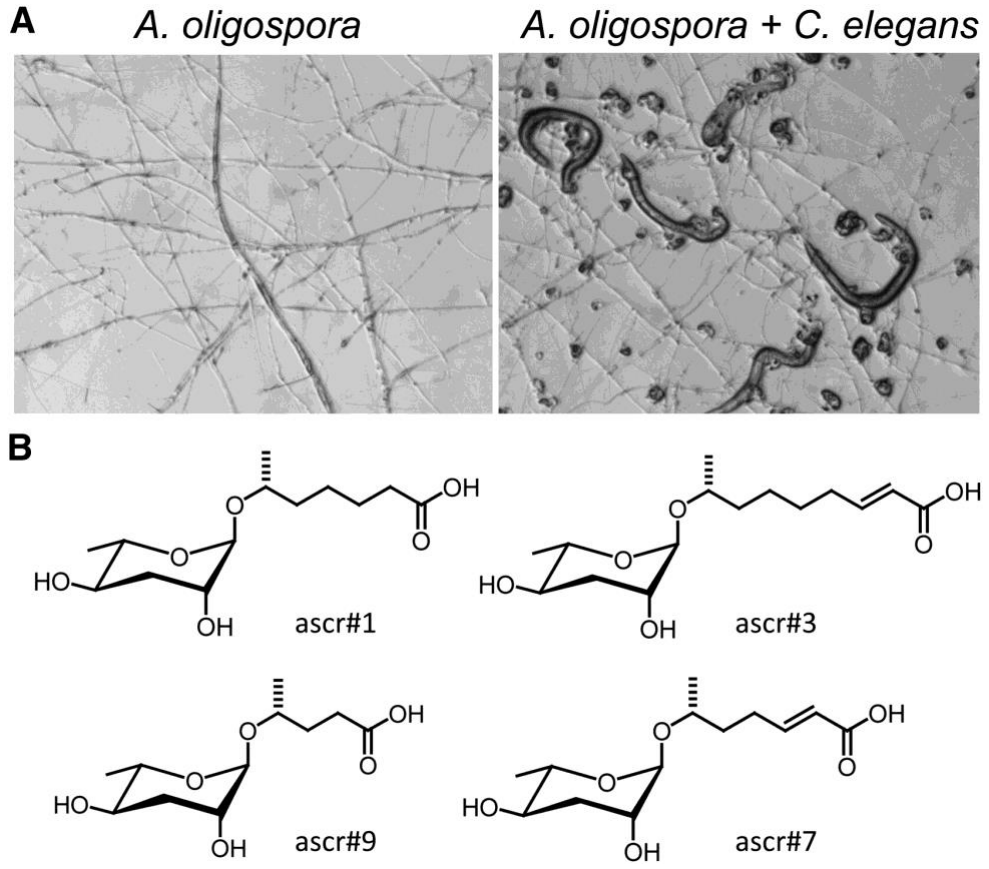

Fig. 4: Nematode-catching fungi form trapping structures in response to the presence of nematodes. (A) *A. oligospora* cultivated with or without *C. elegans* on LNM. **(B)** Structures of several types of ascarosides (Hsueh *et al*., 2013).

After knowing that nematode-derived ascarosides induce the predatory lifestyle under low-nutrient conditions, studies were reported about the involvement of

secondary metabolites secreted by NTF. By detecting and analyzing of volatile compounds derived from *A. oligospora* using gas chromatography and mass spectrometry, it was found that fungi secrete bioactive compounds (Hsueh *et al*., 2017). Several types of fragrances were found from *A. oligospora*, including the sulfur related chemicals dimethyl disulfide (DMDS), 2, 4-dithiapentane (DTP) and S-methyl thioacetate (SMT). These compounds are detectable in aromas of mature or rotting fruits so that they are perceived as food cues by the prey. Insects and nematodes are frequently associated with decaying fruits. Similarly, predatory plants, such as Venus flytraps, sundews, and pitcher plants, create volatiles that resemble fruits and flowers in order to attract the prey (Di Giusto *et al*., 2010; Juergens *et al*., 2009). The dead horse arum and the iconic corpse flower similarly emit rotten odors to induce prey like insects (Shirasu *et al*., 2010; Stensmyr *et al*., 2002). Apart from the food cues, methyl 3-methyl-2-butenoate (MMB) is the most appealing molecule among volatiles of *A. oligospora*, and it induces a substantial sex- and growing phase-specific attraction in several *Caenorhabditis* species. MMB extremely appeals to female but unpleasant to male nematodes and incredibly fascinates adults but not dauers or larvae. The presence of this compound prevents the occurrence of mating so that MMB is considered as a sex pheromone generated by male nematodes (Hsueh *et al*., 2017). This imitation strategy is conserved among different species of predacious fungi, which commonly happens in the feeding style of plants and animals (Flach *et al*., 2006; Haynes *et al*., 2002).

Ascarosides act as inducers of trap formation while MMB as attractant for the nematodes. There is another study performed by our lab as a progressional work of the discovery of SECs and it demonstrates that arthrosporols and 6-MSA play a role as inhibitors of traps in the NTF *A. flagrans* (Yu *et al*., 2021). The expression of genes in the *artA* gene cluster (*pksA* in *A. oligospora*) is individually controlled in time and space. Upon the presence of nematodes, low-molecular-weight compounds are produced with varying effects on fungal development in different regions of hyphae. Without any nematode, polyketide synthase ArtA is synthesized mostly at the tips in a colony since *artB-D* are not expressed at the hyphal tip and then the direct product 6-MSA (6-methyl-salicylic acid) accumulates to inhibit trap development and lure nematodes. *artA* combined with *artB* and *artC* are expressed in the posterior of the hypha, resulting in the generation of arthrosporols, which also prevent trap formation. When nematodes were added to the mycelium, *artA* is down-regulated so that the compounds were significantly decreased resulting in the formation of traps **(Fig. 5)**. This smart strategy enables the fungus to regulate the trap generation accurately by turning on and off the inhibiting effect from arthrosporols and 6-MSA in response to the absence or presence of nematodes correspondingly. Salicylic acid is frequently found as a plant pheromone, and similarly the predacious fungus secretes the methylated isoform of salicylic acid for the interplay of nematodes and fungi (Bouwmeester *et al*., 2019; Clavijo *et al*., 2012).

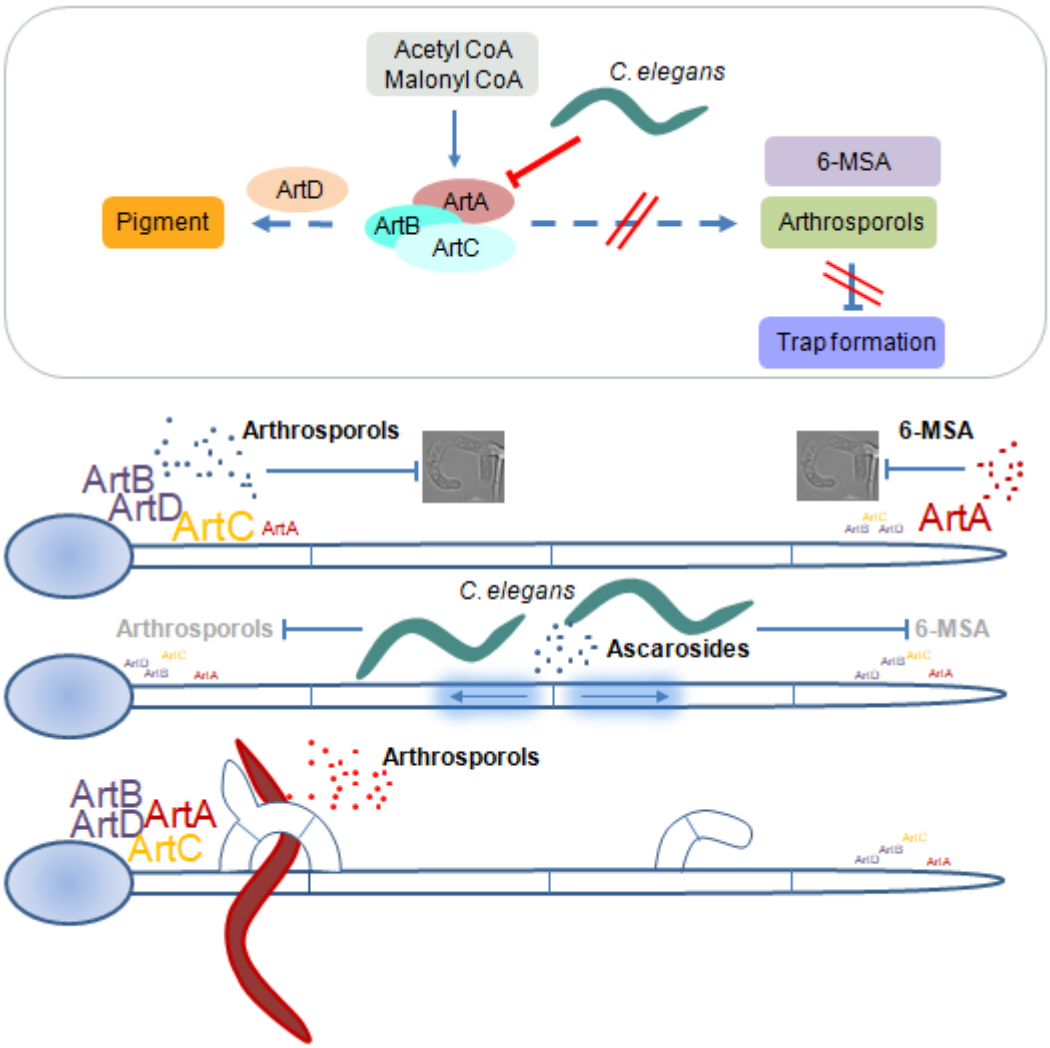

Fig. 5: Scheme depicting the function of the *artA*-gene cluster and the influence of the existence of nematodes. Gradients of arthrosporols and 6-MSA substances and ascarosides mediate trap production in *A. flagrans*. Hyphal tips produce 6-MSA, while rear hyphae convert it to arthrosporols. Both substances inhibit trap morphogenesis. Plenty of nematodes are attracted by 6-MSA and other compounds. Nematode-derived ascarosides cause the downregulation of artA cluster genes, which will result in decreased production of arthrosporols and 6-MSA, leading to trap production. After nematode being digested, *artA* cluster genes are expressed again and arising concentrations of arthrosporols suppress trap generation. Bigger font size refers to higher transcript abundances (Yu *et al.*, 2021).

Considering the secretion of small molecules and the responses performed by the two organisms, the next question is about the recognition of the molecules and the connected signaling cascades leading to differential gene expression. The olfactory neuron of *C. elegans*, AWC, mediates chemoattraction to odors produced by *A. oligospora* (Hsueh *et al.*, 2017). In the toxin-producing nematophagous fungus *P. ostreatus*, there is a cilia-dependent catching mechanism, which is that mycelia induce paralysis of prey by attacking sensory neurons in the cilia (Lee *et al.*, 2017). On the fungal side, a G-protein beta subunit, Gpb1, of *A. oligospora* plays a role in

sensing the presence of nematodes and initiates the production of traps (Yang *et al*., 2020). However, a detailed and comprehensive analysis from the extracellular signal sensing down to the intracellular specific executor is still missing. Therefore, the purpose of this work is to figure out how the fungus senses the existence of nematodes, by which means the fungus transfers the signal into the cells to enable trap induction and if the synthesis of the inhibitory arthrosporols is regulated by upstream factors in the presence of nematodes.

1.4 G-protein signaling pathways

G-proteins are highly conserved among eukaryotes and essential components for detecting and transmitting environmental stimuli into cells to evoke the proper physiological and biochemical responses. The G-protein dependent signaling system is comprised of G-protein-coupled receptors (GPCR), heterotrimeric G-proteins including α, β and γ subunits, and a variety of effectors **(Fig. 6)**. The sequential stimulation and activation of all these G-protein components convert environmental cues into chemical signals, resulting in the production of the proper cellular activities. Regulators of G-protein signaling (RGSs) play a vital role in regulating the magnitude and duration of G-protein signaling (Yu, 2006). In detail, the G-α subunit combines GTP and GDP and plays a role of hydrolyzing GTP to GDP, forming a dimer of the G-β and G-γ subunits. In the inactive conformation, α, β and γ subunits are found in a complex with a GPCR. When the ligand interacts with the receptor, this leads to the activation of the G-α protein to exchange GTP for GDP and dissociation of the G-α and G-βγ dimer (Li *et al*., 2007). In many organisms, both the G-α-GTP and G-βγ dimer influence downstream effector proteins such as phospholipases, phosphodiesterases, adenylyl cyclases, and ion channels (Neves *et al*., 2002). Proper modulation of the sensitivity and frequency of G-protein signaling is required for accurate signal transduction into an appropriate physiological response.

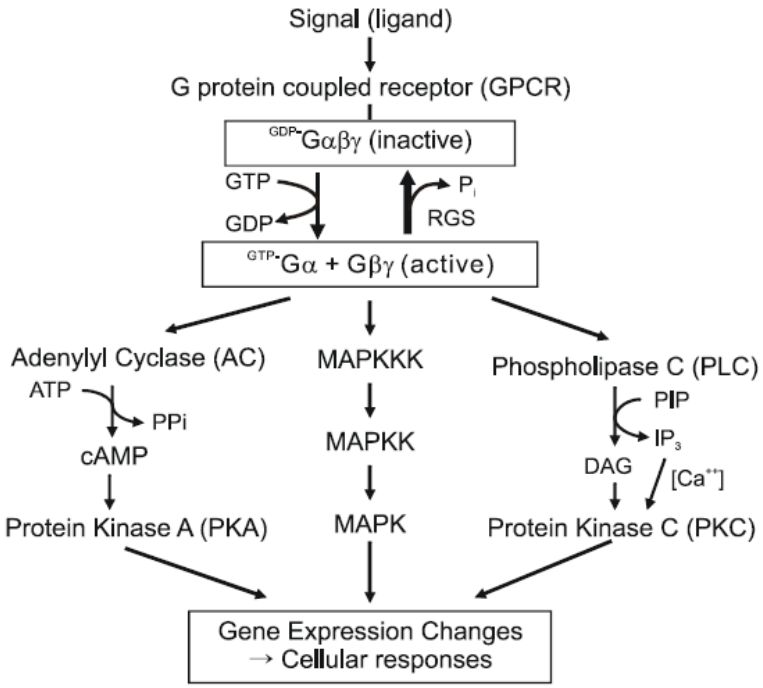

Fig. 6: Schematic representation of heterotrimeric G-protein signaling pathway and downstream signaling in *A. nidulans.* When external signals bind GPCR, it will activate G-alpha subunits to exchange GDP for GTP, which accelerating the dissociation of G-α-GTP from βγ dimer. Both activated complexes pass the signal downstream for proper intracellular responses. RGS performs a negative role to this signaling by inactivating G-α subunit (Yu, 2006).

Among the G-protein system, G-alpha subunits are the most important components since they take essential responsibilities in various aspects of eukaryotic microorganisms. Compared to two alpha subunits contained in *S. cerevisiae* which regulate sexual and asexual development individually, most filamentous fungi harbor three components which are generally classified into three groups (Lengeler *et al.,* 2000; Harashima & Heitman, 2004). Taking *A. nidulans* as an example, the three classes are group I (FadA), group II (GanA) and group III (GanB) respectively (Liu *et al*., 2018). Three subunits perform diverse and abundant functions which are normally indispensable for the colony. In *Cryptococcus neoformans*, the alpha subunit Gpa1 is induced by nitrogen limitation and is essential for the formation of melanin and the capsule which are both related to pathogenesis (Kwon-Chung *et al*., 1982; Kwon-Chung & Rhodes, 1986; Tolkacheva *et al*., 1994). Unlike Gpa1, both Gpa2 and Gpa3 are related to mating and pheromone sensing, and Gpa2 promotes sexual development whereas Gpa3 performs an inhibiting effect (Hsueh *et al*., 2007). Moreover, deletion of *gpaA* increased sporulation while deletion of *gpaB* decreased asexual development and reduced the level of the metabolite gliotoxin in *Aspergillus fumigatus* (Choi *et al*., 2020). In *A. nidulans*, FadA regulates vegetative growth and inhibits mating and toxin generation, and GanB is linked with nutritional sensing and asexual sporulation (Yu, 2006). Interestingly, four homologues of alpha subunits were identified in *Aspergillus flavus*, GanA, GpaB, FadA and GaoC respectively, in which

GaoC is a novel one. As one of the most critical parts, the production of aflatoxin is significantly influenced by the loss of *gpaB* that directly affects fungal virulence (Liu *et al*., 2018). Similarly, in the insect pathogen *Metarhizium robertsii*, MrGpa1 played a role in the formation of appressoria and insect cuticle penetration which accordingly control the fate of the fungus (Tong *et al*., 2020). The identification of G-alpha proteins in a variety of fungi and their corresponding functions in virulence and asexual development are well established. However, the role of G-alpha subunits in NTF is still scarce. Since α subunits are the uppermost elements of G-protein signaling, I assume that alpha subunits are involvedin sensing the nematode-derived pheromones ascarosides and pass down the signal to the nucleus in order to regulate the production of traps.

G-β and G-γ subunits are conserved as well among filamentous fungi and normally only one predicted β and one γ protein are contained. There are some exceptions, such as three beta subunits are identified in *Mucor circinelloides* while *Rhizopus oryzae* harbors four putative beta and five gamma subunits (Valle-Maldonado *et al*., 2020; Li *et al*., 2007). The βγ dimer also performs critical roles besides the active alpha subunits. In *Fusarium oxysporum*, the loss of β subunits Fgb1 leads to reduced pathogenicity on tomato plants and abnormal hyphal growth (Delgado-Jarana *et al*., 2005). Reduced virulence and weak invasiveness into the animal tissue are caused by the lack of the encoding gene of Gpb1 subunit in *M. circinelloides* (Valle-Maldonado *et al*., 2020). Twenty years ago, a beta subunit in the NTF *Arthrobotrys dactyloids* was recognized however no functional analysis was performed (Chen *et al*., 2001). Recently the role of beta subunit Gpb1 in another NTF *A. oligospora* was described in detail that the protein is essential for trap induction and the predatory lifestyle (Chen *et al*., 2020; Yang *et al*., 2020).

Regulator of G-protein signaling (RGS) function commonly as GTPase activatinG-proteins, adversely regulating G-protein signaling (Li *et al*., 2007). RGS proteins stimulate GTPase activity by binding to the transition state during GTP hydrolysis. Each of RGS has an RGS box that is critical for G interaction and may also harbor other domains for membrane targeting or Ras binding. The RGS proteins Sst1p and Rgs2p in the yeast *S. cerevisiae* control the two G-proteins, Gpa1p and Gpa2p, respectively (Hill *et al*., 2006). There are four RGS proteins in *A. nidulans*. The first RGS protein identified in filamentous fungus is FlbA (Lee *et al*., 1994). FlbA promotes asexual sporulation while FadA controls negatively (Yu *et al*., 1996). RgsA, the second discovered RGS in *A. nidulans*, controls colonial expansion, aerial hyphae, and pigment synthesis by negatively regulating the alpha subunit GanB (Han *et al*., 2004). And eight regulators (MoRgs1-MoRgs8) were identified in *Magnaporthe oryzae* and MoRgs1 is related to fungal pathogenesis (Yu *et al*., 2021). The regulators in nematophagous fungi take a critical role in the predation process of nematodes as well. Seven RGS proteins are identified and characterized in *A. oligospora* which are confirmed to perform various functions including promoting mycelia development, stress responses, sporulation and trap production. In particular, AoFlb1 is indispensible for trap formation (Ma *et al*., 2021).

1.5 The relation between G-proteins and downstream central signaling

Several signaling pathways downstream are correlated with G-proteins to transfer the extracellular signal into the cells for the biological responses. The widespread secondary messenger cyclic AMP is one of the components which perform such function. The enzyme adenylyl cyclase produces the ubiquitous intracellular messenger cAMP that is regulated by G-α subunits, which is demonstrated in *S. cerevisiae* and multiple filamentous fungi (Colombo *et al*., 1998; Alspaugh *et al*., 2002; Yang *et al*., 2016). In yeast, the intracellular cAMP level is reduced attributed to the loss of alpha subunits Gpa2 (Colombo *et al*., 1998). In *C. neoformans*, the mutant of the adenylyl cyclase encoding gene *cac1* is in the same morphogenesis as the Δ*gpa1*-mutant strain that the capsule synthesis is diminished, melanin formation reduced and the hyphae are avirulent to mice (Alspaugh *et al*., 2002). PKA is a well-described target of cAMP and constituted of two catalytic subunits and two regulatory subunits. Release of the regulatory subunits is caused by cAMP resulting in the kinase to be activated. Hereafter, catalytic subunits are free to phosphorylate downstream signaling cascade targets (Pukkila-Worley & Alspaugh, 2004). The lack of the catalytic subunit PKA1 of *C. neoformans* shows the same phenotype as the deletion strains of Δ*gpa1* and Δ*cac1*, well describing the consistent signal transduction (D'Souza *et al*., 2001). Similarly in *A. fumigatus*, PKA activity was undetectable in all the deletion strains of encoding genes of PKA, G-alpha subunit and adenylyl cyclase, indicating three belong to the cAMP signaling pathway (Liebmann *et al*., 2004). Apart from the establishment of deletion strains of respective genes, the direct addition of exogenous cAMP restores the defects from the loss of G-proteins, verifying their correlation in an easier way (Yu *et al*., 2017).

G-proteins control the fungal live through cAMP dependent and/or independent pathways. The relationship between G-protein and calcineurin in mammalian cells has been thoroughly investigated. The membrane phospholipid phosphatidylinositol-4, 5-bisphosphate (PIP2) is hydrolyzed by phosphatidylinositol-specific phospholipase C (PI-PLC), in order to produce the inositol-1, 4, 5-triphosphate (IP3, a universal Ca^{2+} mobilizing second messenger) and diacylglycerol (DAG, a kind of protein kinase C (PKC)) (Rebecchi & Pentyala, 2000). However, in filamentous fungi, there are only few reports about the functional relationship between PLC signaling and G-proteins. In the fungus *Botrytis cinerea* there is a link between one G α component and the calcineurin signaling pathway (Schumacher *et al*., 2008).

Additionally, Mitogen-activated protein kinase (MAPK) cascades are also crucial signal transducers that employ protein phosphorylation/dephosphorylation cycles to transmit signals across evolutionarily conserved pathways. MAPKKK (MAPK kinase kinase) phosphorylates two Ser and/or Thr residues inside the activating complex of MAPK kinases (MAPKK). Activated MAPKK then activates MAPK by dual phosphorylation of a highly conserved activation loop with the pattern -TXY-. Activated MAPK phosphorylates downstream targets, influencing their biochemical characteristics and eliciting particular output reactions (Hamel *et al*., 2012). To activate the pheromone response pathway in *S. cerevisiae*, the GPCR (Ste2p or Ste3p)

senses extracellular signals and then the G-proteins are dissociated, activating Ste20p, Ste50p, and the Far1p/Cdc24p complex, which activates the Fus3p MAPK cascade (mak-2 ortholog) (Bardwell, 2005). The cross-talk of several signaling modules has been described in *B. cinerea*: rich media induction is slightly reliant on the MAP kinase BMP1, induction of carbon sources requires G-alpha subunit 3, cAMP, and BMP1, and hydrophobic surfaces-contacting induction is completely dependent on BMP1 (Doehlemann *et al*., 2006). Likewise, in the pathogenic fungus *A. fumigates*, MAP kinase MpkB acts the role of signal transduction in the production of dihydroxynaphthalene (DHN)-melanin by cross-connecting with G-protein GpaA and the linked receptor GprM (Manfiolli *et al*., 2019). Among nematophagous fungi, the connection is well established between G-β subunit Gpb1 and STE7-FUS3 (MAPKK-MAPK) in *A. oligospora*, and this signaling transmits the signal and induces trap morphogenesis (Chen *et al*., 2021).

1.6 Ascaroside sensing

The transmission of chemical signals between organisms is a ubiquitous characteristic of living organisms. Ascarosides secreted by nematode are signals for communications between themselves and other creatures like fungi and plants in the natural environment. Fungi or plants perform powerful methods to sense the compounds from nematodes in order to respond physiologically in a proper time. For plants, pathogen or microbe associated molecular patterns (PAMPs) has been well described and the recognition of substances by plant species is regulated by germline-encoded pattern recognition receptors (PRRs), triggering the intrinsic pattern-triggered immunity (PTI) (Gust *et al*., 2017; Jones *et al*., 2016; Lolle *et al*., 2020). However there is still no ascaroside-sensing receptor in plants characterized (Siddique *et al*., 2022). It is only known that plants respond to ascarosides and induce defenses reactions. For example, the plant *Arabidopsis* takes advantage of the preserved process of peroxisomal β-oxidation to metabolize specific types of ascarosides from nematodes (Klessig *et al*., 2019; Manosalva *et al*., 2015; Manohar *et al*., 2020).

G-protein coupled receptor (GPCR) is one of the biggest classes of transmembrane receptors and able to transmit signals from extracellular to intracellular in response to different stimuli, including light, carbon, Calcium, volatiles, amino acids, nitrogen and enzymes. All GPCRs have the same basic architecture to contain a seven transmembrane domain (TM) and share the same signal transduction process, but display a remarkable variation in coding sequences and biological functions. Activated GPCRs promote the exchange of GTP for GDP on G-α proteins, resulting in the separation of G-α proteins from G-βγ dimer and physiological adaptations governed by downstream signaling (Maller, 2003; Xue *et al*., 2003). Due to their localization on the cellular membrane and essential functions in cell signaling, around 40 % of current medicines target to human GPCRs, demonstrating that these receptors are in theory druggable (Wacker *et al*., 2017; Eglen *et al*., 2007; Brown *et*

al., 2018).

In contrast to *S. cerevisiae* harboring only three receptors covering Ste2, Ste3 and Gpr1, most filamentous fungi contain a variety of GPCRs (Thevelein & de Winde, 1999; Dohlman & Thorner, 2001). The classification is well grouped by Brown *et al*. (2018). Based on sequence and structural similarity, ten groups of fungal GPCRs have been classified **(Fig. 7)**. The six classical groups of GPCRs consist of pheromone (classes I and II), carbon (class III), nitrogen (class IV), cAMP receptor-like (class V), and microbial opsin (class IX) receptors respectively. Subsequently, bioinformatics and backward genetics enable the discovery of a number of non-classical fungal GPCRs. These include RGS-domain-containing receptors (VI), homologues of MG00532 (*Magnaporthe oryzae*) (VII), progesterone like receptors (VIII), and Pth11 receptors (X).

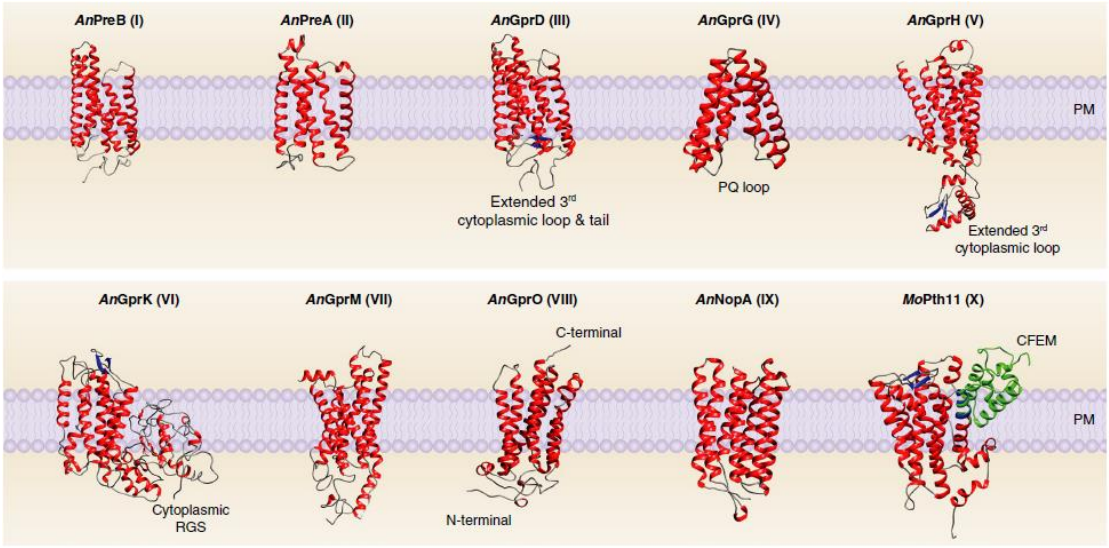

Fig. 7: The ten classical groups of G-protein coupled receptors containg diverse structures. The class names and the plasma membrane (PM) are indicated. The 7-TMs are in red color, β-sheets in blue color, and the eight-cysteine-containing domain (CFEM) in green color. Structural models of GPCRs were predicted with Phyre2 (Brown *et al*., 2018; Kelley *et al*., 2015).

The function of receptors in carnivorous fungi has not been reported yet, and the receptor which senses ascarosides remains to be identified. However, in other fungi multiple GPCRs are characterized. The Gpr4 of *C. neoformans* is the homologue of Gpr1 of *S. cerevisiae* and belongs to the carbon class (III). It is responsible for capsule production, which is essential for fungal virulence, and GprH of *A. nidulans* coming from the group V regulates production of secondary metabolites (Xue *et al*., 2006; Dos Reis *et al*., 2019). Receptors in both, group III and group V contain the 7-transmembrane-domain and play an important role in regulating fungal pathogenicity, which can be used as a good reference to choose the receptor from *A. flagrans*. The group I and II sense sexual pheromone which are chemical substances, so I will figure out if pheromone ascarosides derived from nematodes are sensed by

the homologues of both groups. There are as well abundant reports about the virulence-mediating receptors such as Pth11 in plant pathogenic fungi (Kou *et al*., 2017; DeZwaan *et al*., 1999).

Among the nematode community, ascarosides play critical roles as chemical signals to modulate sex attraction, antagonism, accumulation, sensory plasticity, and entrance into dauer stage, indicating that ascarosides influence a broad spectrum of *C. elegans* activities (Jeong *et al*., 2005; Butcher *et al*., 2007; Pungaliya *et al*., 2009; Golden *et al*., 1982). The receptors in *C. elegans* which sense ascarosides are partly characterized **(Fig. 8)**. Considering that there is no clue of conserved receptors employed by NTF for sensing ascarosides, I hypothesized that one or several receptors in carnivorous fungi are derived from nematodes by horizontal gene transfer (HGT) during the long co-evolution process of both organisms.

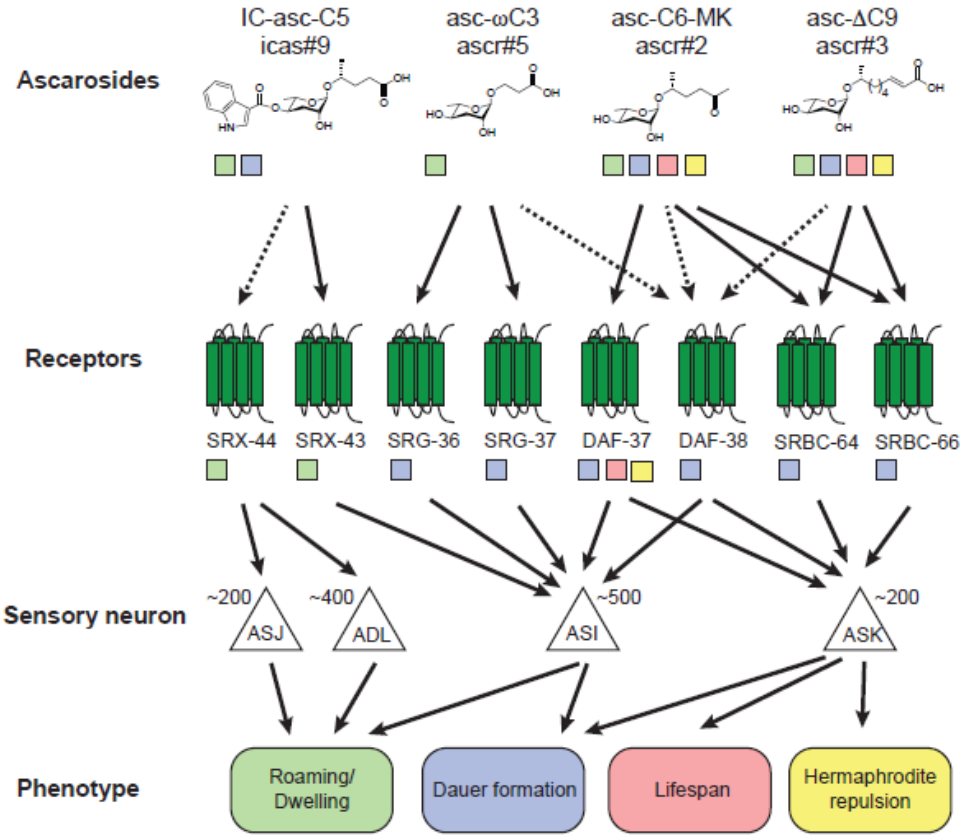

Fig. 8: Illustration of the connections between ascarosides, their corresponding receptors, sensory neurons, and the morphological consequences they induce. Lines between ascarosides and receptors are based on heterologous expression or pull-down assays. Dashed lines refer to repredicted ascaroside-GPCR interactions. Lines between receptors and sensory neurons mean expressional patterns. Numbers represent the putative amount of GPCRs expressed by specific neuron. The squares below indicate developmental processes regulated by ascarosides and receptors (McGrath & Ruvinsky, 2019; Vidal *et al.*, 2018).

Horizontal (or lateral) gene transfer is the interchange and permanent integration of

genetic code across strains or species of different origins. In contrast, vertical gene transfer refers to the natural passage of genetic information from generation to generation (DoolittleWF, 1999; Fitzpatrick, 2012). HGT has evolved between microbes with shared ecological niches or that have close relationships, such as host and pathogen, bacterial prey and predator, and symbiotic partners (Andersson *et al.*, 2003; Wang *et al.*, 2020; Beiko *et al.*, 2005; Jones *et al*., 2005; Richardson & Palmer, 2007; Haegeman *et al.*, 2011). There are major metabolic and developmental differences between nematodes and fungi, yet they share an intimate relationship of predating and being preyed. In fact, GPCRs in fungi are intensively conserved with 7-TM domain and considered to be inherited from the evolutionary parent, suggesting that nematode-fungi HGT might be a largely unknown factor in their cooperatively evolutionary history.

The mechanism of HGT is till ambiguous. Mostly HGT is defined when the distinguishing traits of encoding genes are apparent, such as a discrepancy between the clades of the genetic sequences in question and the generally recognized phylogeny of the organisms, a relatively high DNA or derived amino acid resemblance

between elements found in evolutionarily distanced life forms, uncommon distribution of a genetic element in a variety of species, related genes shared by organisms within a geographical region or specific ecosystems regardless of their genetic relatedness; and gene characteristics (G + C content, codon usage, intron, etc.) that are conflicting with the resident genome (Mitreva *et al.*, 2009). Unquestionably, the rising availability of genome analysis and subsequent developments in bioinformatics opens up possibilities for revealing HGT. Around 18 % of the *Escherichia coli* genome is composed of laterally transferred sequences and more than 100 putative HGT genes were explored by genome-wide screening in the insect pathogenic fungus *Metarhizium robertsii* (Zhang *et al.*, 2019; Mitreva *et al.*, 2009).

1.7 Effector and virulence proteins are important in many organismal interactions

During the attack against nematodes, carnivorous fungi secrete functionally secondary metabolites to lure the prey and regulate themselves for trap induction. Apart from it, fungi can also secrete small proteins which are virulent to the counterparts to manipulate their defense responses and physiology, namely effectors or virulent factors. In bacteria and plan-pathogenic fungi, effectors are well characterized. One of first steps of bacterial pathogens to attack is attachment of host epithelial barriers. Defense mechanisms of the host are responsible for recognition of microbial associated molecular patterns (MAMPs) by specific effectors such as membrane-anchored Toll-like receptors (TLRs). While bacteria secreted virulent factors to interact with TLRs in order to trigger the activation of host defenses and gain entry into the host. A secreted invasion protein InvA of *Yersina* sp.

involves in entry of pathogens into the host cell (Owen *et al.*, 2007). Bacterial effectors target G-protein signaling cascades, MAPK and ubiquitination pathways (Hardt *et al.*, 1998; Fu & Galan, 1999; Orth *et al.*, 2000; Mukherjee *et al.*, 2006; Kim *et al.*, 2005). Among effectors of fungal plant pathogens, there are proteases secreted to promote colonization into host and growth of pathogens. A serine protease Sep1 and a metalloprotease Mep1 are secreted by *Fusarium oxysporum* f. sp. *Lycopersicum*. They act to interrupt chitinases of host in order to inhibit their activity in degrading cell walls of fungi (Jashni *et al.*, 2015). The big class of secreted effectors, NLPs, induces necrotic cell death of plant host that is dependent on host cell damage induced by toxin (Ottmann *et al.*, 2009). In attacking nematodes by predatory fungi, there are not multiple reports about virulent factors. A systeine-rich protein (CyrA) among small-secreted proteins (SSPs) is characterized in *A. flagrans*. The transcript abundance of *cyrA* gene is induced in trap cells by nematodes. Before trapping *C. elegans*, CyrA accumulates at the inner rim of traps while after penetration into nematodes, the protein localizes in the fungal infection bulb. Heterologous expression of CyrA in nematodes reduces their lifespan and the protein accumulates in coelomocytes of *C. elegans* (Wernet *et al.*, 2021a). Besides this report, master thesises of our lab characterized other effector proteins that are induced by nematodes including HinA and NipA (Menzner, 2020; Wang, 2022). I aimed to reveal functions of more effectors that are essentially involved in interactions of nematodes and *A. flagrans*.

1.8 Aim of this work

As a downstream inhibitor of trap formation, the polyketide synthase ArtA is an important enzyme to synthesize the trap-inhibiting substances arthrosporols, and the expression of its encoding gene *artA* is suppressed by the existence of nematodes. In order to reveal the ascaroside-sensing signaling pathway in *A. flagrans*, this work aims to clarify whether G-proteins behave as the first element to sense the presence of nematodes and produce signals to the downstream cascades, targeting in the ultimate *artA* gene cluster in order to regulate trap morphologenesis. In several filamentous fungi, the production of secondary metabolites is mediated by signal transmission of G-α-cAMP/PKA pathway (Hu *et al*., 2018; Yu *et al*., 2017; Tag *et al*., 2000; Choi *et al*., 2020). Ste12 acts as a signal transductor between Gpb1 and the FUS3-MAPK cascade and is predicted by transcriptome sequencing as the upstream of a gene encoding a putative polyketide synthase in *A. oligospora* (Chen *et al*., 2021). The hypothesis was proposed that GPCRs bind nematode-secreted ascarosides and activate G-proteins, activated G-alpha subunits transform ectracellular cues into intracellular signals such as cAMP or calcium flow second messengers, these signals activate kinases in the downstream central signaling and are brought to nuclei, and here the transcriptional factor is commanded to regulate the expression of the *artA* gene cluster for trap induction.

In addition, the functionality of effector proteins will be characterized. I hypothesized

that an effector is induced by the presence of nematodes and will be secreted by trap cells. The effector takes an effect on the attack of hyphae against nematodes, such as digesting cuticles, targeting to immune system or modulating the physiological processes of the nematode prey.

2 Results

2.1 Ascarosides cause downregulation of the arthrosporols synthesized gene *artA*

Trap formation in *A. flagrans* depends on interplay of low-molecular weight compounds derived from the fungus and from the nematode (Xu *et al*., 2015; Hsueh *et al*., 2013). *A. flagrans* produces arthrosporols, which inhibit trap formation. On the other hand, *C. elegans* secretes ascarosides as pheromones, which are sensed by *A. flagrans* and thereby induce trap formation. I followed the hypothesis that the ascarosides cause downregulation of the genes required for arthrosporol biosynthesis. To test this hypothesis, I enriched ascarosides from nematode cultures as described (Zhang *et al*., 2013). Around 90,000 nematodes were cultured in liquid for 9 days in a large scale culture (150 ml). Afterwards the cultural supernatant was collected by centrifugation and condensed by freeze-dried, evaporated from the organic solution and freeze-dried again since the compounds are amphiphilic. In order to monitor *artA* expression, a reporter strain was used (SXY17), where the promoter of the *artA* gene was fused with *h2b* and *mCherry*. The mCherry signal was visible in the tips of the hyphae. After addition of nematodes, the signal disappeared. This also happened upon addition of the ascarosides fraction **(Fig. 9A**; Yu *et al*., 2021**)**. To further characterize the expression levels of the *artA* cluster genes in the presence of nematodes, 10^6 conidia were spread on thin low nutrient media in petri dishes and incubated for 24 h. *C. elegans* of different developmental stages was washed off from 7-day old NGM plates and applied on the germinated conidia for co-incubation for 6 h and 24 h before isolation of RNA. As a sample of uninduced mycelia, the same amounts of conidia were inoculated for 30 h and 48 h. Then the expression level of *artA* cluster genes were examined in both induced and uninduced mycelia by quantitative real time RT-PCR. The transcript abundances of all four genes were downregulated upon addition of *C.elegans*, which was consistent with the microscopical observation of the reporter **(Fig. 9B)**.

After the analysis that ascarosides cause downregulation of the *artA* gene cluster, I wondered which signaling cascades are involved and how the hyphae detect ascarosides and control the expression of *artA*. Because G-protein signaling pathways are central cascades which pass extracellular signals to the intracellular, I assumed that G-proteins act upstream of *artA* expression.

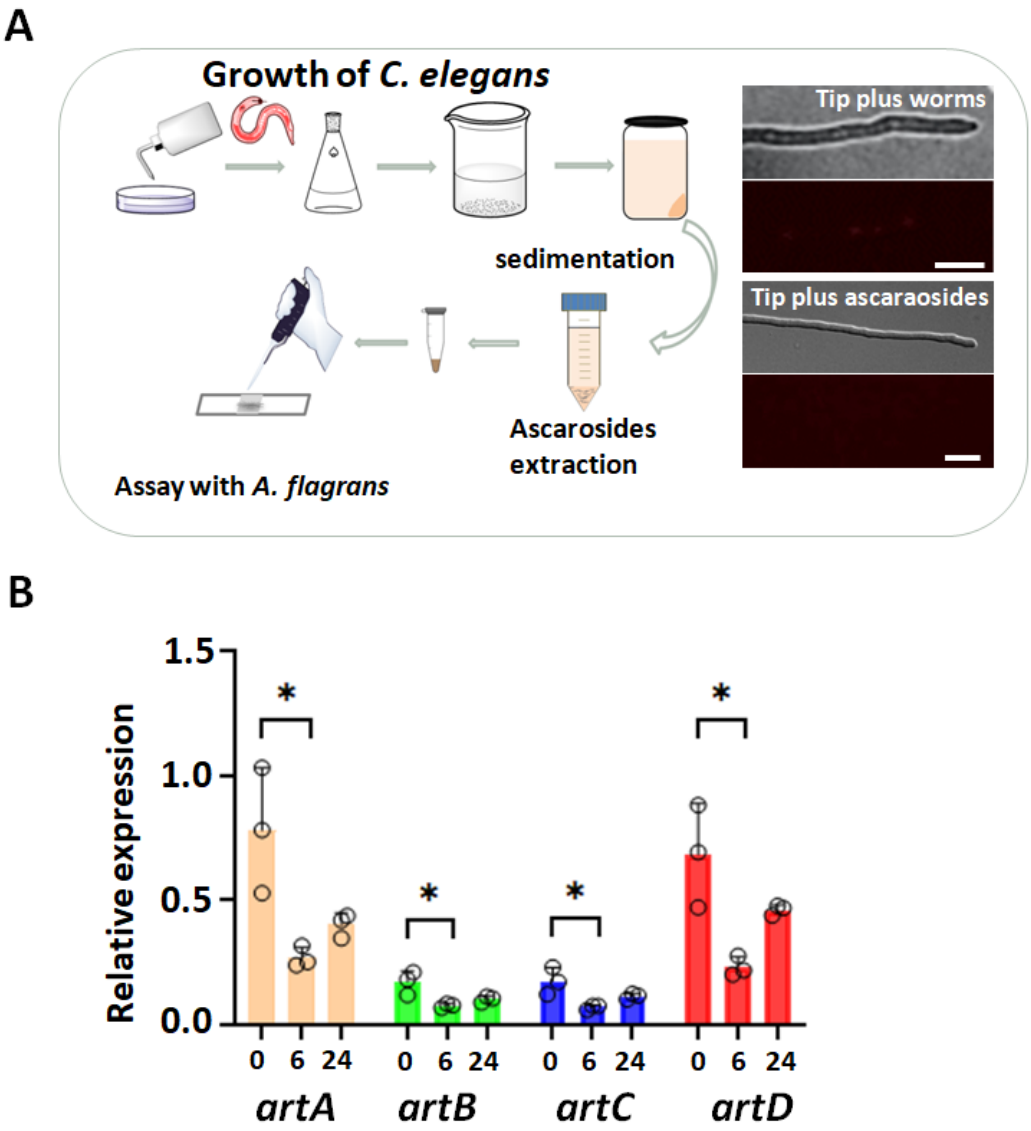

Fig. 9: Isolated ascarosides from *C. elegans* suppress the expression of *artA*. (A) Scheme of the ascarosides extraction process (left, drawn with ChemDraw software). The microscopic pictures show hyphae exposed to nematodes or to the ascarosides fraction. The fluorescent pictures show very weak signals in both cases (right). Scale bar, 20 µm. **(B)** The transcript abundances of four genes (*artA-D*) of *artA* gene cluster. Conidia of *A. flagrans* were added evenly on cellophane on LNA media for overnight incubation at 28° C. About 50,000 mixed-stage nematodes from NGM plates were added on the germinated conidia, and mycelia were collected at the indicated time points and processed for analysis by qRT-PCR. Expression data were normalized to actin. (mean ± SD, n = biological and technical triplicates; asterisks indicate significant differences as measured with the unpaired t test compared between induction and uninduction; *p < 0.05. *artA* 0 h vs. 6 h, p-value is 0.025; *artB* 0 h vs. 6 h, p-value is 0.027; *artC* 0 h vs. 6 h, p-value is 0.030; *artD* 0 h vs. 6 h, p-value is 0.020).

2.2 *A. flagrans* contains three G-protein α subunits

To identify putative G-alpha subunits I used the sequences of FadA (XP_658255.1), GanA (XP_660694.1) and GanB (XP_658620.1) of *A. nidulans* as bait to search for orthologues in the *A. flagrans* genome. Three putative G-protein α subunits were identified and named as GasA (DFL_009501), GasB (DFL_000801) and GasC (DFL_009358). Their open reading frame (ORF) encodes proteins of 353, 356 and 354 amino acids, respectively. The three Gα subunits were aligned and compared based on their amino acid sequences. GasA shared 99.43 % and 90.37 % similarity with AOL_s00075g181 and FadA from *A. oligospora* and *A. nidulans* respectively, GasB shared 98.03 % and 79.21 % identity with AOL_s00109g19 and GanB respectively, and GasC shared 98.31 % and 51.81 % identity with AOL_s00075g14 and GanA. All three α subunits contain one G-α domain including an ADP-ribosylation factor domain.

To show its conservation between different species of fungi, a phylogenetic tree was constructed with the three putative Gas proteins of *A. flagrans* with orthologues from *A. oligospora*, *Arthrobotrys entomopaga*, *Dactylellina haptotyla*, *Dactylella cylindrospora*, *Metarhizium robertsii*, *Beauveria bassiana*, *A. nidulans*, *Aspergillus fumigatus*, *Aspergillus flavus*, *Aspergillus terreus*, *Cryptococcus neoformans* and *Saccharomyces cerevisiae* **(Fig. 10)**. G-alpha subunits are subdivided into three classes, and all fungi harbor two to four homologous proteins. Likewise, the three proteins of *A. flagrans* GasA, B and GasC belong to the three classes. The bootstrap values by the colors indicated that yeast fungi like *C. neoformans* and *S. cerevisiae*, non-nematode catching fungi and NTF are distant relatives from each others.

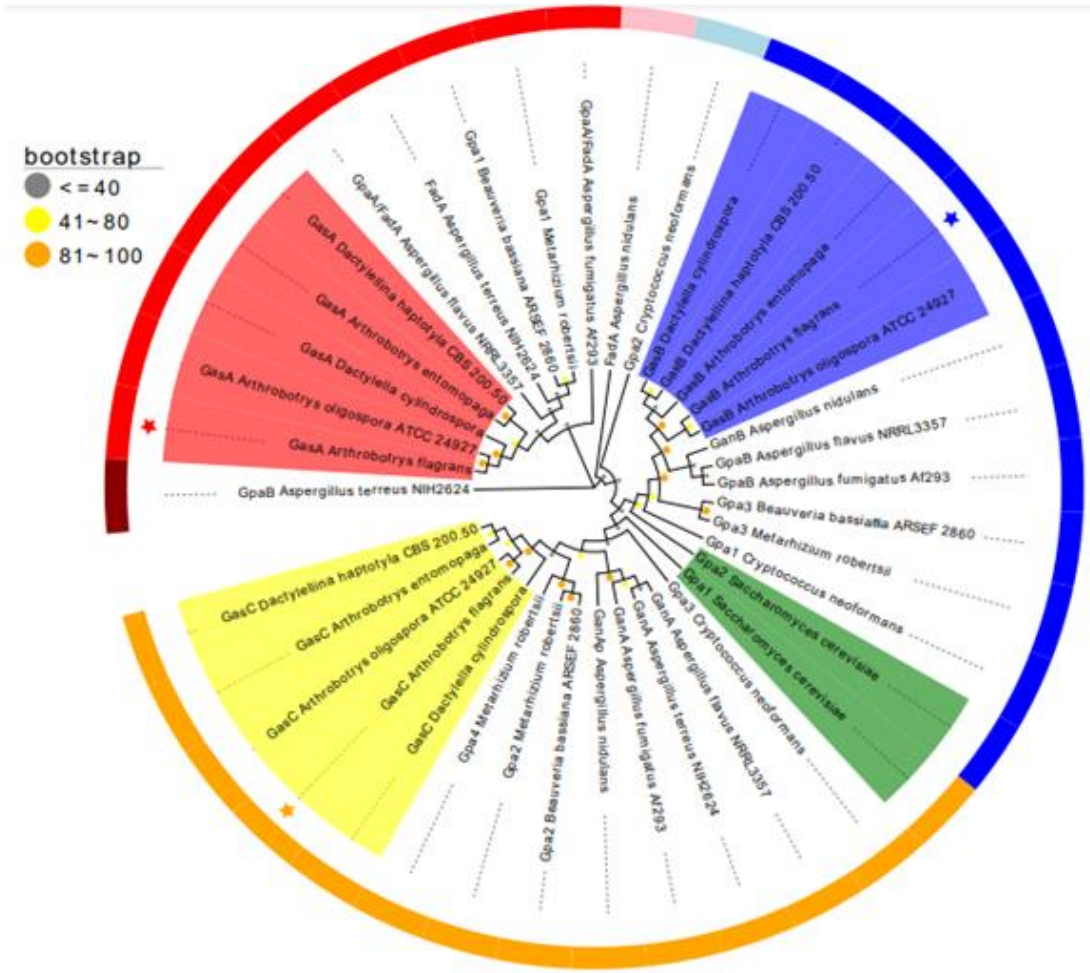

Fig. 10: A phylogenetic tree of three G- protein α subunits from several fungal species. The sequence was aligned with Mega X, and the evolution tree was illustrated with EvolView2 (https://evolgenius.info/evolview-v2/#login). Three classes of GasA, GasB and GasC are shaded with the colors in the periphery (red, blue and yellow), and the other colorful bands peripherally indicate distant proteins. The colors in the fan forms indicate proteins from NTF (red, yellow and blue) and *S. cerevisiae* (green). *A. flagrans* GasA-C are represented by red, yellow and blue asterisks. The bootstrap value was displayed by the respective colors which are marked at the top left.

2.3 The G-protein α subunits GasA and GasB control pigmentation, conidia formation, conidia germination and trap formation

2.3.1 GasA is required for the germination of spores

To examine the molecular function of GasA, the *gasA* open reading frame was deleted by homologous recombination of the flanking regions using the hygromycin cassette as selection marker. The left border was amplified by PCR from the template of genomic DNA with the primers GasALB-pjet-ol-for and GasALB-H-ol-rev, and the

right border of the ORF with the primers GasARB-H-ol-for and GasARB-pjet-ol-rev, and the hygromycin cassette was amplified with the primers H-GasALB-ol-for and H-GasARB-ol-rev from a plasmid with this region. The three fragments were ligated to pJET with the help of corresponding overlaps in the primers by means of Gibson. Then the deletion cassette without overlap (LB-Hyg-RB) was amplified with GasA_LB_for and GasA_RB_rev for transformation into protoplast. After obtaining the transformants, they were verified by amplifying the deletion cassette with the primers GasAko_up_for and GasAko_down_rev, and also checking the lack of the ORF with GasA_ORF_for and GasA_ORF_rev. Since the lengths of the *gasA* ORF and hygromycin cassette are different, wild type and mutant should show different lengths of bands by amplifying the deletion cassette, 3148 and 3716 bp respectively **(Fig. 11A, B)**. The deletion event in the eight selected transformants was confirmed by Southern blot. The left border was used as the probe and the genomic DNA of respective strains was digested with the restriction enzyme *Xba*I. In wild type a band of 4678 bp was detected, whereas in the deletion strains a band of 2357 bp appeared. In the deletion strains no extra bands were detected suggesting that there were no ectopic integrations.

One of the deletion strains (SXD39) was used for further analysis. In order to show that the observed phenotypes were due to the deletion of *gasA,* a wild-type copy of *gasA* was introduced into the mutant strain. SXD39 was transformed with plasmid PXD71 (SXD42). The same amount of spores of wild type, the Δ*gasA*-deletion strain, and the re-complemented strain were inoculated on PDA plates and incubated for several days. The colony of the deletion strain grew smaller than wild type and the re-complemented strain **(**WT**, Fig. 11C, D)**. This could be due to delayed germination or to reduced hyphal extension. To distinguish between the two possibilities, conidia of WT and mutant were inoculated in low nutrient medium and incubated in the dark for 4 h before counting the number of germinated conidia. Whereas 36.78 % of wild type had germinated, only 31.35 % did of the mutant strain. In the re-complemented strain the defect was rescued and 35.81 % of the conidia had germinated **(Fig. 11E)**. This result suggests that a delay in germination is responsible for the reduced colony diameter since an observation of the extension rate of hyphae in the strains showed no obvious difference **(Fig. 11F)**. A difference in the production of spores between WT and mutant was not observed.

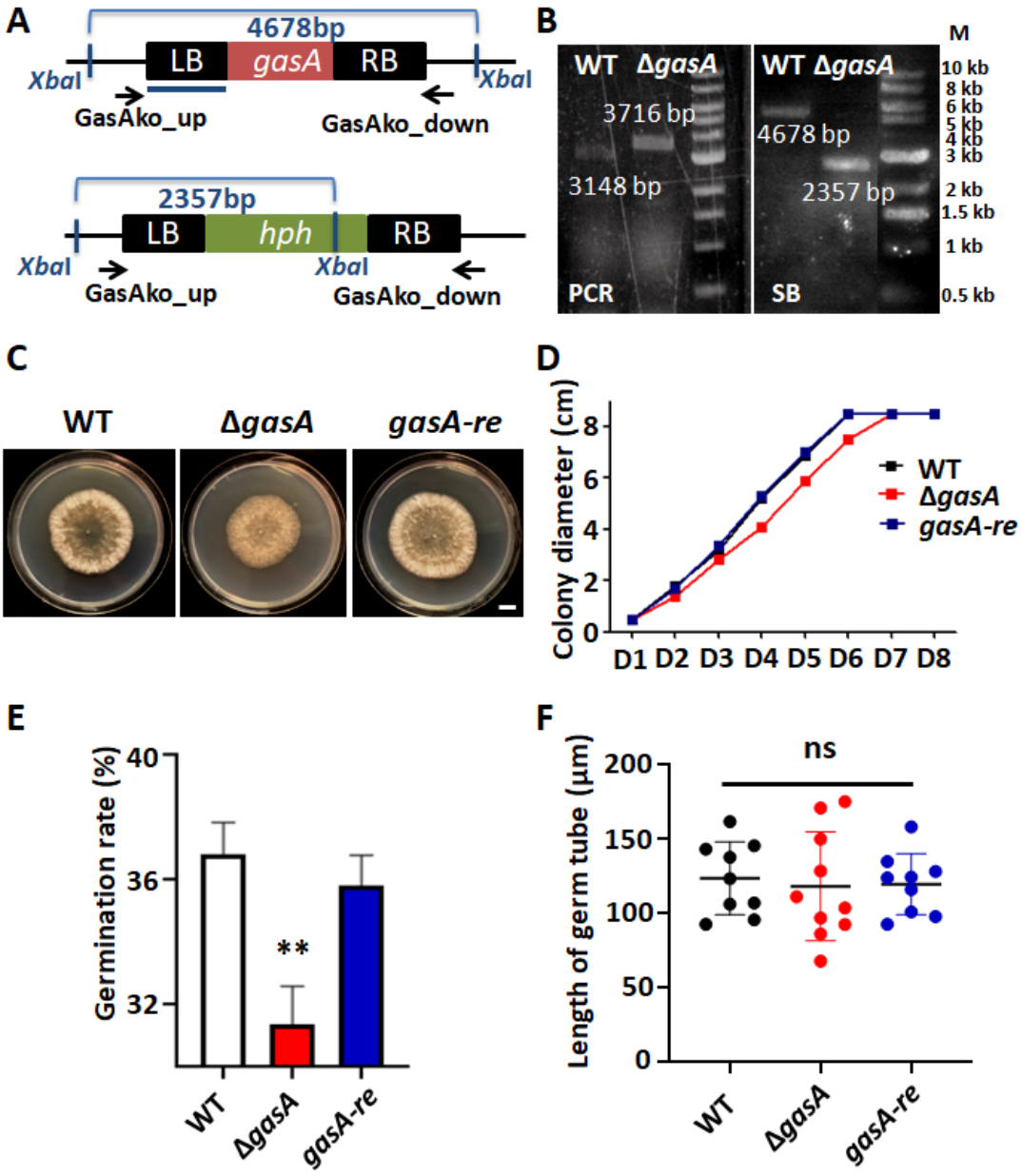

Fig. 11: Analysis of the *gasA* gene in *A. flagrans*. (A) Scheme of the *gasA* gene and the confirmation strategy of the knockout strain. Arrows indicate the primers used for PCR and the blue line below LB region indicates the probe for the Southern blot. **(B)** Left: PCR amplification of the fragments indicated in (A) using genomic DNA of WT and the Δ*gasA*-deletion strain as template. PCR fragments were separated on a 0.8 % agaraose gel. Right: The Southern blot analysis of the fragments indicated in (A) using the enzyme *Xba*I for digestion of gDNA of wild type and the Δg*asA*-deletion strain. **(C)** Morphology of wild type, the Δ*gasA*-deletion strain and the re-complemented strain (*gasA-re*, SXD42) after growth on PDA plates for 4 days after inoculation of 10^5 conidia. Scale bar, 1 cm. **(D)** Growth curves of WT, Δ*gasA* and *gasA-re* by measuring the diameter of the colony for 8 days after inoculation of conidia. **(E)** Germination rate of conidia of WT, the Δ*gasA*-deletion and the *gasA-re* strains after 4 h of incubation at 28° C. **(F)** Comparison of the lengths of germ tubes of WT, the deletion and the re-complemented strains. Conidia were inoculated on LNA and incubated

for 4 h in 28° C before measuring the length of the germ tube. Data are presented as mean ± SD, and error bars indicate the standard deviation. Asterisks shows significant levels based on unpaired t test between WT and mutants; **p < 0.01 and ns suggests not significant. (E) p-value is 0.004; (F) p-value is 0.714.

2.2.2 GasB is involved in the regulation of conidia production and the control of melanin biosynthesis

The *gasB*-open reading frame was deleted in the same way as *gasA* in wild type and with the selection marker hygromycin. The left border, hygromycin and right border were amplified individually with the primers GasBLB_pjet_ol_for, GasBLB-H-ol-rev, H-GasBLB-ol-for, H-GasBRB-ol-rev, GasBRB-H-ol-for and GasBRB-pjet-ol-rev. The 4085 bp band was obtained from transformants by amplification with GasB_KO_up_for_n and GasB_KO_down_rev_n, which was different with the 3725 bp band from WT, generating the Δ*gasB*-deletion strain **(Fig. 12A, B)**. The deletion event was verified with Southern blot by digesting the genomic DNA of nine transformants with enzyme *XmnI* and using the right border as the probe. As a result, the bands of different lengths of 1797 bp in WT and 5752 in mutants were detected and there was no additional band observed suggesting that no ectopic integration happened. One of the deletion trains (SXD40) was chosen for further analysis. In order to show that the defect came from the lack of *gasB*, a wild-type copy of *gasB* was re-introduced into the Δ*gasB*-deletion strain by transforming the plasmid PXD72 into the mutant strain SXD40, generating the re-complemented strain (*gasB-re*, SXD43).

10^5 conidia of WT, the *ΔgasB*-deletion and the *gasB-re* strains were inoculated at the center of PDA plates. At the beginning of growth on PDA plates, the colony of the Δ*gasB*-deletion strain showed significantly less aerial hyphae compared to WT and *gasB-re* whereas all colonies shared similar growth rates **(Fig. 12C)**. After being cultured for more than 5 days, the Δ*gasB*-deletion strain started to appear darker than WT and the re-complemented strain in the substrate hyphae at the reverse side of the PDA plate. The above side of the colonies of the strains did not show obvious differences in pigmentation. The conidia yields were collected and calculated from 10-day-old plates of these strains inoculated with 10^5 conidia. The Δ*gasB*-deletion strain produced obviously reduced numbers of conidia as compared to wild type and *gasB-re* **(Fig. 12D)**. These results suggest that GasB is involved in the generation of conidia and aerial hyphae, and the control of pigment production in substrate hyphae.

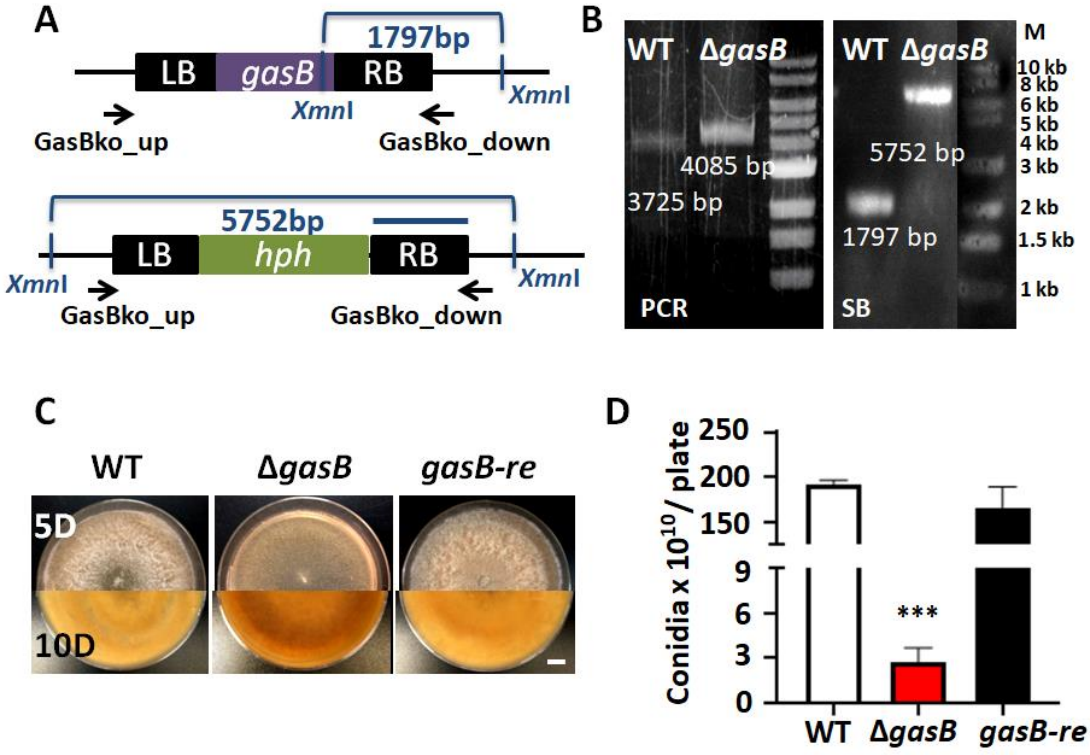

Fig. 12: Analysis of the *gasB* gene in *A. flagrans*. (A) Illustration of the *gasB* gene and the homologous recombination strategy. Arrows indicate the primers used for PCR verification and the blue line indicates the probe for the Southern blot. **(B)** Left: PCR amplification of the fragments indicated in (A) using genomic DNA of WT and the Δ*gasB*-deletion strain as template. PCR fragments were separated on a 0.8 % agaraose gel. Right: The Southern blot analysis of the fragments indicated in (A) using the left border region of *gasB* as a probe and enzyme *Xmn*I for digestion of gDNA of wild type and the Δg*asB*-deletion strain. **(C)** Morphogenesis of WT, the Δ*gasB*-deletion and the re-complemented strain grown for 5 days (aerial hyphae, above) and 10 days (substrate hyphae, below). Scale bar, 1 cm. **(D)** Measurement of the number of conidia produced by strains collected after 10 days of incubation at 28° C of 10^5 conidia (mean ± SD, n = three biological replicates and three technical replicates; asterisks indicate significant levels based on unpaired t test between strains; ***p < 0.001, the Δ*gasB*-deletion strain p-value = 0.000).

2.3.3 GasC is not obviously involved in morphology control

I also studied the function of the third G-alpha subunit of *A. flagrans,* GasC. The *gasC* gene was deleted using the same approach as for *gasA* and *gasB* and confirmed by PCR (not shown). In order to reveal any function at the colony level, the same amount of conidia (around 10^5) was inoculated in the canter of PDA plates and the growth was observed for several days. However, the Δ*gasC*-deletion strain (SXD91) did not show any obvious changes in the appearance of the colony on PDA plates compared to wild type **(Fig. 13)**, including germination rate, growth speed, conidia production or pigment formation.

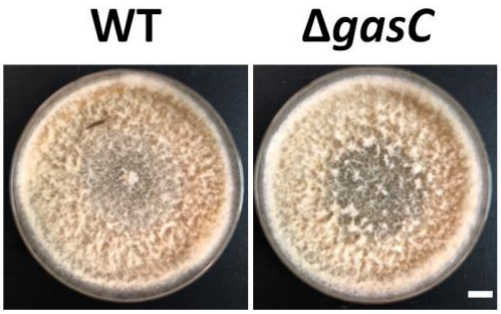

Fig. 13: Comparison of colonies of wild type and the Δ*gasC*-deletion strain. 10^5 of conidia of WT and the Δ*gasC*-deletion strain were inoculated at the center of the PDA plate and incubated for 10 days in the dark of 28° C. Scale bar, 1 cm.

2.3.4 GasA and GasB are involved in the control of trap production

Next, I examined roles of GasA and/or GasB and/or GasC in the control of trap production and/or the capturing of nematodes. The agar for the microscope slides was made of low nutrient media in order to mimic the deprivation of nutrient. Same amounts of conidia of wild type, the Δ*gas*-deletion and the corresponding re-complemented strains, were inoculated on the agar, and afterward incubated for 16 h. *C. elegans* of mixed developmental stages was grown on NGM for seven days and applied to conidia and co-incubated for another 16 h. Then traps were quantified microscopically in a 2.5 cm x 2.5 cm area of the agar on the slide. Wild type produced 472.96 ± 63.23 traps, the Δ*gasA*-deletion strain 9.39 ± 3.28, *gasA-re* strain 444.00 ± 53.39, the Δ*gasB*-deletion strain 237.60 ± 39.85, and *gasB-re* 486.40 ± 75.16 **(Fig. 14B)**. The Δ*gasA*-deletion strain lost almost completely the ability to produce traps **(Fig. 14A)**. Trap formation was less affected in the Δ*gasB*-deletion strain but not as severe as with the Δ*gasA*-deletion strain. The re-complemented strains produced again similar numbers of traps. There was no difference of the trap numbers between the Δ*gasC*-deletion strain and WT.

Next, the numbers of nematodes either trapped or digested by traps was calculated in wild type and mutant strains. The number of trapped nematodes followed the numbers of traps in the different strains. Wild type *A. flagrans* caught 40.53 ± 4.60 nematodes, the Δ*gasA*-deletion strain 1.92 ± 0.85, the Δ*gasA*-deletion strain 17.28 ± 2.93 and the re-complemented strains have caught similar numbers of nematodes **(Fig. 14C)**. The different numbers of trapped nematodes reflect the different numbers of traps formed in the different strains. The decreased numbers of traps of mutants compared to wild type demonstrated that GasA and GasB positively regulate the production of traps, whereas GasC appears to play no role in the process.

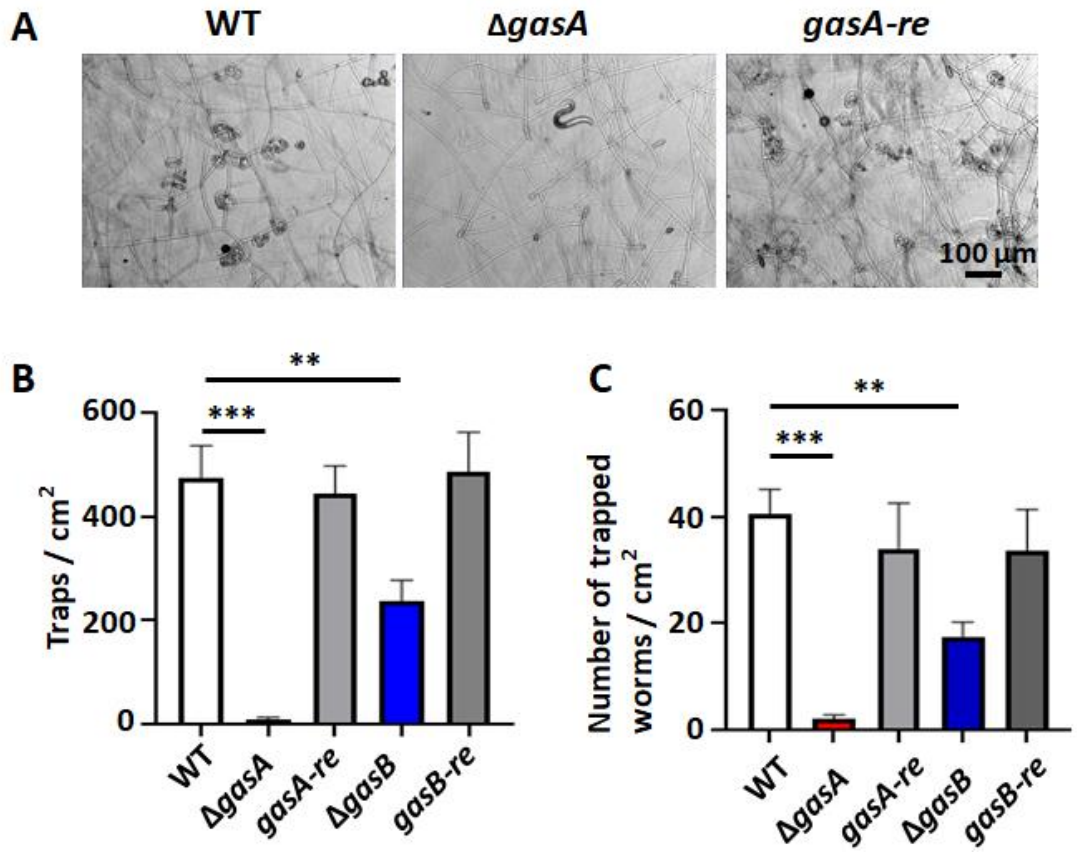

Fig. 14: GasA and GasB are involved in trap formation. (A) Trap production of wild type, the Δ*gasA*-deletion and the re-complemented strain (*gasA-re*) observed under the microscope (scale bar, 100 µm). **(B)** Quantification of the trap number of WT, the Δ*gasA*-deletion strain, the Δ*gasB*-deletion strain and their corresponding re-complemented strains. 10^5 conidia were inoculated on the agar of the slide for overnight growth. *C. elegans* was added on the mycelia and incubated again overnight. Trap numbers were calculated counted on the entire slide. **(C)** Quantification of *C. elegans* that were trapped or being digested by strains. Data were processed as mean ± SD, and error bars indicate the standard deviation. Asterisks show significant levels based on unpaired t test between WT and mutants; **p < 0.01 and ***p <0.001. (B) For trap number, WT vs. Δ*gasA*-deletion strain, p-value is 0.000; WT vs. Δ*gasB*-deletion strain, p-value is 0.005; (C) For number of trapped nematodes, WT vs. Δ*gasA*-deletion strain, p-value is 0.000; WT vs. Δ*gasB*-deletion strain, p-value is 0.002.

2.3.5 GasA is involved in ascaroside sensing

Prerequisites for the initiation of trap formation in *A. flagrans* are growth on low-nutrient medium and the presence of nematodes. The process is triggered by low molecular weight compounds of fungal origin, the arthrosporols, and of nematode origin, the ascarosides (Hsueh *et al*., 2013). Arthrosporols inhibit trap formation and ascarosides inhibit arthrosporol production (Xu *et al*., 2015; Yu *et al*., 2021). Because G-protein-dependent signaling pathways are important sensing systems for intra- and extracellular signals, we speculated that GasA and/or GasB

sense the presence of nematodes and causes the downregulation of the arthrosporol biosynthesis. To test this hypothesis, I studied the expression of the *artA* cluster genes (*artA*, *artB*, *artC*, *art*D gene), which are required for arthrosporol biosynthesis (Yu *et al*., 2021). To this end, quantitative real-time RT-PCR analysis were performed in wild type and Δ*gasA*-, Δ*gasB*-deletion strains under both induced and uninduced conditions, which were represented by incubating the growing hyphae together with nematodes for 0 h and 6 h individually. A decrease of the transcript abundance of *artA* was observed in wild type in the presence of nematodes in comparison to uninduced mycelia of WT, and other *art* genes in wild type displayed similar tendency as *artA*. However no change was detected between the induced and uninduced *ΔgasA*-deletion strain among all four *art* cluster genes. The same downregulation as in WT was detected in induced compared to uninduced mycelia of the Δ*gasB*-deletion strain **(Fig. 15A)**.

The differences in *artA* transcript levels were not very large, which can be explained by the fact that there are still substrate hyphae in induced mycelia and the genes were not expressed homogenously in all hyphae. To circumvent this problem a reporter assay with cellular resolution was used. The *artA* promoter was fused with the *h2b* (histone 2 b) gene and *mCherry*, and the construct introduced in both, wild type and mutants. If the artA gene is expressed, there will be red signals in the nuclei. To monitor the expression, *C. elegans* was added to the growing mycelia of *A. flagrans* on low nutrient media for overnight induction. For wild type, strong fluorescence signals were detected in nuclei in hyphal tips whereas there was no detectable signal in the presence of nematodes, suggesting inhibition of *artA* **(Fig. 15B)**. Strikingly, there was no obvious response in the Δ*gasA*-deletion strain, that is, the fluorescent signal was detected no matter if nematodes were present or not. This suggests that there was no inhibition of *artA* in the absence of GasA. In contrast in the *ΔgasB*-deletion strain, the nematode-induced downregulation of *artA* occurred like in wild type. These results demonstrate the validity of the assumption that GasA is responsible for the sensing of the presence of nematodes and that the *artA* gene is one of the targets of the GasA-signaling pathway.

The next question was how GasA senses the nematodes. *C. elegans* pheromone, the ascarosides, has been shown to induce trap production in *A. oligospora* (Hsueh *et al.*, 2013). Therefore, we assumed that sensing of these compounds involves GasA. To test the hypothesis, I enriched the ascarosides as mentioned above and reported before (Zhang *et al.,* 2013). 20 µl of the isolated substance fraction was applied to germinated conidia of WT, the Δ*gasA*-deletion and Δ*gasB*-deletion strains for overnight co-incubation before microscopic observation. Consequently, the occurrence of the downregulation of *artA* in these strains was similar to the situation after addition of nematodes **(Fig. 15B)**.

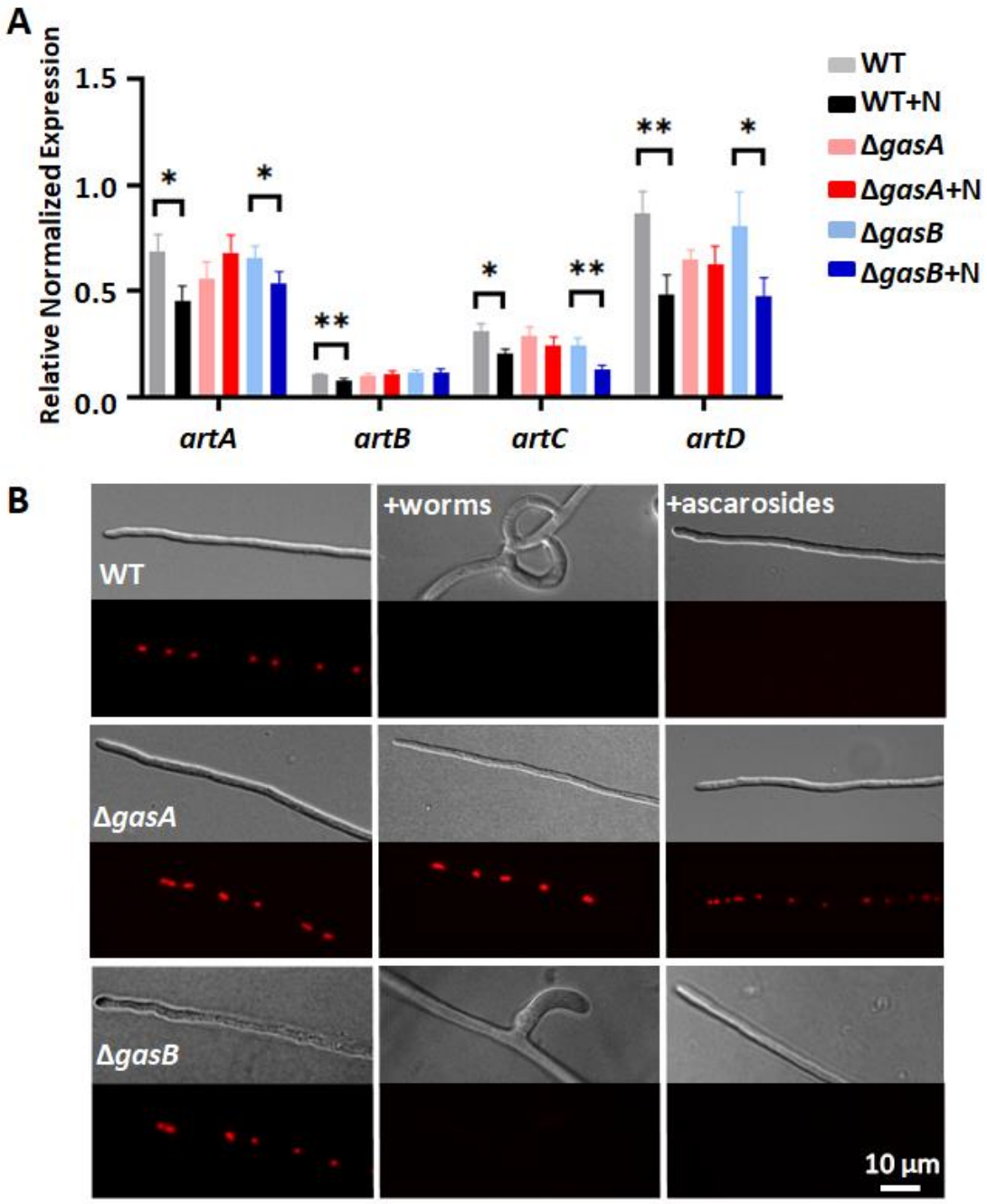

Fig. 15: Role of GasA and GasB in the regulation of the expression of the *artA* gene cluster. **(A)** The transcript abundances of *artA* cluster genes in un-induced and induced mycelia of both wild type and mutants. *A. flagrans* conidia of corresponding strains were spread on cellophane membrane on LNA and grown at 28 °C for 24 h. Then about 50,000 nematodes cultivated on NGM medium were collected and added on growing mycelia for another 24 h. Mycelia were harvested from cellophane at indicated time points and RNA isolated for qRT-PCR. Scale bars indicate standard deviation of three technical replicates. *artA*: un-induced vs. induced WT, p-value = 0.019, the un-induced vs. induced Δ*gasA*-deletion strain, p-value = 0.133, the un-induced vs. induced Δ*gasB*-deletion strain, p-value = 0.048; *artB*: un-induced vs. induced WT, p-value = 0.009, the un-induced vs. induced Δ*gasA*-deletion strain, p-value = 0.281, the un-induced vs. induced Δ*gasB*-deletion strain,

p-value = 0.978; *artC*: un-induced vs. induced WT, p-value = 0.014, the un-induced vs. induced Δ*gasA*-deletion strain, p-value = 0.324, the un-induced vs. induced Δ*gasB*-deletion strain, p-value = 0.007; *artD*: un-induced vs. induced WT, p-value = 0.009, the un-induced vs. induced Δ*gasA*-deletion strain, p-value = 0.738, the un-induced vs. induced Δ*gasB*-deletion strain, p-value = 0.038. **(B)** Spatial examination of *artA* expression at cellular resolution with the reporter assay. The *h2b-mCherry* reporter was under the control of *artA* promoter in either the Δ*gasA*-deletion strain or the Δ*gasB*-deletion strain, generating the reporter strains SXD44 and SXD45 respectively. Conidia were inoculated on the LNA slide and for induction, *C. elegans* or enriched ascarosides was added on the growing hyphae and after co-incubation for overnight, the photos were taken. Scale bar, 10 µm.

2.3.6 GasB represses *artA* cluster gene expression

The expression levels of *artA* were compared in the last chapter between un-induced and inducted mycelia of both, wild type and mutants. Since △*gasB* mutants grow poorly on low nutrient media, the expression level of *artA* was not well comparable between strains. In order to analyze the expression differences of *artA* between wild type and mutants, the transcript abundances of the *artA* cluster genes were quantified in wild type and the Δ*gasA*-deletion and Δ*gasB*-deletion strains by culturing conidia in PDB liquid media for two days. Interestingly the transcript abundances of all four *artA*-cluster genes were obviously increased in the Δ*gasB*-deletion strain but not Δ*gasA*-deletion strain as compared in wild type, suggesting that the expression level of *artA* is repressesd by *gasB*, while *gasA* does not influence the *artA* expression in substrate hyphae **(Fig. 16A, B)**. The darker pigmentation observed in the Δ*gasB* deletion strain as compared to WT verified the increased expression level of *artA* as well **(Fig. 12C)**.

To figure out if the enhanced pigmentation and the reduced number of traps was due to higher expression level of *artA*, the *artA*-open reading frame was deleted by homologous recombination with the selection marker geneticin in the Δ*gasB*-deletion strain. Deletion was confirmed by PCR and Southern blot **(Fig. 16C, D)**. The double mutant Δ*gasB* Δ*artA* (SXD50) produced dramatically increased amounts of traps after strains were incubated in the presence of *C. elegans* on low nutrient medium **(Fig. 16B)**. However, the darker pigmentation did not disappear after the deletion of *artA* **(Fig. 16E)**.

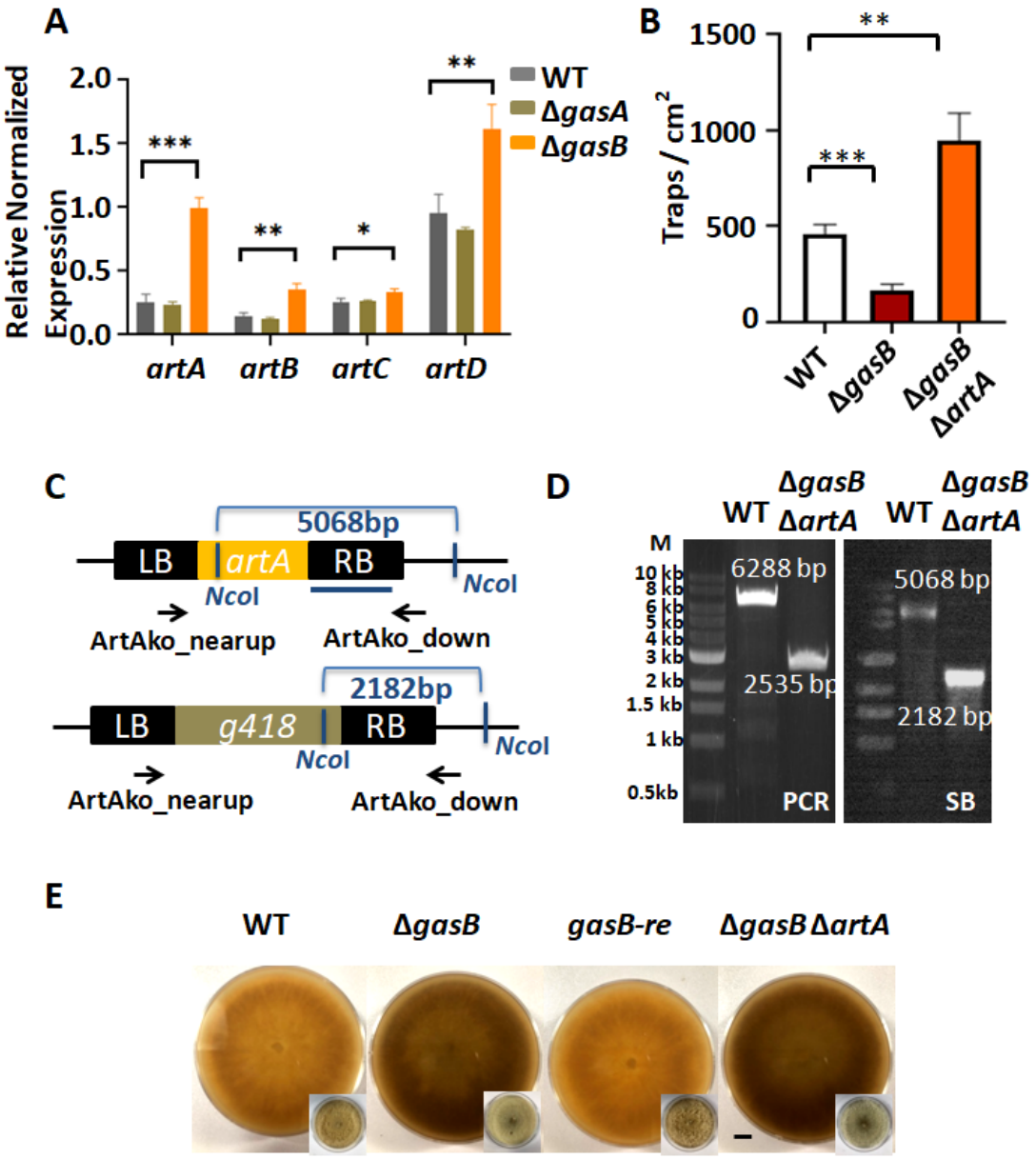

Fig. 16: GasB represses the induction of the *artA*-gene cluster. (A) Relative expression levels of *artA* cluster genes in the strains indicated. Expression data were normalized to actin. **(B)** Quantification of trap productivity in WT, the Δ*gasB*-deletion strain and the double mutant Δ*gasB* Δ*artA.* **(C)** Scheme of the homologous recombination event. *Nco*I restriction sites was used for the Southern blot. Arrows indicate the primers used for PCR verification and the blue line indicates the probe of the right border of *artA* for the Southern blot. **(D)** Left: PCR amplification of the fragments indicated in (C) using genomic DNA of WT and the Δ*gasB* Δ*artA*-double deletion strain as template. PCR fragments were separated on a 0.8 % agaraose gel. The left border, geneticin cassette and the right border were amplified individually with artALB_pjet_ol_for and artALB_hph_ol_rev, H-artALB-ol-for and H-artARB-ol-rev, artARB_hph_ol_for and artARB_pjet_ol_rev. The deletion cassette without overlap was amplified with artA_LB_for and artA _RB_rev. The transformants were verified by being amplified the latter part of deletion cassatte with primers artAKO_nearup_for and artAKO_down_rev. Right: The Southern blot analysis of the fragments indicated in (C) using

the right border of *artA* as a probe and enzyme *Eco*I for digestion of gDNA of wild type and the Δ*gasB* Δ*artA*-double deletion strain. **(E)** Colonial morphogenesis of wild type, the Δ*gasB*-deletion, the re-complemented of *gasB* and the Δ*gasB* Δ*artA*-double deletion strains grown for 10 days (big: reverse side; small: above side of PDA plates). Scale bar, 1 cm. Error bars indicate standard deviation of technical triplicates. Asterisks suggest significances. *p < 0.05, **p < 0.01, ***p < 0.001. (A) *artA* WT vs. the Δ*gasA*-deletion strain, p-value = 0.566, WT vs. the Δ*gasB*-deletion strain, p-value = 0.000; *artB* WT vs. the Δ*gasA*-deletion strain, p-value = 0.298, WT vs. the Δ*gasB*-deletion strain, p-value = 0.003; *artC* WT vs. the Δ*gasA*-deletion strain, p-value = 0.605, WT vs. the Δ*gasB*-deletion strain, p-value = 0.032; *artD* WT vs. the Δ*gasA*-deletion strain, p-value = 0.182, WT vs. the Δ*gasB*-deletion strain, p-value = 0.009; (B) WT vs. the Δ*gasB*-deletion strain, p-value = 0.001; WT vs. the Δ*gasB* Δ*artA*-double-deletion strain, p-value = 0.005.

2.4 The cAMP-PKA signaling pathway acts downstream of GasB

2.4.1 GasB regulates the biosynthesis of intracellular cAMP

The G-alpha proteins GasA and GasB were proven to act upstream of the *artA* gene. The next question was how the signal is transmitted further. Three pathways were reported to perform such a function, namely the MAP Kinase pathway, the cAMP-PKA and the PLC signaling pathways (Shimizu & Keller, 2001; Chen *et al.*, 2021; Schumacher *et al.*, 2008).

In order to determine whether the deficiency of G-alpha subunits resulted in decreased levels of cAMP, 5 mM of the cAMP analog 8'-Bromo-cAMP was applied to growing mycelia of wild type and mutants on PDA plate for morphological observation and on LNA agar for examination of trap productivity **(Fig. 17A)**. We anticipated that the analog would recover the defects of the deletion strains. Interestingly, the Δ*gasB*-deletion strain displayed normal pigment levels, normal mycelial growth and regular conidia amount as wild type in the presence of the analog in PDA plates **(Fig. 17B, D)**. Likewise, trap formation was recovered when the Δ*gasB*-deletion strain was grown on low nutrient medium with 8'-Bromo-cAMP **(Fig. 17E)**. However, the defect in trap morphogenesis of the Δ*gasA*-deletion strain was not restored by the addition of the analog **(Fig. 17C)**. These results suggest that the defect of the Δ*gasB* deletion was due to decreased levels of intracellular cAMP and GasB regulates the biosynthesis of cAMP in *A. flagrans*.

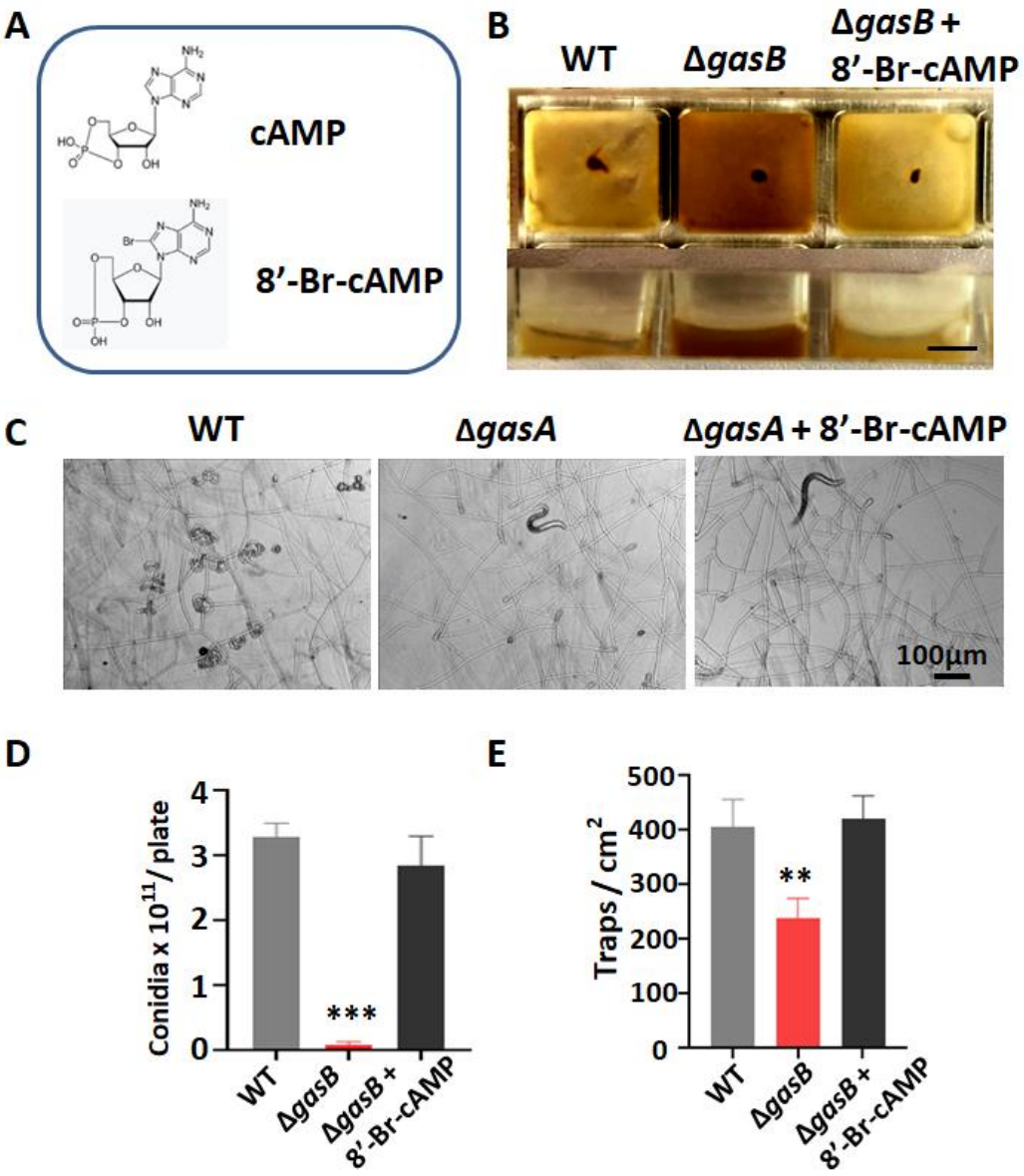

Fig. 17: Regulation of the biosynthesis of intracellular cAMP by Gas proteins. (A) The chemical structures of cAMP and its analog 8'-Bromo-cAMP. **(B)** Recovery of the production of mycelia and pigment upon the addition of 5 mM of the cAMP analog 8'-Bromo-cAMP in PDA plates of the Δ*gasB*-deletion strain, in contrast to wild type and the unadded Δ*gasB*-deletion strain. 10^4 conidia were grown on the PDA plates in the wells for 3 days. Up: the reverse sides; down: the lateral sides. Scale bar, 0.5 cm. **(C)** Microscopic observation of trap morphogenesis in wild type, the Δ*gasA*-deletion strain and the Δ*gasA*-deletion strain supplemented with the cAMP analog. Scale bar, 100 µm. **(D, E)** Quantification of conidia and traps of the Δ*gasB*-deletion strain additionally with 8'-Bromo-cAMP. Conidia were harvested from PDA plates and measured after growth of 10 days. Traps were produced on LNA media and counted after overnight germination of conidia followed by overnight co-incubation with *C. elegans*. Error bars indicate standard deviation of technical triplicates. Asterisks suggest significances. (D) p-value is 0.000; (E) p-value is 0.009.

2.4.2 Analysis of the GasA-signaling pathway

Whereas the cAMP analog rescued the *gasB*-mutant phenotype, it did not rescue the *gasA* defects, suggesting another signaling pathway for GasA **(Fig. 17C)**. Since the genome of *A. oligospora* and *A. flagrans* share 88 % similarity and the FUS3 MAPK cascade was reported to be related to G β subunit Gbp1 in *A. oligospora*, I considered that this MAP kinase might act downstream of GasA (Youssar *et al*., 2019; Chen *et al*., 2021). An orthologue of FUS3 (DFL_000344) in *A. flagrans* was identified and named as MakB (PhD thesis, Valetin Wernet, 2021). The protein displays 99.71 % identical amino acids. The gene was deleted and the trap induction was still observed in the Δ*makB*-deletion strain. Another MAK kinase MakA (DFL_005546) was identified that is homologous to SLT2 of *A. oligospora*, which was reported to be essential for the formation of trapping structures, the deletion strain of its encoding gene *makA* showed significantly reduced growth on LNA but the traps were still formed suggesting that they were not critical for trap morphogenesis (Zhen *et al*., 2018; PhD thesis, Valetin Wernet, 2021).

Another possibility for a MAK downstream of GasA is the transfer of MakB into the nucleus in the presence of nematodes. To test this hypothesis, a MakB-GFP expressing strain (SXD90) was created. Its conidia were incubated on LNA slides overnight, and 200 nematodes were added and further incubated overnight. As a control conidia were incubated without nematodes. No shuttle of MakB was observed.

Next, I tested an involvement of phospholipase C in the GasA signaling. The survey of the genome and comparison with yeast and other filamentous fungi showed two predicted isozymes of PLC, *plc1* (*dfl_009590*) and *plc2* (*dfl_003061*) **(Fig. 18)**. The two genes were deleted individually by homologous recombination using the hygromycin cassette for selection (SXD92, SXD93). It was anticipated that one of the deletion strains of *plc* could show similar deficiency in the production of traps as Δ*gasA*. However, none of the two deletion strains was affected in trap formation (not shown). This may be due to the redundancy of functions of the two PLCs. A double knockout has not been created yet to test this hypothesis.

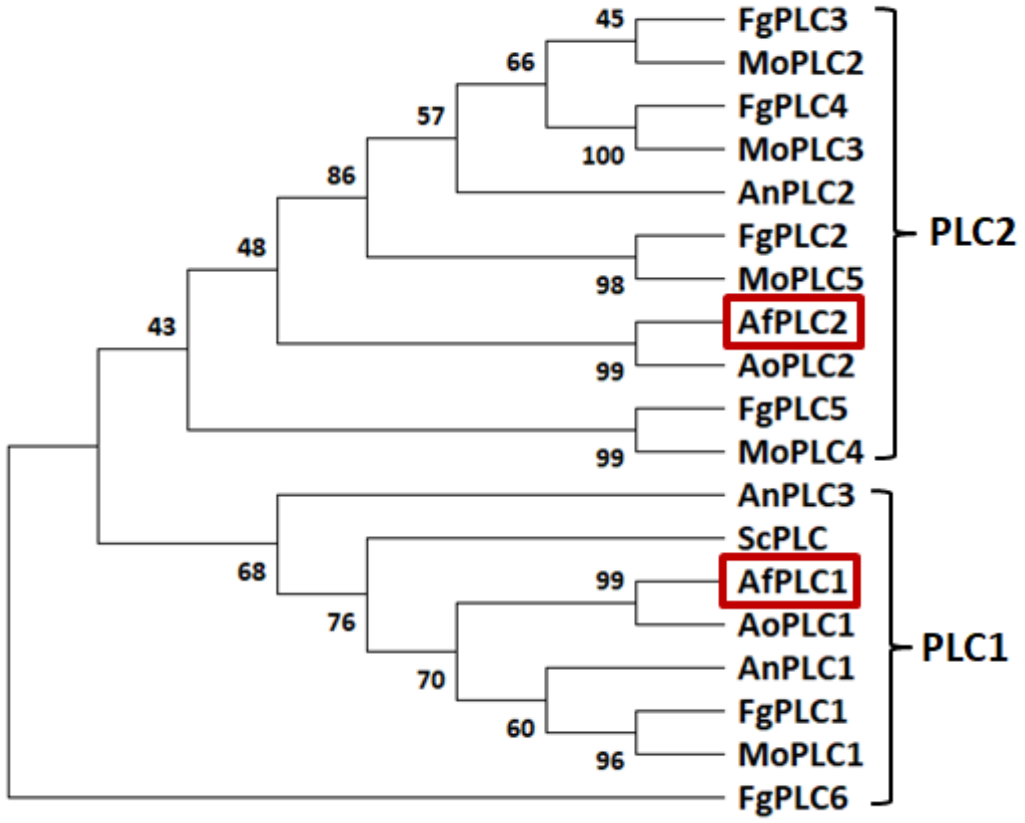

Fig. 18: Phylogenetic tree of Phospholipase C in respective microorganisms. Af: *A. flagrans*, Ao*: A. oligospora*, Sc: *S. cerevisiae*, Fg: *Fusarium graminearum*, Mo: *Magnaporthe oryzae*, An: *A. nidulans.* The value in the branches indicated the similarities between homologous proteins.

2.5 The transcriptional factor Ste12 acts upstream of the *artA* gene cluster

2.5.1 The Tetratricopeptide repeat (TPR) containinG-protein ArtR

After the examination of the signaling pathway, I tried to identify the transcriptional factor upstream of *artA*. The first candidate was a putative regulator in the *artA* cluster, ArtR (Yu *et al*., 2021). In contrast to the homologous gene cluster in other nematode trapping fungi, ArtR (DFL_002600) is the unique protein which contains 6 tetratricopeptide repeats **(Fig. 19A, B)**. TPR is probably involved in protein-protein interactions (Marck *et al*., 1993). Transcriptional factors found in gene clusters for secondary metabolites often control the expression of the other cluster genes. To test if ArtR controls the expression of *artA-D*, the open reading frame of *artR* was disrupted by the deletion cassette containing hygromycin as selection marker. The mutant was confirmed by PCR amplification **(Fig. 19C)**. However, the Δ*artR*-deletion strain (SXD60**)** was still able to form similar numbers of traps like wild type.

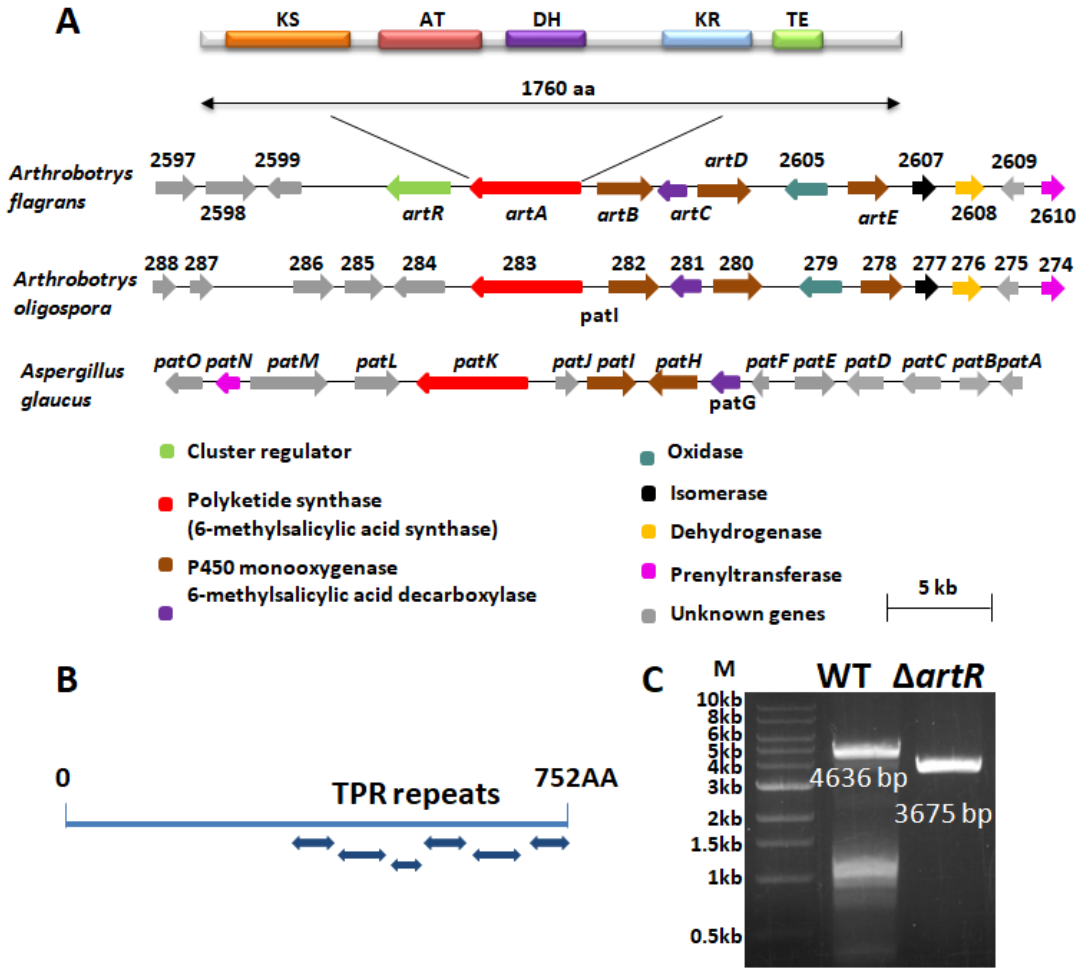

Fig. 19: Analysis of the role of ArtR in *A. flagrans*. (A) Scheme of the *artA*-gene cluster in several filamentous fungi (Yu *et al.*, 2021). **(B)** Structure of the *artR* gene and the 6 tetratricopeptide repeats. **(C)** PCR amplification of the fragments using genomic DNA of WT and the Δ*artR*-deletion strain as template. The fragments were amplified with primers TPRko_up_for and TPRko_down_rev. PCR fragments were separated on a 0.8 % agaraose gel. The lengths of generated bands were marked in the gel. The left and right flanking regions and hygromycin cassette were amplified, respectively with the primers of TPRLB_pjet_ol_for and TPRLB_H_ol_rev, TPRRB_H_ol_for and TPRRB_pjet_ol_rev, H_TPRLB_ol_for and H_TPRRB_ol_rev.

2.5.2 Role of Ste12 as a transcriptional factor controlling trap formation

The transcriptional factor Ste12 was reported to act downstream of the signaling pathway of the G-β subunit Gpb1 and the FUS3 MAPK cascade of the carnivorous fungus *A. oligospora*. Therefore, it can be assumed that Ste12 acts downstream of the G-α subunits in *A. flagrans* (Chen *et al.*, 2021). I found a Ste12 ortholog (DFL_001239) in *A. flagrans*. In order to study a role as a transcription factor, the predicted *ste12* gene was fused with the green fluorescent protein gene (*GFP*) and

expressed under the control of the constitutive *oliC* promoter. The construct was introduced into wild type and positive transformants were visualized and confirmed by microscopy (SXD48). In order to make sure that the signal was in nuclei, Hochst33258 was used to stain the DNA. The fluorescent signals of the fusion protein Ste12-GFP and the nuclear dye Hochst33258 overlapped, suggesting the localization of Ste12 protein in nuclei **(Fig. 20A)**. Since *ste12* was expressed under the control of a constitutive promoter, the *ste12-GFP* strain was considered to over-express *ste12* in comparison to wild type. To confirm this, a quantitative RT-PCR was formed. The expression level of *ste12* gene in the *ste12-GFP* strain was obviously higher than it in wild type **(Fig. 20B)**.

In order to characterize the role of Ste12, a deletion strain of *ste12* (SXD56) was generated by disruption of the ORF with the hygromycin cassette. The deletion cassette was derived by the amplification of left border (LB), hygromycin (H) and right border (RB) individually with primers of Ste12LB_pjet_ol_for and Ste12LB_H_ol_rev, H_ste12LB_ol_for and H_ste12RB_ol_rev, Ste12RB_H_ol_for and Ste12RB_pjet_ol_rev. The deletion cassette was introduced to wild type protoplast. After the substitution of the open reading frame (ORF) of *ste12* by the deletion cassette, the transformant was confirmed to be a pure mutant by PCR and Southern blot. The gDNA of wild type and mutant was digested with the restriction enzyme *Eco*RV, and hybridized with the probe of the right border. Different bands of WT (6014 bp) and the Δ*ste12*-deletion strain (3228 bp) were detected **(Fig. 20D, E)**. The Δ*ste12*-deletion strain produced bushy mycelia that gathered around of the petri dish **(Fig. 20C)**. In order to confirm the defect was due to the lack of *ste12*, a re-complemented strain (*ste12 re*) was gained by introducing the expression cassette (*LB-ste12-RB*) and the geneticin cassette into the Δ*ste12*-deletion strain. The normal mycelia were retrieved by the expression of *ste12* gene. Interestingly the *ste12-GFP* strain displayed rare hyphae around the plate and a small bunch of hairy mycelia at the center **(Fig. 20C)**.

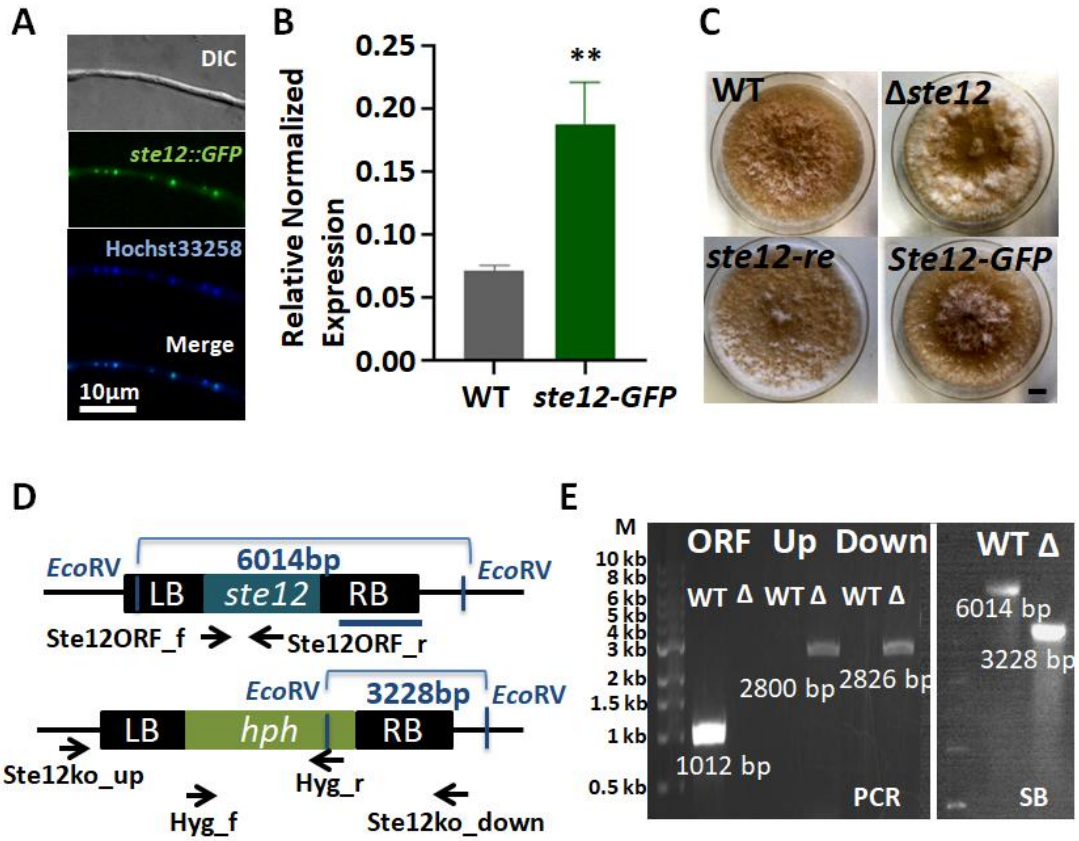

Fig. 20: Analysis of Ste12 localization and the generation of a Δ*ste12*-deletion strain. (A) The nuclear localization of the fusion protein Ste12-GFP. The *GFP* gene was fused with *ste12* and expressed under the control of the constitutive *oliC* promoter. Conidia of the *ste12-GFP* strain were inoculated on a LNA slide and incubated for 24 h before microscopic inspection. The nuclear dye Hochst33258 was used at a concentration of 10 µg/ml. Scale bar, 20 µm. **(B)** The relative expression levels of *ste12* in wild type and the *ste12-GFP* strain. Expression data were normalized to actin. Error bars indicate standard deviation of technical triplicates. Asterisks suggest significances. p-value is 0.004. **(C)** The colonial morphology of wild type, the Δ*ste12*-deletion, the re-complemented (*ste12-re*, SXD63) and *ste12-GFP* strain. Conidia of strains were inoculated at the center of PDA plate and grown for 10 days. Scale bar, 1 cm. **(D)** Scheme of the homologous recombination strategy. *Eco*RV restriction enzyme was used for the Southern blot and the right border of *ste12* as a probe. Arrows indicate primers used in PCR confirmation **(E)** Left: PCR amplification of the fragments using genomic DNA of WT and the Δ*ste12*-deletion strain as template. The upstream fragment of deletion cassette (2800 bp) and downstream (2826 bp) were amplified with the primers Ste12ko_up_for and Hph_rev, Hph_for and Ste12ko_down_rev. The absence of ORF region was confirmed by amplification with Ste12ORF_for and Ste12ORF_rev. PCR fragments were separated on a 0.8 % agaraose gel. Right: The Southern blot analysis of the fragments indicated in (D) using the right border of *ste12* as a probe and enzyme *Eco*RV for digestion of gDNA of wild type and the Δ*ste12*-deletion strain.

2.5.3 Ste12 inhibits the formation of trap networks

To figure out if Ste12 regulates trap productivity, conidia and nematodes were added on low nutrient medium in succession. After overnight co-incubation, the trap numbers were quantified. The Δ*ste12*-deletion strain presented large trap networks and normal trap production was restored in *ste12 re* strain, but the over-expressing strain failed to produce any traps **(Fig. 21A)**. The quantification of traps confirmed the microscopic examination. The Δ*ste12*-deletion strain formed increased numbers of traps (1282.13 ± 149.48) in contrast to WT (387.63 ± 71.82) and the rescued strain produced similar amount of traps (399.36 ± 56.36) as wild type, but no traps were observed in the *ste12-GFP* strain **(Fig. 21B)**. Based on further monitoring, larger trap networks were visualized in the Δ*ste12*-mutant strain than in wild type. There were on average 22 traps per network in the Δ*ste12*-deletion strain, but 10 in wild type and 10 in *ste12*-re strain **(Fig. 21C)**. The ability to form more and bigger trap networks in the Δ*ste12*-deletion strain indicates that Ste12 plays a role in repressing the production of trap network.

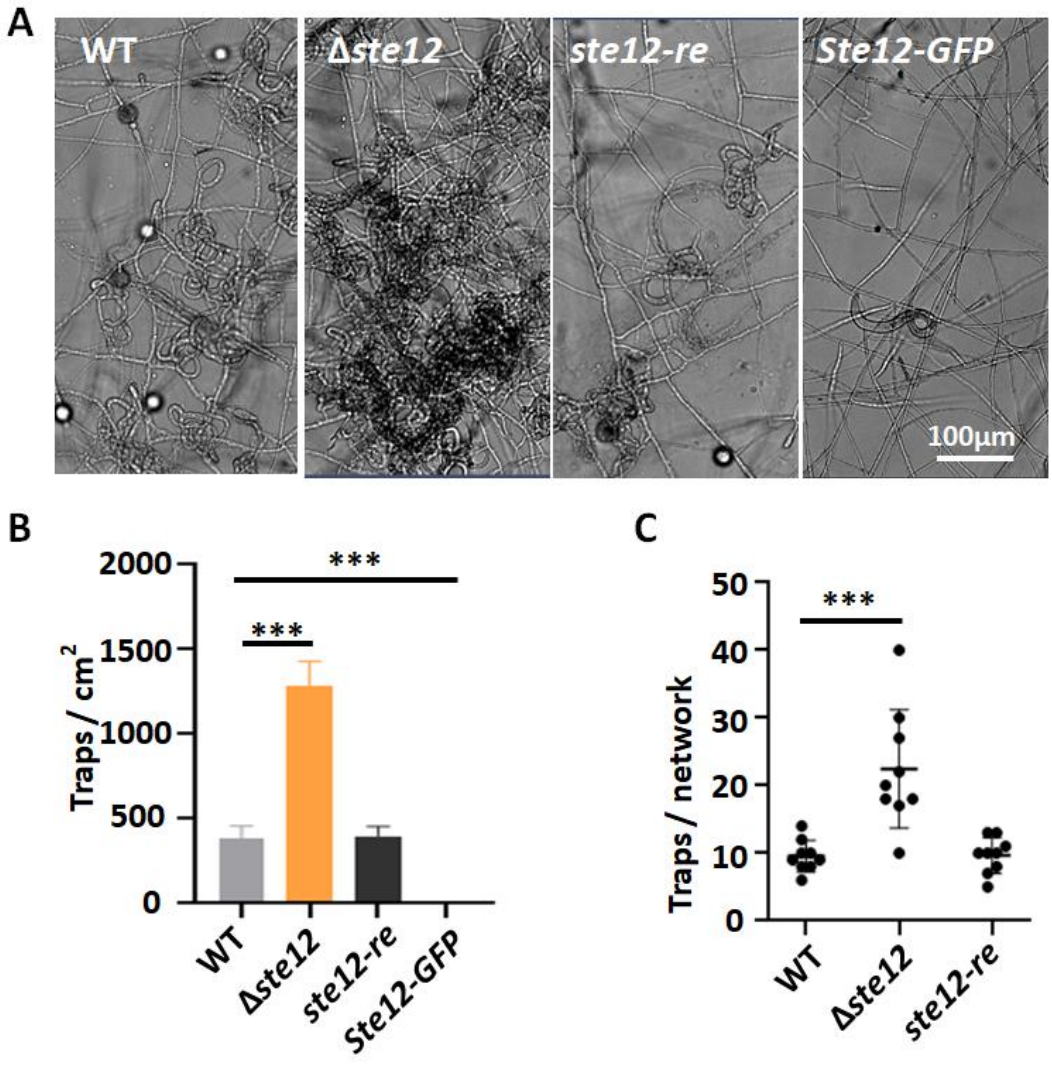

Fig. 21: The effect of *ste12* expression on trap morphogenesis. (A) Microscopic observation

of trap productivity of wild type, the Δ*ste12*-deletion, the *ste12* re-complemented (*ste12 re*) and *ste12*-GFP strain. Scale bar, 100 µm. **(B)** Quantification of trap number produced by indicated strains. Conidia were spread on the LNA slides for overnight and around 300 *C. elegans* were added on the growing hypha and co-incubated for 16h in the dark. The trap number was calculated under an optical microscope. WT vs. the Δ*ste12*-deletion strain, p-value = 0.001; WT vs. the *ste12-GFP* strain, p-value = 0.001. Error bar indicates standard deviation of technical triplicates. **(C)** Quantification of mean trap number in one network. p-value = 0.001. **p < 0.01, ***p < 0.001.

2.5.4 The transcriptional factor Ste12 regulates the expression of *artA*

The next question was if Ste12 regulates *artA*-gene-cluster gene expression. This could explain the effect of *ste12* deletion on trap formation. To test this hypothesis, conidia of wild type and the Δ*ste12*-mutant strain were grown in liquid PDB for 2 days at 28° C. The substrate hyphae were harvested, RNA isolated and quantitative real time RT-PCR performed. The transcript abundances of *artA* cluster genes were examined. By comparison with wild type, the expression levels of *artA*, *artB*, *artC* and *artD* in hyphae of the Δ*ste12*-deletion strain were significantly reduced **(Fig. 22A)**. The down-regulation of the *artA* cluster in the Δ*ste12*-mutant strain suggests decreased production of arthrosporols. Therefore, the inhibition by arthrosporols was reduced so that plenty of traps were formed. It indicates that Ste12 acts upstream of *artA* gene cluster and activates the arthrosporols biosynthetic pathway.

It was reported that *artA* expresses highly in uninduced hyphae to inhibit trap production, after 6 hours induction with nematodes the transcript abundance was decreased to enable the formation of traps, and when the traps are well formed and nematodes digested after 24 h, the expression levels turned up again to inhibit the production of too much traps (Yu *et al*., 2021). According to this, I assumed that the extensive trap networks in Δ*ste12*-null strain were formed because Ste12 limits the number of traps in trap networks. To prove this, I studied the expression levels of *artA*-cluster genes in the Δ*ste12*-deletion strain. Conidia of Δ*ste12*-mutant strain were inoculated on cellophane for overnight incubation, and nematodes added for induction for 6 h, and 24 h respectively. The mycelia were collected and processed for quantitative RT-PCR. As a result, after 6 h of induction, the expression levels of the *art* genes were down regulated in contrast to uninducted mycelia, and after 24 h, the expression was still significantly lower than the uninduced time point **(Fig. 22B)**. There results suggest that Ste12 transcription factor regulates the expression level of the *artA*-cluster-gene in order to control the formation of proper amount of traps.

As for the correlation of Ste12 with GasA and GasB, the expression level of *ste12* was not significantly influenced by the lack of any G-alpha subunit (not shown). The G-protein signaling pathway might regulate the activity of Ste12 by phosphorylation, which needs to be further proven.

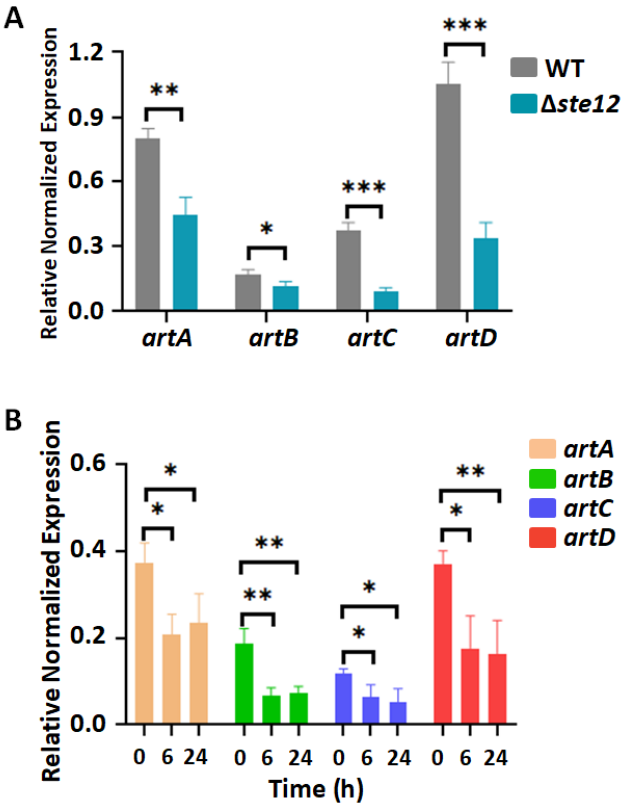

Fig. 22: The involvement of Ste12 in the regulation of expression of *artA* gene cluster. (A) The relative expression levels of *artA* cluster (*artA*, *artB*, *artC* and *artD*) in wild type and the Δ*ste12*-deletion strain. Expression data were normalized to actin. 10^5 conidia were inoculated in PDB liquid medium and incubated for 2 days in the dark at 28° C. The mycelia were harvested and processed for quantitative real time RT-PCR. *artA* WT vs. the Δ*ste12*-deletion strain, p-value = 0.003; *artB* WT vs. the Δ*ste12*-deletion strain, p-value = 0.040; *artC* WT vs. the Δ*ste12*-deletion strain, p-value = 0.000; *artD* WT vs. the Δ*ste12*-deletion strain, p-value = 0.001. **(B)** The transcript abundances of four genes in *artA* gene cluster in un-induced and induced mycelia of the Δ*ste12*-deletion strain. 10^5 conidia were spread evenly on the cellophane membrane on thin LNA medium for 24 h, and 50,000 *C. elegans* in mixed stages collected from 7-day-old NGM plates were applied to the growing hypha for co-incubation for indicated time at 28° C. The mycelia were scraped from the cellophane membrane and RNA isolated of. Error bar indicates standard deviation of technical triplicates. *artA* 0 h vs. 6 h, p-value = 0.011, 0 h vs. 24 h, p-value = 0.040; *artB* 0 h vs. 6 h, p-value = 0.006, 0 h vs. 24 h, p-value = 0.007; *artC* 0 h vs. 6 h, p-value = 0.036, 0 h vs. 24 h, p-value = 0.026; *artD* 0 h vs. 6 h, p-value = 0.013, 0 h vs. 24 h, p-value = 0.012. *p < 0.05, **p < 0.01, ***p < 0.001.

2.6 Dominant activation of Gα subunits

I attempted to overexpress *gas* genes to stimulate trap formation. *gasA* was expressed under the control of the constitutive *oliC* promoter in wild type (SXD46). However, the amount of traps was reduced rather than increased. The G-proteins were successfully activated by site-directed mutagenesis in several filamentous fungi

causing deficient GTPase activity, so it was tried as well in *gasA* and *gasB* of *A. flagrans* (Regenfelder *et al*., 1997; Zuber *et al*., 2002; Kraakman *et al*., 1999). The directed sites for mutagenesis of *gas* genes were taken from the examples of dominant activation including Gpa2^{G132V}, GasA^{G42R} from *S. cerevisiae* and *Talaromyces marneffei* and Gpa3^{Q206L} in *U. maydis* (Regenfelder *et al*., 1997; Zuber *et al*., 2002; Kraakman *et al*., 1999). By alignment the amino acid sequences of GasA and GasB behaved conserved with G α subunits reported above. G^{42} from GasA and G^{45} from GasB are homologous to G^{132} of Gpa2 in *S. cerevisiae* and G^{42} of GasA in *T. marneffei*, and Q^{204} in GasA and Q^{208} in GasB are conserved with Q^{206} of Gpa3 from *U. maydis* **(Fig. 23A, B)**. To this end the sites were directly mutated based on the mutation examples in other fungi, which was performed with site mutated primers and the Gibson Assembly, generating the strains of GasA^{G42R} (SXD95), GasB^{G45R} (SXD96), GasA^{Q204L} (SXD97) and GasB^{Q208L} (SXD98).

Then the mutagenesis cassettes were transformed into the protoplast of wild type of *A. flagrans*. Unexpectedly the site mutated strains did not produce a plenty of traps but less amount. And the decreased level depended on different transformant strains. It might be due to different copy numbers integrated in the genome. The correct sites in *gas* genes of *A. flagrans* need to be identified.

Fig. 23: Site directed mutagenesis of GasA and GasB. (A) Alignment of conserved amino acid sequences of G-alpha proteins in *A. flagrans* (Af), *S. cerevisiae* (Sc), *T. marneffei* (Tm) and *U. maydis* (Um). And the sites for mutation, GasA^{G42R} and GasB^{G45R} (in yellow frame) of *A. flagrans* (AGA was used as the Arginin codon), Gpa2^{G132V} of *S. cerevisiae* and GasA ^{G42R} of *T. marneffei* (in red frame). **(B)** The site mutagenesis of GasA^{Q204L} and GasB^{Q208L} of *A. flagrans* (TTG was used as the Leucine codon) (in yellow), and Gpa3^{Q206L} from *U. maydis* (in red).

2.7 The G-protein β subunit GbsA is required for trap formation

It was reported that in the nematophagous fungus *A. oligospora*, the G-β subunit

Gpb1 is essential for ascarosides sensing and trap formation (Yang *et al*., 2020). The question was if the orthologue in *A. flagrans* also possesses a similar function. By blast in NCBI, a homologous gene *dfl_004756* of *A. flagrans* was identified and named as *gbsA* (G-protein beta subunit A). The gene was disrupted by homologous recombination as described for the other deletion strains. To construct the deletion cassette, left border, hygromycin and right border were amplified individually, with primers gbsA LB_pjet_ol_for, gbsA LB_H_ol_rev, H_ gbsALB_ol_for, H_ gbsARB_ol_rev, gbsARB_H_ol_for and gbsARB_pjet_ol_rev. The Δ*gbsA*-deletion strain was confirmed by PCR confirmation with the ORF primers of gbsA_ORFin_for and gbsA_ORFin_rev, and the knockout verification primers of gbsAko_up_for and gbsAko_down_rev (SXD94). Interestingly a similar trap morphogenesis was discovered in the Δ*gbsA*-deletion strain. There was strongly defect in trap formation **(Fig. 24)**. But for the trap forming ability, the microscopic picture of the Δ*gbsA*-deletion strain presented mycelia with various curves. The curly hyphae might indicate the additional role of GbsA.

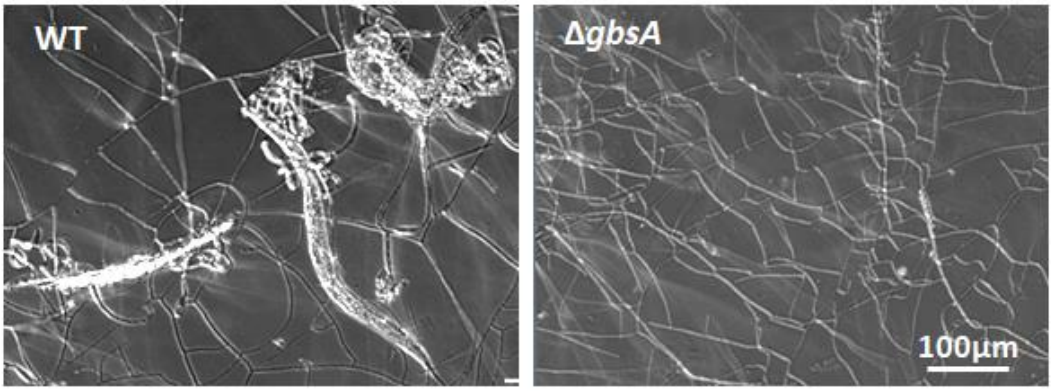

Fig. 24: The microscopical visualization of trap productivity of wild type and the Δ*gbsA*-deletion strain. Scale bar, 100 µm. Conidia were inoculate on the LNA media for overnight incubation and followed by addition of nematodes for another overnight incubation.

2.8 GprC senses ascarosides and may be obtained by horizontal gene transfer

2.8.1 Identification of conserved putative GPCRs

Many of the G-protein coupled receptors were identified in plenty of microorganisms including *S. cerevisiae*, *A. nidulans*, *A. fumigatus*, *N. crassa*, *A. oryzae*, *M. grisea* and *C. neoformans* (Lafon *et al*., 2006; Dos Reis *et al*., 2019; Xue *et al*., 2006; Borkovich *et al*., 2004; Jung *et al*., 2016 Kou *et al*., 2017). Among the survey of genes encoding seven-transmembrane domain containinG-proteins, more than 100 genes were identified in *A. flagrans*. As a first step, the receptors of nine classical groups of *A. nidulans* and *S. cerevisiae* were used as baits to identify the homologues in the genome of *A. flagrans* **(Table 1)** Class I includes GprA (DFL_009538) that is similar to

the Ste2-like pheromone receptor GprA in *A. nidulans* however GprB from *A. nidulans* has no homologue in *A. flagrans*. The class III includes GprB (DFL_005837), GprD (DFL_007781) and GprC (DFL_001370), in which the former two putative receptors are similar with Gpr1 in *S. cerevisiae*, and GprC is homologous to Gpr4 of *Neurospora crassa*. GprF (DFL_008204), GprG (DFL_000166) and GprJ (DFL_008382) are the homologues of three putative nutrient receptors in class IV from *A. nidulans*. With the baits of GprF and GprJ of *A. flagrans*, GprF1 (DFL_002229) and GprJ1 (DFL_000712) were identified individually. Only GprH (DFL_002583) was found belonging to cAMP receptor group but no any RGS domain containing homologue was identified. VII group contains GprM (DFL_004146) putatively. GprO (DFL_004609) and GprP (DFL_007848) were assumed to be Haemolysin III related sensors since each has a HlyIII domain and similar to those in *A. nidulans*. Lastly NopA (DFL_008784) was proposed to be involved in light sensing since it is homologous to NopA in *A. nidulans*.

Table 1: List of GPCR candidates of *A. flagrans.*

GPCR classification	**Domain**	***S. cerevisiae***	***A. nidulans***	***A. flagrans***
I Ste2 like pheromone receptor	Ste2	Ste2	GprA (PreB) AN2520	GprA DFL_009538
II Ste3 like pheromone receptor	Ste3	Ste3	GprB (PreA) AN7743	--
III Carbon receptor	7tm (Git3)	Gpr1	GprC AN3765 GprD AN3387 GprC AN9199	GprB DFL_005837 GprC DFL_001370 GprD DFL_007781
IV Putative nutrient receptor	PQ loop	SCRG_01312 SCRG_02823 SCRG_00179	GprF GprG GprJ AN5720	GprF DFL_008204 GprF1 DFL_002229 GprG DFL_000166 GprJ DFL_008382 GprJ1 DFL_000712
V cAMP receptor	7tm		GprH AN8262 GprI GprL	GprH DFL_002583
VI RGS domain containing receptor	RGS		GprK AN7795	--
VII --	7tm		GprM AN6680 GprN AN5508	GprM DFL_004146
VIII Haemolysin III related proteins	HlyIII		GprO AN4932 GprP AN5151	GprO DFL_004609 GprP DFL_007848
IX Microbial Opsin	7tm Opsin-1		NopA AN3361	NopA DFL_008784

2.8.2 Deletion and characterization of *gprC*

Based on the quantitative real time RT-PCR, the transcript abundance of *gprC* was significantly higher in mycelia induced by *C. elegans* for 6 h than it of uninduced. It indicated that GprC is a nematode-induced receptor **(Fig. 25A)**. To characterize its function to trap regulation, the gene *gprC* was disrupted by homologous recombination with the resistance gene hygromycin (SXD57) **(Fig. 25C)**. The primers used for amplification of the flanking regions left border, right border and the resistance cassette are GprCLB_pjet_ol_for and GprCLB_H_ol_rev, GprCRB_H_ol_for and GprCRB_pjet_ol_rev, and H_GprCLB_ol_for and H_GprCRB_ol_rev. The deletion cassette was introduced into protoplast of wild type for homologous recombination. Transformants were confirmed with PCR amplification and Southern blot. The primers of GprCORF_for and GprCORFin_rev were used for the verification of the absence of the ORF in the Δ*gprC*-deletion strain. And GprCko_up_for, Hyg_rev, Hyg_for and GprCko_down_rev were employed for the detection of the integration of the deletion cassette in the right location of the genome **(Fig. 25C, D)**. For the Southern blot, the genome of wild type and the Δ*gprC*-deletion strain was digested by the restriction enzyme *Eco*RV and the fragment right border was taken as probe. By blotting, the different bands from wild strain and Δ*gprC*-mutant strain were detected, confirming the mutant genotype.

The productivity of trap networks of the Δ*gprC*-deletion strain was measured. By growing conidia on low nutrient agar for 4h, *C. elegans* was added to the hyphae for co-culture. After incubation for 24 h, the slide was taken out and observed under the optical microscope. The number of traps was calculated. The Δ*gprC*-null strain displayed a reduced trap number compared to wild type **(Fig. 25B)**. In order to confirm the deficiency was due to the lack of the *gprC* gene, a re-complemented strain (*gprC-re*) was constructed by introducing a wild-type copy into the Δ*gprC*-deletion strain G418 as a selection marker. The normal ability of trap morphogenesis was restored in the *gprC-re* strain **(Fig. 25B)**. Overall, the nematode-activated expression level of *gprC* and trap defect in the Δ*gprC*-deletion strain indicated that the receptor GprC is involved in trap production and probably ascaroside sensing.

G-protein coupled receptors normally interact with G-alpha subunits. To manifest the connection between GprC and GasA and/or GasB, a yeast two hybrid assay (Y2H) was performed in the *S. cerevisiae* strains AH109 and Y187. A receptor normally anchors at the plasma membrane, but Y2H happens in the nuclei. The binding of GPCR and G-alpha proteins is mediated by the third intracellular loop and the C-terminus (Brown *et al*., 2018; Ansari *et al*., 1999; Yun *et al*., 1997). The transmembrane helices were predicted by the online server TMHMM-2.0. Only the cDNA of 3rd cytoplasmic loop and the N-terminal tail of GprC were used in this experiment for the combination with GasA or GasB subunits. Unfortunately the haploid yeast strains can grow on the LW plates (leucine$^-$, tryptophan$^-$) but not on the selective TDO plates (leucine$^-$, tryptophan$^-$, histidine$^-$) (not shown). It indicated that there was no protein

interaction between loop 3 or tail 4 with GasA or GasB. The failure might because the interaction with GasA or GasB needs the oligomeric structure formed by the 3rd inner loop and the tail (Xue *et al.*, 2006). It also might due to the incorrect prediction of secondary structure of GprC.

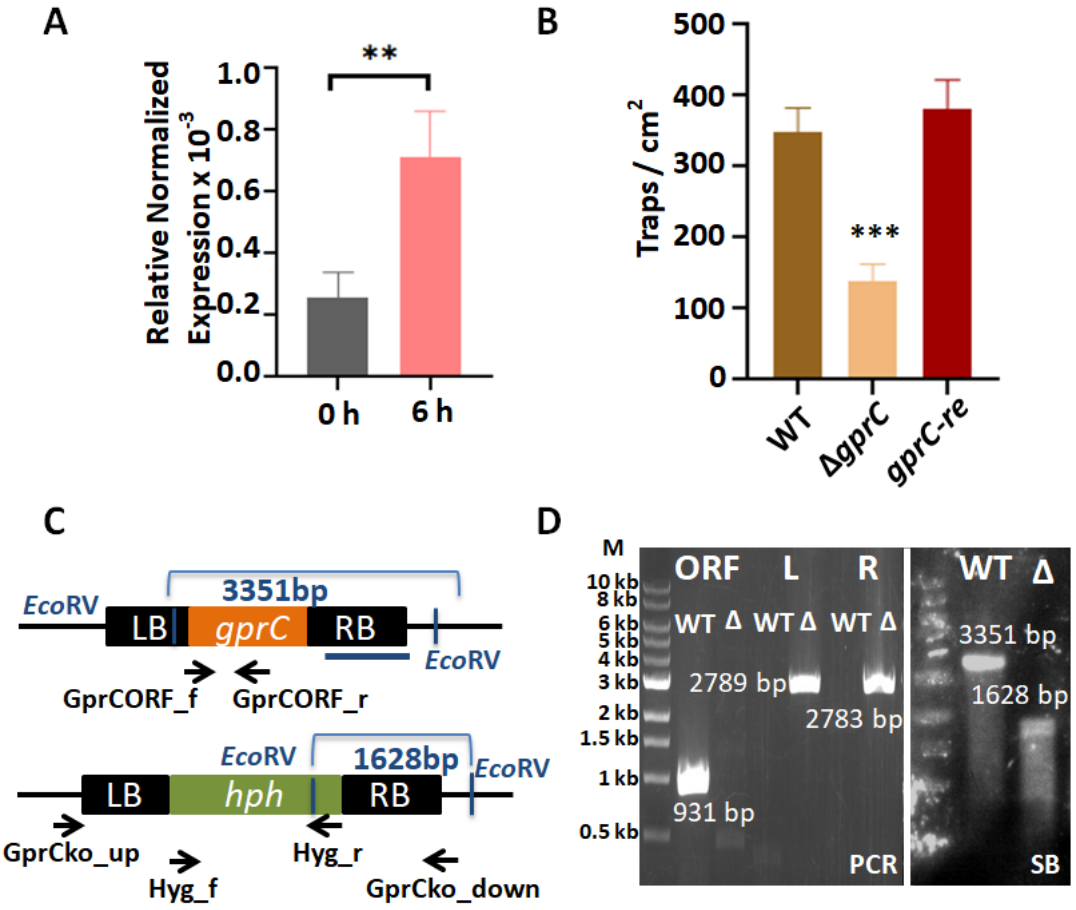

Fig. 25: Analysis of the GprC receptor (A) The expression levels of *gprC* in uninduced (0 h) and induced mycelia (6 h). Conidia of wild type were inoculated on cellophane membrane on LNA media for 24 h, and 50,000 *C. elegans* were collected from seven-day-old NGM plates and applied to the growing mycelia for co-incubation for 24 h. The mycelia were harvested and processed for quantitative RT-PCR. Error bar indicates standard deviation of technical triplicates. p-value = 0.010. **(B)** Quantification of trap numbers produced by wild type, the Δ*gprC*-deletion and the re-complemented strain (*gprC-re*, SXD62). 10^4 conidia of indicated strains were inoculated on LNA agar for 4 h and 300 *C. elegans* were added to the germinating conidia for overnight co-culture. Trap numbers were calculated under the microscope. p-value = 0.001 **(C)** Scheme of deletion of *gprC* by homologous recombination. The blue line indicates the probe for the Southern blot. Asterisks represent primers used for PCR confirmation. **(D)** Left: PCR amplification of the fragments indicated in (C) using genomic DNA of WT and the Δ*gprC*-deletion strain as template. PCR fragments were separated on a 0.8 % agaraose gel. Right: The Southern blot analysis of the fragments indicated in (C) using the right border of *gprC* as a probe and enzyme *Eco*RV for digestion of gDNA of wild type and the Δ*gprC*-deletion strain.

2.8.3 The receptor GprC behaves as an ascarosides sensor and may be obtained by horizontal gene transfer

Receptors of *C. elegans* that sense ascarosides were reported, including Daf-37, Daf-38, SRBC-64, SRBC-66, SRX-43, SRX-44, SRG-36 and SRG-37 (McGrath & Ruvinsky, 2019). However, there is no research about ascaroside-sensing receptors in fungi though multiple species of nematode-trapping fungi were characterized. Considering the co-evolution of nematodes and NTF and intimate relationship between them, it is reasonable that NTF have the ability to sense nematode-secreted pheromone ascarosides. Since the receptor GprC is essential for trap formation, I proposed that GprC is an ascaroside sensor. To prove it, the receptors in *A. flagrans* were aligned with other filamentous fungi, including carnivorous fungi and non-NTF. Surprisingly, GprC and the other two receptors in Carbon Receptor Class, GprB and GprD, presented obviously lower similarities with homologues in non-NTF even no homologous protein of three was found in some species, but high homology with other NTF was observed **(Fig. 27C)**. Receptors of other classes (GprF, GprO and NopA) showed an identical level in the correlation with either NTF or non-NTF. These results indicate that GprC and its class members are specific receptors in nematophagous fungi and their possible role of sensing ascarosides. All the three genes *gprB*, *gprC* and *gprD* were knocked out individually as described here and in a related master thesis (Mai, 2021). The Δ*gprC*-deletion strain displayed the biggest defect (50 %, **Fig. 27B**) in forming traps while each of the Δ*gprB*-deletion and the Δ*gprD*-deletion strains produced 75 % of traps. So GprC was chosen for the following research.

The role of the ascaroside-sensing receptor GprC stimulated the hypothesis that the *gprC* gene was transferred from nematodes to NTF during the co-evolution by horizontal gene transfer (HGT). To test the prediction, re-complementation experiments of the Δ*gprC*-deletion strain was performed with *C. elegans* receptors. It is known that GPCR localizes at the cytoplasmic membrane and harbors seven transmembrane domains. The N-terminal region and loops outside the membrane take a role of sensing ligands, and the cytoplasmic loop and the C-terminal tail interact with G-alpha subunits. In order to enable accurate interaction of receptors with *A. flagrans* Gas subunits, the C-terminus of GprC was maintained and fused with the N-terminus of nematode ascaroside-sensing receptors, generating chimeric sensory proteins **(Fig. 27A)**. The nematode GPCR *octr-1* which regulates longevity and immunity was used as negative control (Wibisono *et al*., 2021). To construct the chimeric protein, in the *gprC* plasmid used for re-complementation (left border-*gprC*-right border), the N-terminal region of *gprC* was replaced with the cDNA of the N-terminus of the nematode receptors. The construct was transformed into protoplast of the Δ*gprC*-deletion strain under the selection of geneticin418. Only ascaroside sensors SRBC-64, SRBC-66, DAF-37, DAF-38 and OCTR-1 were analysed in this experiment. SRX-43, SRX-44, SRG-36 and SRG-37 were not amplified successfully from cDNA perhaps due to low transcript abundance. I anticipated that the chimeric

proteins would rescue the defect in producing traps of Δ*gprC*-null strain. Surprisingly normal trap morphogenesis was restored in several re-complemented strains with the fusion proteins. *srbc-64-re* (SXD83) produced 611.95 ± 143.35 numbers of traps, *srbc-66-re* (SXD99) 489.28 ± 40.74 and *daf-38-re* (SXD84) 529.28 ± 170.23, which were in similar level as wild type (526.40 ± 51.25). However, *daf-37-re* (SXD82, 220.27 ± 52.19) and the negative control (183.15 ± 29.86) formed similar amount of traps as the Δ*gprC*-deletion strain (SXD85, 229.87 ± 36.01) **(Fig. 27B)**. The successful re-complementation suggests that GprC shares the same function as SRBC-64, SRBC-66 and Daf-38 of sensing ascarosides and is probably the homologue of those sensors. The genome of *A. flagrans* possibly obtained *gprC* by horizontal gene transfer from nematodes.

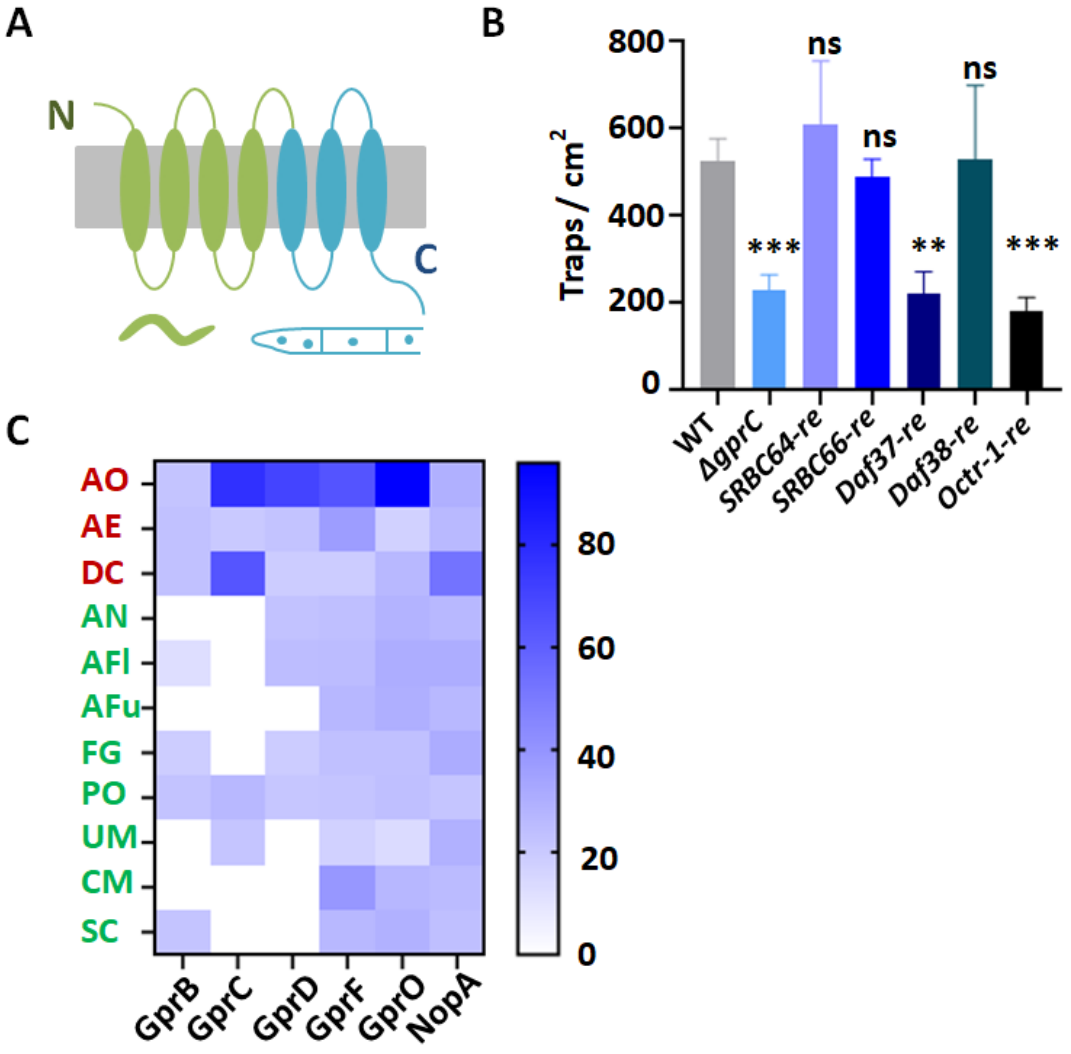

Fig. 27: Analysis of GprC as a NTF-specific GPCR and homology with nematode ascaroside receptors. (A) Schematic representation of the chimeric receptor formed by combining the N-terminus of ascaroside-sensing receptors of nematodes (SRBC-64, SRBC-66, Daf-38 and Daf-37) with the C-terminus of GprC in *A. flagrans*. The green color shows the origin of *C.elegans* and the blue color of *A. flagrans*. **(B)** Quantification of trap numbers in indicated strains. The chimeric protein was expressed in the Δ*gprC*-mutant strain for

re-complementation. *SRBC-64-re*, *SRBC-66-re*, *Daf-38-re*, *Daf-37-re* and *Octr-1-re* (SXD85) indicate the re-complemented strains by expressing respective chimeric proteins. Error bar indicates standard deviation of technical triplicates. Asterisks indicate the significance in trap productivity of re-complemented strains compared to wild type. Δ*gprC*, p-value = 0.001; *SRBC-64-re*, p-value = 0.386; *SRBC-66-re*, p-value = 0.382; *Daf-38-re*, p-value = 0.979; *Daf-37-re*, p-value = 0.002; *Octr-1-re*, p-value = 0.001. **(C)** The heat map of similarities between the receptors in *A. flagrans* (GprB, GprC, GprC, GprF, GprO and NopA) and the homologues from the other fungi including nematode-trapping fungi *A. oligospora* (AO), *A. entomopaga* (AE) and *Dactylella cylindrospora* (DC), which are labeled in red color, and the non-NTF *A. nidulans* (AN), *A. flavus* (AFl), *A. fumigatus* (AFu), *F. graminearum* (FG), *Pyricularia oryzae* (PO), *Ustilago maydis* (UM), *C. neoformans* (CN) and *S. cerevisiae* (SC) written in green. Values at the right represent the homology index.

2.9 The characterization of the regulators of G-protein (RGS)

The regulators of G-proteins are believed to inhibit G-alpha subunits (Li *et al*., 2007). In the nematode trapping fungus *A. flagrans*, four *rgs* genes were identified by alignment using the *rgs* gene in *A. nidulans flbA*, *rgsA*, *rgsB* and *rgsC* as a bait (Han *et al*., 2004), namely *rgs1* (*dfl_002387*), *rgs2* (*dfl_000272*), *rgs3* (*dfl_005207*) and *rgs4* (*dfl_007421*) respectively.

In order to analyze the role of RGSs in *A. flagrans* in regulating Gas proteins and trap morphogenesis, the four genes were over-expressed under the constitutive *oliC* promoter with the selection marker of hygromycin, generating four over-expressing strains *rgs1-oe* (SXD86), *rgs1-oe* (SXD87), *rgs1-oe* (SXD88) and *rgs1-oe* (SXD89) individually. If RGSs inhibit G-alpha, the over-expression of *rgs* will constitutively inhibit the activation of Gas proteins so that trap production fails to be induced. Conidia of over-expressing strains were inoculated on LNA agar for incubation for 4 h, and *C. elegans* was applied to the germinated conidia for co-incubation for overnight to induce trap formation. Trap morphogenesis was still observed and no significant down-regulation in trap numbers occurred. The results indicate that RGS does not negatively regulate the activation of G-proteins in the nematode catching fungus *A. flagrans* and the role of RGS is probably diverse among different fungi.

2.10 Analysis of the effector protein PefD

2.10.1 The small effector protein PefD is induced by nematodes

A survey of the genome of *A. flagrans* for putative secreted proteins revealed many small-secreted proteins which are probably involved in fungal virulence toward nematodes (Youssar *et al*., 2019). The possibility as an effector was predicted by the server EffectorP (Sperschneider J *et al*., 2018). AmonG-proteins that meet criteria, a putative effector protein D (PefD, DFL_005559) was chosen for further analysis. It is

composed of 72 amino acids and harbors a signal peptide and a propeptide predicted with Prop 1.0 Server **(Fig. 28A)**. It does not contain any conserved domain and no report of its homologue was investigated. In order to figure out its relationship with nematodes, a quantitative real time RT-PCR in un- and induced mycelia was performed. Conidia of wild type were inoculated on cellophane membrane on LNA medium to grow 24 h, after that mixed stages *C. elegans* was applied to the germinated conidia for trap induction of 24 h. The uninduced mycelia were prepared by growing conidia on LNA for 48 h. Then mycelia were scraped off and processed for quantitative RT-PCR. As a result, the expression level of *pefD* in induced mycelia was significantly higher than in vegetative hyphae **(Fig. 28D)**. It indicated that the expression level of *pefD* is induced by addition of *C. elegans*. The induced mycelia are mix of traps and substrate mycelia since not every hypha produces traps upon the presence of nematodes. Therefore, a reporter assay with cellular resolution was performed. The promoter of *pefD* was fused with *h2b* and *mCherry* (SXD14). When pefD is activated, the red fluorescent signal will be observed in nuclei. Conidia of the strain *pefD(p)::h2b:mCherry* were inoculated on LNA and co-incubated with *C. elegans* for 24 h. Red signals were visualized in trap cells and hyphae around or in the nematodes **(Fig. 28B)**. In contrast, vegetative hyphae did not display observable signals. The fluorescent intensity in traps and substrate hyphae were measured by ImageJ. By comparison, intensities in induced hyphae are significantly higher than those in uninduced hyphae **(Fig. 28C)**. It indicated that *pefD* is specifically induced by nematodes and the induction only occurs in the nematode-attacking hypha.

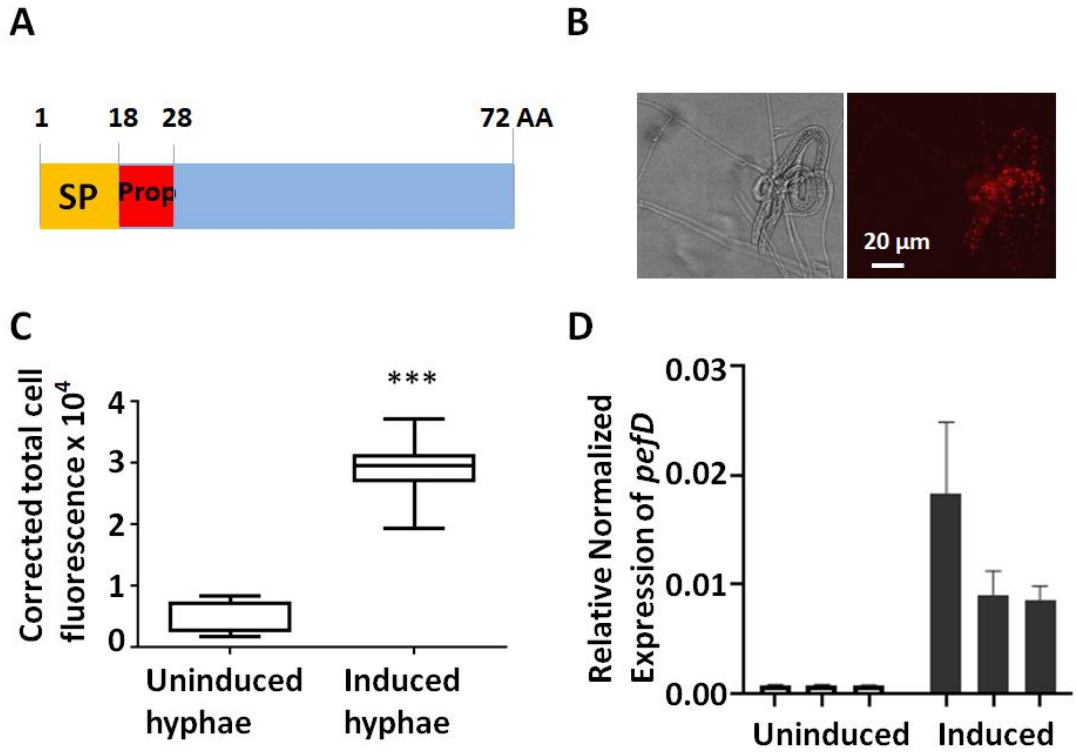

Fig. 28: Analysis of the putative effector protein PefD. (A) Schematic representation of the PefD protein. The 72 amino acid lonG-protein contains a predicted signal peptide (SP) and a

predicted propeptide (Prop). **(B)** Spatial observation of *pefD* expression in a transcriptional reporter assay. The *h2b-mCherry* fused protein was expressed under the control o the *pefD* promoter (SXD14). Conidia of the strain were incubated for 24 h and co-incubated with *C. elegans* for another 24 h before microscopy. Scale bar, 20 µm. **(C)** The average fluorescence of each nucleus of the reporter strain in un-induced and induced hyphae. Conidia were grown on LNA agar for 24 h with or without nematodes. For induced hyphae, pictures were taken of the trap cells (n = 26) while for uninduced hyphae, were of vegetative mycelium (n = 32). ImageJ was performed to measure the fluorescence. p-value = 0.000. **(D)** Expressional levels of *pefD* in *A. flagrans* of un- and induced mycelia normalized to actin. Biological triplicates are displayed respectively. The error bar means the standard deviation of technical triplicates. p-value = 0.024.

2.10.2 PefD is a secreted protein

In order to test the functionality of the signal peptide, *pefD* was fused with *lccC*, a laccase C encoding gene (*A. nidulans*), without the LccC signal peptide and expressed in *A. flagrans* under the control of the constitutive *oliC* promoter (SXD13). If the signal peptide of *pefD* works, the fusion protein PefD-LccC$^{\Delta SP}$ will be secreted out of hyphae. The laccase catalyzes the oxidation of ABTS (2, 2'-azino-bis (3-ethylbenzothiazoline-6-sulfonic acid)) to blue-green cation radical (Mander *et al*., 2006). Conidia of wild type and the strain *pefD::lccC*$^{\Delta SP}$ were inoculated on LNA plate containing ABTS (1 mM). After incubation for 2 days in the dark, the blue-green color was observed in the area of *pefD::lccC*$^{\Delta SP}$ strain while not in wild type **(Fig. 29A)**. It suggests that laccase fused to PefD was secreted out of cell into the agar and the predicted signal peptide works.

The next question was whether PefD is not secreted out of the traps when the signal peptide was deleted. To this end, *pefD* without the signal peptide was fused with a C-terminal *GFP* and expressed under *oliC* promoter control (SXD15). By introducing to wild type, the conidia and nematodes were incubated on LNA agar for 24 h. Green fluorescent signals were observed in hyphae, and signals were dispersed in cells **(Fig. 29B)**. It suggests that the fusion protein PefD$^{\Delta SP}$-GFP localizes in cytoplasm and fails to be secreted out.

By prediction of WolF PSORT, PefD without the predicted signal peptide and without the predicted propeptide localizes in nuclei. To test this, the strain *pefD*$^{\Delta SP\Delta Prop}$*-mCherry* was performed by fusing 29th-72nd amino acids of PefD with GFP. The construct was introduced to a strain (SNH14) containing *h2b-GFP* construct, generating the co-localization strain (SXD41). 200 *C. elegans* was used to induce trap production of the strain. Green signals are not over-lapped with red signals **(Fig. 29C)**. The propeptide is assumed to be clipped off the protein when it is in the nematode body. If the cleaved protein was poisonous to nematodes, it could also be unhealthy for fungal development. To confirm this, *pefD* without the propeptide was expressed in wild type (SXD38). By observation of vegetative growing on PDA plates, no defect was observed yet.

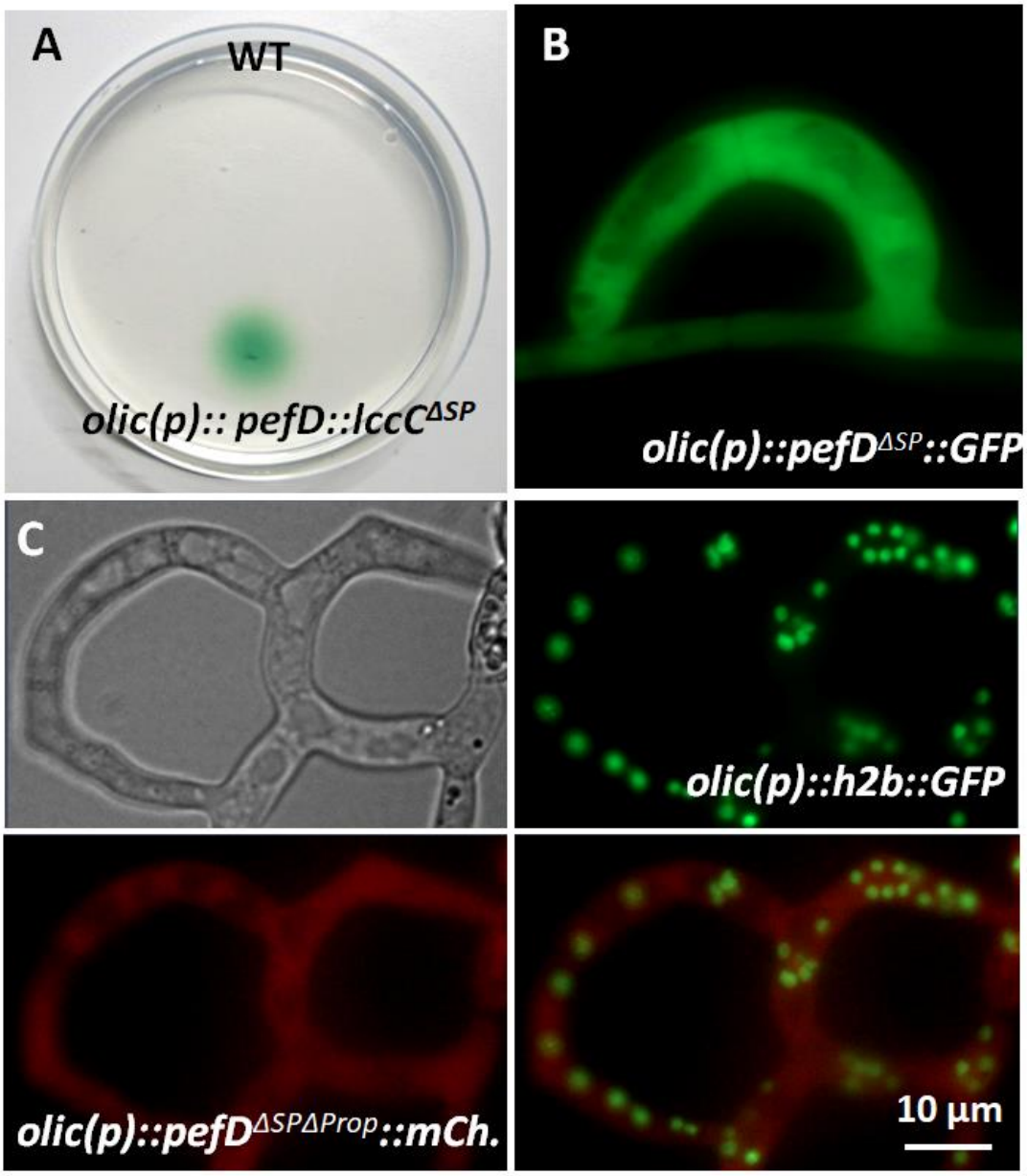

Fig. 29: Characterization of the secretion and localization of PefD. (A) Secretion assay. Wild type and the PefD-LccC expressing strain were incubated on LNA medium containing 1 mM ABTS for 2 days. **(B)** Microscopic observation of PefD$^{\Delta SP}$-GFP fused protein under the control of constitutive *oliC* promoter. **(C, D, E and F)** Localization analysis of PefD$^{\Delta SP\Delta Prop}$ fused with mCherry and H2B-GFP under *oliC* control. Scale bar, 10 µm.

2.10.3 PefD localizes in infection site during attacking nematodes

In order to study the role of PefD in trapping nematodes, *pefD* was fused with a C-terminal *GFP* gene and the construct expressed under the control of the *pefD* promoter. By introducing it into wild type, the strain *pefD(p)::pefD::GFP* was gained (SXD26). The conidia were inoculated on LNA agar for 4h of germination, after that *C. elegans* was applied on it for co-incubation for 24 h. By microscopical visualization, the green fluorescent signals were

observed in the infection site where trap penetrates the cuticle of nematode **(Fig. 30A, B)**. The specific localization of PefD-GFP fusion protein indicated that PefD involves in the penetration of hypha into nematode body.

Small, spot-like signals were visualized in the trap cell as well. In order to enrich the protein in traps for observation, the expression cassette *pefD-GFP* was introduced into wild type under the control of constitutive promoter (SXD24). By inducing the hyphae with *C. elegans*, traps were produced by *oliC(p)::pefD::GFP* strain. The green fluorescent signals occurred in traps and a cluster of signals were accumulated at the inner rim of the trap, indicating the fusion protein was being secreted from there **(Fig. 30C)**.

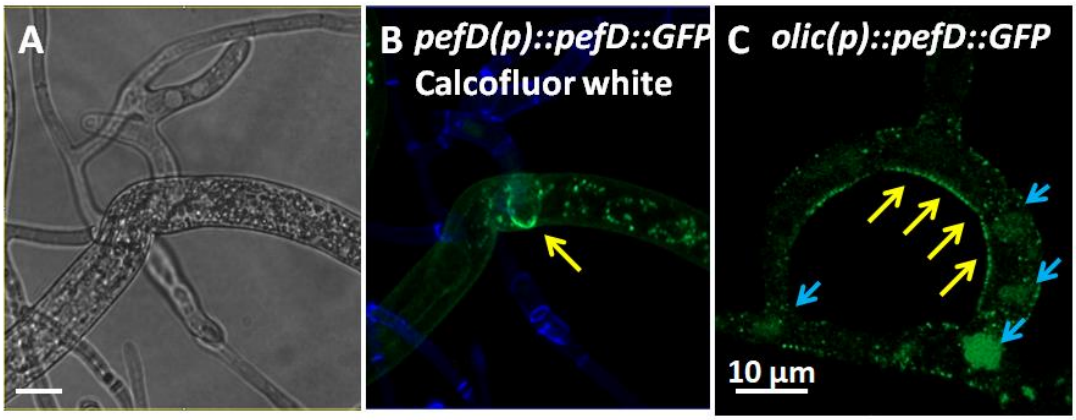

Fig. 30: PefD localizes at the penetration site during the attack. (A, B) The localization of PefD during trapping nematodes. The *pefD(p)::pefD::mCherry* expressing strain was co-cultured for 24 h at 28˚ C with *C. elegans*. The mycelia were stained with cell wall dye Calcoflour White. The arrow indicates the infection site where hypha enters nematode body. **(C)** The microscopical visualization of PefD-GFP localization under constitutive promoter. Yellow arrows indicate the accumulation of fluorescent signals at the inner rim of a trap cell. Blue arrows suggest the localization in vesicles. Scale bar, 10 µm.

2.10.4 Co-localization of PefD and other proteins

Several effector proteins in *A. flagrans* were studied including CyrA, NipA and HinA (Wernet *et al*., 2021a; Menzner, 2020; Wang, 2022). In order to figure out if they localize in the same sites as PefD, co-localization experiments were performed. The *pefD* gene was fused with *mCherry* and expressed under its own promoter for natural expression. The expressing construct was introduced into the *cyrA* gene expressing strain *cyrA-GFP* (SNH30), generating the co-expressional strain *cyrA::GFP + pefD::mCherry* (SXD28). By induction with *C. elegans*, the red and green signals were observed. Both signals were at the same sites during penetration into the nematode body **(Fig. 31A)**. Likewise, a strain (SXD30) for co-localization of PefD and NipA was performed by transforming the construct *nipA::mCherry* into *PefD* expressing strain (SXD26). But no overlap was visualized of red and green signals. PefD in green localized in infection site while NipA in red color in trap cells **(Fig. 31B)**. By co-expressing *pefD* and *hinA* (SXD33), overlap was observed by red signals of

HinA-mCherry and green of PefD-GFP, as the same as CyrA and PefD **(Fig. 31C)**.

In the observations of constitutive expressed *pefD*, some green signals occurred in vesicles apart from the accumulation at the trap borders (**Fig. 30C**). I assumed that the vesicles might represent endosome. To confirm if PefD localizes in endosome, a late endosome related gene (*dfl_008616*) in the genome of *A. flagrans* was identified by using *rab7* from *A. nidulans* as bait. Co-localization was performed by fusing PefD with GFP and Rab7 with mCherry under the control of the constitutive promoter (SXD34). After the induction of hyphae with *C. elegans* for overnight, the signals were observed under the fluorescence microscope **(Fig. 31D)**. Both, the red and green signals localized in big vesicles in vegetative hyphae (blue arrows) but not in traps. Green signals of PefD-GFP were observed in the margin of the trap cells (red arrow) while Rab7-mCherry appeared in big vacuoles (yellow arrow). The results indicate that PefD does not localize in vesicle represented by Rab7. Since Rab7 localizes in late endosomes and lysosomes (Bucci *et al*., 2000), the observed overlap of both proteins might indicate that the effector PefD is being degraded in lysosomes since it was expressed constitutively.

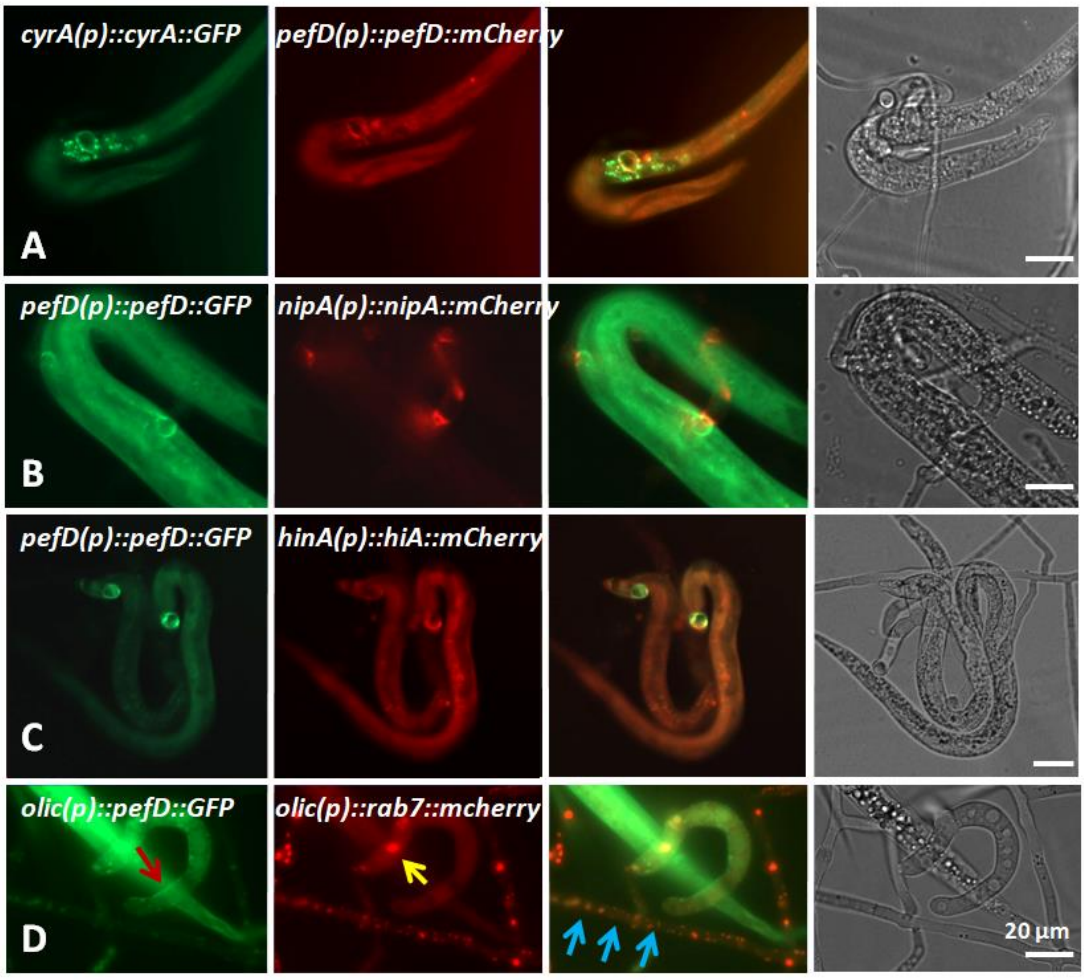

Fig. 31: Co-localization of PefD with other effector proteins and Rab7. (A) Overlapped co-localization of CyrA-GFP and PefD-mCherry under the promoters of *cyrA* and *pefD* individually. **(B)** Visualization of localization of PefD-GFP (*pefD*(*p*)) and NipA-mCherry

(*nipA*(*p*)). **(C)** The observation of *pefD(p)::pefD::GFP* and *hinA(p)::hinA::mCherry* in one strain during attacking nematodes. **(D)** Co-localization of PefD-GFP and Rab7-mCherry under constitutive *oliC* promoter. Red arrow indicates the PefD-GFP signal at the trap rim, yellow indicates signal of Rab7-mCherry in vacuole and blue arrows show the overlap of both signals in substrate hypha. Scale bar, 20 μm.

2.10.5 PefD is involved in nematicidal activity

It was confirmed that PefD is secreted from trap cell and accumulated in penetration site during attack against nematodes. In order to characterize its role in catching nematodes, the gene *pefD* was deleted by homologous recombination with the deletion cassette **(Fig. 32A)**. It is composed of left border, hygromycin and right border, which are amplified by the primers of 5559LB-pjet-ol-for, 5559LB-H-ol-rev, hyg_for, hyg_rev, 5559RB-H-ol-for and 5559RB-pjet-ol-rev. The deletion cassette was introducing in wild type and positive transformants were selected by PCR confirmation and Southern blot. Primers 5559ko_up_for and 5559ko_down_rev were used as the verification of accurate integration (2334 bp in WT and 3890 bp in the Δ*pefD*-deletion strain SXD35). The primers of 5559_ORF_for and 5559_ORF_rev were also employed for the detection of the ORF. Meanwhile right border of *pefD* gene was used as probe for the Southern blot and different lengths of bands were detected from gDNA of wild type (1669 bp) and the Δ*pefD*-deletion strain (3225 bp). No extra integration was detected, confirming the purity of the mutant **(Fig. 32C)**. By co-incubation for conidia and nematodes for 24 h in the dark, normal trap morphogenesis and prey attacking were observed in the Δ*pefD*-mutant strain. The penetration-site-expression indicates that PefD might take a role in penetrating or digesting. If the gene *pefD* was disrupted, the duration of penetration or digestion could be longer in Δ*pefD*-mutant strain than in wild type. To prove it, the virulence assay needs to be further performed.

To the same end, an over-expressing strain of *pefD* (*pefD-oe*, SXD37) was obtained by introducing a constitutively expressed *pefD* in wild type **(Fig. 32B)**. The extra integration (1910 bp) of over-expression was detected by Southern blot except for the gene *in situ* as wild type **(Fig. 32D)**. The ORF of *pefD* was employed as a probe. Conidia were inoculated on the LNA agar for 4 h growing, after that 300 *C. elegans* were added to the germinated conidia for trap induction. After hyphae arresting nematodes, microscopy was performed. Nematodes that are swimming or trapped have auto-fluorescence normally. But when they are fully digested and totally dead, the auto-fluorescence becomes obviously stronger. The amounts of alive and dead nematodes were quantified by the criteria of auto-fluorescent intensity. As a result, 30 and 38 nematodes in normal fluorescence were observed in co-incubation with WT and *pefD-oe* strain individually which are in the comparative levels. However, the over-expressing strain fully digested 44 nematodes (in strong auto-fluorescence) which were significantly more than wild type (10 nematodes). The larger amounts of dead nematodes indicate that *pefD-oe* strain has a stronger nematicidal activity.

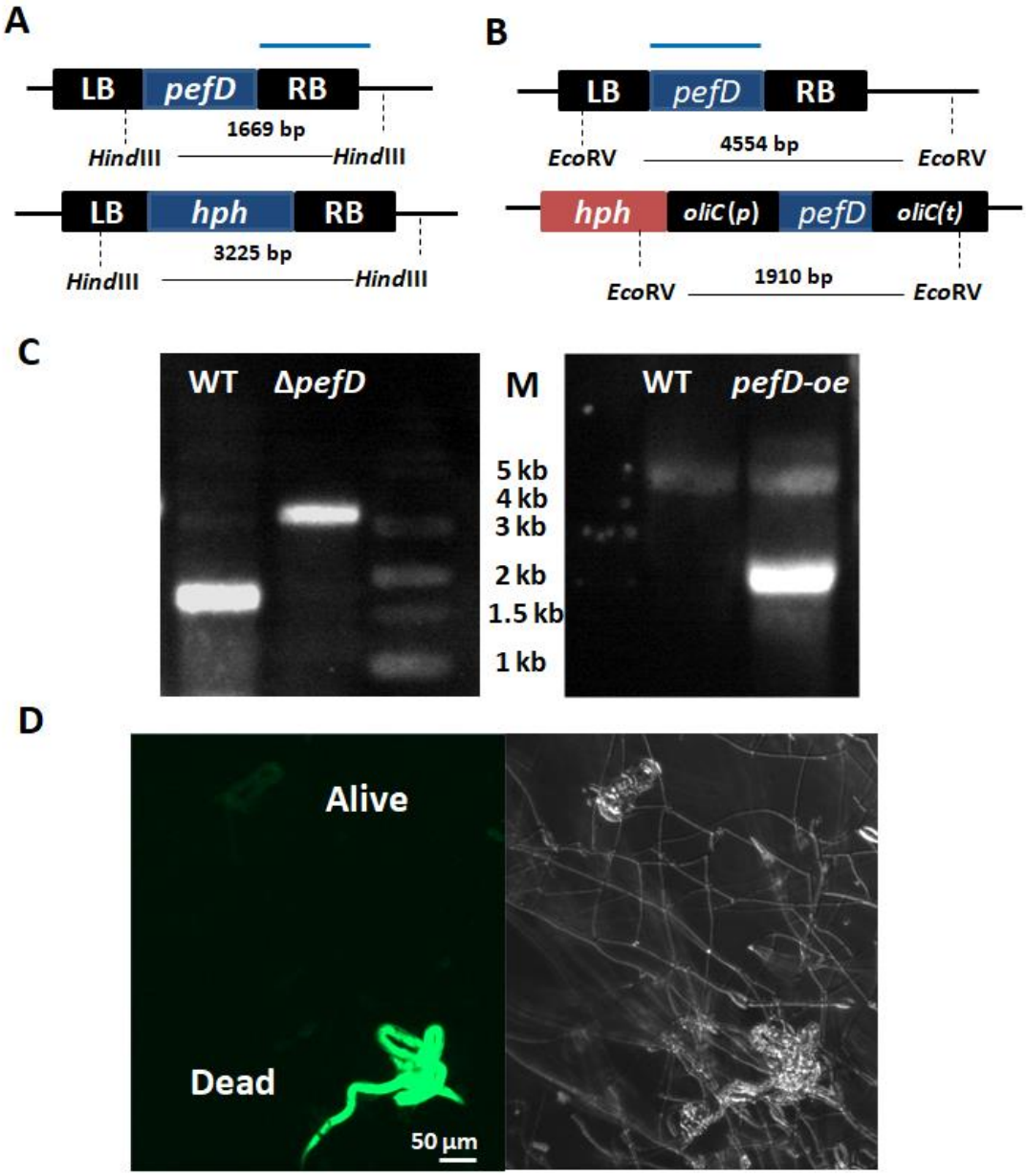

Fig. 32: Deletion and over-expressing strains of *pefD*. (A, B) Schematic representation of deletion (left) and over-expression (right) of *pefD* individually. Blue lines indicate probes for the Southern blot. *Hind*III and *Eco*RV were employed for digestion of genomic DNA of indicated strains. **(C)** Left: The Southern blot analysis of the fragments indicated in (A) using the right border of *pefD* as probe and enzyme *Hind*III for digestion of gDNA of wild type and the Δ*pefD*-deletion strain. Right: The Southern blot analysis of the fragments indicated in (A) using the ORF of *pefD* as probe and enzyme *Eco*RV for digestion of gDNA of wild type and the *pefD* over-expressing strain (*pefD-oe*). **(D)** The visualization of trapped (alive) and digested nematodes (dead). Scale bar, 50 µm.

2.10.6 Heterologous expression in *C. elegans*

In order to figure out the function of PefD in attacking nematodes and the potential target, pefD was expressed in *C. elegans*. To control its proper expression and keep the nematode from death, a heat inducible promoter *hsp-16.48* was used. The construct *hsp-16.48(p)::pefD::GFP::unc-54UTR* (WXD3) and the co-marker *myo-2p::tomato* were introduced into *C. elegans* as extra-chromosomal array. The control strain without *pefD* was generated (*hsp-16.48(p)::GFP*, WXD2). The positive nematode transformants were selected by observing a red head coming from the tomato signal. In order to activate the expression of *pefD*, the nematode strain was heat-shocked at 37˚ C for 2 h and the activation of promoter was checked under the fluorescent stereomicroscope. As a result, the GFP signals were equally distributed throughout the nematode body in both control strain and *pefD::GFP* strain **(Fig. 33)**. And no movement or shaped defect was observed by expressing *pefD*.

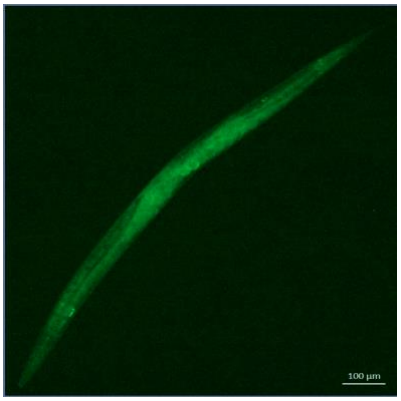

Fig. 33: Expression of *pefD* in *C. elegans*. The *pefD* gene with its signal peptide was fused to *GFP* and expressed under the heat inducible *hsp-16.48* promoter. The expression was induced by heat shock for 2 h at 37˚ C in the dark. Scale bar, 100 µm.

The fluorescent signals induced by heat shock were not consistent among different transformant worm strains, the constitutive all-tissue or specific-tissue promoters should be considered.

3 Discussion

G-protein signaling pathways perform multiple functions to regulate sexual and asexual development, pathogenicity, the production of secondary metabolites and stress responses in all filamentous fungi (Neves *et al*., 2002; Li *et al*., 2007; Yu, 2006; Lengeler *et al.,* 2000). One important component is the G-alpha subunits (Harashima & Heitman, 2004; Kwon-Chung *et al*., 1982). Therefore, it was assumed that G-protein signaling is important in the interaction of nematodes and NTF for sensing the presence of nematodes and the environmentally nutritional conditions for producing trap networks.

Three G-α subunits and one G-β subunit (Gpb1) were identified in *A. oligospora*, and the deletion strain of *gpb1* exhibited strong defects in trap morphogenesis (Yang *et al*., 2020). Gpb1 acts upstream to activate the Fus3 MAPK cascade by phosphorylation to enable trap formation (Chen *et al*., 2021). However G-alpha subunits (Gas) are not characterized yet in NTF. In this work I studied first the role of G-α subunits in the nematode-catching fungus *A. flagrans*. Two Gas proteins showed important roles in trap production in the interspecies interaction. Besides the G-alpha subunits, the G-beta subunit, the upstream GPCRs and downstream signaling components were studied which are all involved in the regulation of the *artA*-gene cluster. My results allow reconstructing a complete signaling cascade from the sensing of ascarosides to the repression of the arthrosporol biosynthesis. The GprC receptor senses ascarosides and activates the Gas proteins. The activated Gas-GTP complex or the G-βγ dimer passes the signal to downstream cascades including the cAMP-dependent signaling pathway. And the expression of the *artA*-gene cluster is inhibited, leading to less production of arthrosporols. The trap-inhibiting effect from arthrosporols is released, enabling trap morphogenesis. This work displays an intensive and elaborate research of the involvement of the G-protein signaling pathway for the interactions of *A. flagrans* with nematodes and should be a valuable significance for other nematode trapping fungi.

3.1 An interplay of low-molecular weight compounds derived from NTF and nematodes

In the recent decade, research about the participation of secondary metabolits in interactions between NTF and nematodes are arising and attractive (Hsueh *et al*., 2013; Xu *et al*., 2015; Hsueh *et al*., 2017). The trap structure is one of the most important indicators of shifting from saprotrophic to the predatory lifestyle in the nematode-trapping fungi. It can be induced by several nematode-derived pheromones, the ascarosides, which are secreted and employed for developmental processes by nematodes (Hsueh *et al*., 2013). In turn, carnivorous fungi secrete appealing volatile compounds to lure nematodes to enter traps (Hsueh *et al*., 2017).

Arthrosporols are NTF-derived compounds and are produced during saprptrophic growth of fungi. NTF secrete arthrosporols to inhibit trap production. When nematodes are lured by attractive substances, they will come near hyphae. At this time, the fungus senses the presence of the prey, and hyphae will turn down the secretion of trap-inhibiting arthrosporols. The trap inhibition from these substances is released and traps are formed by the fungus. In this work, enriched ascarosides were used to induce trap formation, which is direct evidence that these are the effective nematode molecules. The isolated ascarosides suppress the expression of the *artA* cluster. Genes in the cluster encode enzymes including polyketide synthase to synthesize arthrosporols. The differences in expression levels were not significant since upon the induction of nematodes the colony is mixed with traps and the substrate hyphae. However, the reporter assay of *artA* showed downregulation of expression specifically in trap structures. It demonstrated that the trap-inhibiting arthrosporols are suppressed by nematode-derived ascarosides. Ascarosides are important for developmental processes of *C. elegans*. Therefore, they cannot just be modified to escape the recognition by the fungus. In evolution there is always a race between the two partners. If the fungus recognizes a nematode molecule, nematodes would have an advantage in which the molecule is not produced anymore or modified.

3.2 Gas proteins enable trap formation by suppressing the *artA* cluster

I hypothesized that the G-protein signaling pathway sensens ascarosides to regulate the expression of the *artA*-gene cluster. The prediction is well confirmed by the study in the G-protein dependent signaling pathway in *A. flagrans*. As the uppermost components of G-protein signaling pathway, Gas proteins exhibit important functions on the predatory lifestyle of *A. flagrans*. In wild type of *A. flagrans*, the presence of nematodes or enriched ascarosides can be sensed by G-protein signaling pathway, and the signal is transferred into the cell in order to suppress the expression of the *artA* cluster to enable trap formation. It is proven by both the detection of the expressional levels of the *artA*-cluster genes and the microscopic observation of promoter activity of *artA*. However, in the Δ*gasA*-deletion strain, upon the induction of *C. elegans*, the transcript abundances of genes in the *artA*-cluster were similar to the ones in uninduced hyphae. This phenomenon is consistent to the reporter assay. *C. elegans*-induced hyphae of the Δ*gasA*-deletion strain showed intensive signals of the *artA* promoter reporter like uninduced hyphae. Likewise, the induction with enriched ascarosides displayed identical result in the reporter assay. It suggests that the Δ*gasA*-deletion strain does not respond to nematodes anymore. In contrast, when the Δ*gasB*-deletion strain was induced by nematodes, the expression of the *artA*-gene cluster genes was down-regulated. Therefore, the Δ*gasB*-deletion strain still has the ability to sense ascarosides to induce the biological responses. Although the Δ*gasB*-deletion strain can still respond to the presence of nematodes, it is deficient in trap production and nearly produced half the number of traps compared to wild type. Further experiments found that GasB suppresses the expression of the

artA gene cluster. In substrate hyphae of the Δ*gasB*-deletion strain, obviously higher expression levels of the *artA* gene cluster genes were detected compared to wild type. Higher expression leads to more secretion of the product arthrosporols of the *artA* gene cluster. More trap-inhibiting substances, arthrosporols, lead to stronger inhibition to trap formation upon the induction by nematodes. That answers why the Δ*gasB*-deletion strain responded to nematodes but produced less traps. The Δ*gasB* Δ*artA*-double deletion strain produced much more traps than wild type, suggesting the strong inhibiting effect in the Δ*gasB*-deletion strain is released by the deletion of *artA.* It demonstrated that GasB suppresses the role of the *artA*-gene cluster.

It seems that both GasA and GasB suppress the inhibitory role of ArtA and contribute to trap formation, but their underlying mechanisms are different. As the biological responses to the presence of nematodes and the inducing substances ascarosides, wild type turns down the expression of the *artA* gene cluster and forms traps. When *gasA* is deleted, the fungus can not sense nematodes so that can not make any responses of becoming a predator, no matter how many nematodes are added. When *gasB* is deleted, the fungus can still sense nematodes but the expression of the *artA*-gene cluster is still high. The concentration of arthrosporols, however, probably does not reach the threshold that entirely inhibits trap formation, and traps are formed in lower amounts. To conclude, GasA plays a role as an on-off shutter of predatory ability. The shift from saprotrophic to predatory lifestyle needs the functionality of GasA, while GasB acts as a negative regulator of arthrosporols production to facilitate trap formation. GasB maintains arthrosporols in a proper concentration in order to keep a balance between two types of lifestyles. Both Gas proteins work for production of trap networks.

3.3 Central signaling pathways downstream of G-proteins

In *A. oligospora*, G-beta subunit acts upstream of the FUS3-MAPK cascades to regulate trap formation, and all deletion strains of *gpb1* (G-β encoding gene), *ste7* (a MAP kinase kinase encoding gene) and *fus3* (a MAP kinase encoding gene) display defects in trap morphogenesis (Chen *et al*., 2021). The question if Gas proteins in *A. flagrans* pass through this signaling as well was considered. The deletion strain of *makB* (the homologous gene of *fus3*) can produce traps, and the deletion strain of another MAPK encoding gene *makA* forms quite weak mycelia but still has trap morphogenesis (PhD thesis, Valetin Wernet, 2021). HogA in *A. oligospora* affects trap formation and the functionality of its homologous protein in *A. flagrans* remains unknown (Kuo *et al*., 2020).

The interactions between G-alpha subunits and cAMP-PKA signaling pathway are common in *S. cerevisiae* and filamentous fungi (Colombo *et al*., 1998; Alspaugh *et al*., 2002; Yang *et al*., 2016). G-α subunits regulate the enzyme adenylyl cyclase to produces the second messenger cAMP. I predicted that in *A. flagrans*, there is a same interaction. When Gas protein is activated, it regulates the putatively existing adenylyl cyclase to generate cAMP, and this molecule as a second messenger

regulates downstream cascades for biological responses. But if Gas is deleted, the extracellular signal can not be transformed into cAMP, and lower amount of cAMP fails to regulate downstream cascades. To confirm this, 8'-Bromo-cAMP (an analog of cAMP) was added exogenously on the Δ*gasA*-deletion and the Δ*gasB*-deletion strain individually. If the hypothesis is right, the additional analog would re-complement defects in mutants. Normal production of traps, pigment, conidia and aerial hyphae is restored in the Δ*gasB*-deletion strain by the introducing 8'-Bromo-cAMP. It demonstrates that GasB acts upstream of the cAMP-PKA signaling pathway. The recovery of the Δ*gasA*-deletion strain did not happen in this assay, suggesting GasA does not regulate the production of cAMP. In *Candida albicans*, the small GTPase Ras1 activates the adenylate cyclase Cyr1 directly, causing an increase in the intracellular level of cAMP (Leberer *et al*., 2001). There might be cross-talk between GTPase and dowenstream signaling in *A. flagrans*.

Interactions of GasA proteins with other signaling cascades were considered. In animals, phospholipase C commonly interacts with G-proteins (Rebecchi & Pentyala, 2000). In the filamentous fungus *B. cinerea*, the connection between a G-alpha subunit and the related calcineurin signaling pathway two components is found (Schumacher *et al*., 2008). But there are not many related reports among yeast and fungi. A Phospholipase C (PLC2) in *A. oligospora* regulates trap formation and other developmental processes but the interaction with G-proteins is not mentioned (Xie *et al*., 2022). Two homologous genes encoding PLCs, *plc1* and *plc2*, were identified in the genome of *A. flagrans*. No defect in trap formation was observed in the Δ*plc1*-deletion and Δ*plc2*-deletion strains. There might be redundancy upon functions of two PLCs. The nematode-induced signals passed from upstream G-proteins might be shared by two PLCs or with other signaling pathways as well. The sophisticated role as a predator of NTF is probably achived by cross-talks between several pathways including calcineurin, cAMP-PKA, MAP kinase dependent pathways.

In *S. cerevisiae*, the GPCR Gpr1p and G-alpha subunit Gpa2p are upstream components of the cAMP signaling pathway and regulate glucose sensing (Xue *et al*., 1998; Winderickx *et al*., 1999; Colombo *et al*., 1998). In *A. nidulans*, a homologous protein of Gpa2p, GanB, also mediates activation of the cAMP-PKA signaling in respond to glucose. The addition of glucose led to a rapid and transient increase in the level of intracellular cAMP (Lafon *et al*., 2005). As GasB regulates the generation of cAMP in *A. flagrans* as well, it is possible that GasB senses nutrients like glucose. It could be that GasA senses nematode-derived ascarosides and GasB senses glucose or nitrogen. The presence of nematodes and the lack of nutrient sources are the prerequisites for trap formation. Both G-alpha subunits together with their coupled receptors work for production of traps.

3.4 The transcriptional factor Ste12 regulates the *artA* cluster

The transcriptional factor Ste12 takes multiple functions in virulence, asexual sporulation and filamentous development (Chen *et al*., 2021; Bayram *et al*., 2012).

The transcriptome sequencing of the Δ*ste12*-deletion strain identified a putative polyketide synthase encoding gene (EYR41_000001) probably downstream of Ste12 (Chen *et al*., 2021). Since *artA* is also a polyketide synthase encoding gene, I considered it might be controlled by Ste12 in *A. flagrans*. Further experiments have confirmed my hypothesis, and raised the question about the role of Ste12 in the regulation of the *artA* gene cluster. When nematodes are around, G-proteins send signals of the presence of prey to inhibit the *artA* gene cluster. Traps will be formed. If *ste12* is deleted, much more traps are formed in the presence of nematodes. It indicates that Ste12 stimulates the expression of the *artA*-gene cluster genes. When the concentration of nematode-derived ascarosides drops to a threshold, G-proteins will stop the suppressing effect to the expression of the *artA*-gene cluster to stop trap formation. But if *ste12* is deleted, trap formation seems not to be stopped, leading to larger trap networks. It suggests that when G-proteins facilitate the expression of *artA-C*, the restorement of the expression needs the help of Ste12. Without Ste12, the expression of the *artA* gene cluster can not be turned up again. Trap formation will not be stopped then, leading to the limitless expansion of trap networks.

The expressional levels of *ste12* were similar in WT and the *gasA* and *gasB* mutants, suggesting post-transcriptional regulation of the phosphorylation status. *In S. cerevisiae*, the phosphorylation of Ste12 mediates the induction of downstream genes (Song *et al*., 1991). In *A. oligospora*, Ste12 acts as a downstream transcriptional factor of the FUS3-MAPK cascades for trap induction (Chen *et al*., 2021). The relation between Ste12 and MAP kinases in *A. flagrans* needs to be elucidated.

3.5 The ascaroside-receptor GprC could be obtained by horizontal gene transfer

The alignment revealed putative G-protein coupled receptors (GprF, GprO and NopA) in *A. flagrans* highly similar with their homologues in *S. cerevisiae* and *A. nidulans*. But putative receptors in the carbon receptor class, GprB, C and D, have higher identities with homologues in NTF (*A. oligospora*, *A. entomopaga* and *Dactylella cylindrospora*) but quite lower with other fungi (*A. nidulans*, *A. flavus*, *A. fumigatus*, *F. graminearum*, *Pyricularia oryzae*, *Ustilago maydis*, *C. neoformans* and *S. cerevisiae*). It suggests the carbon receptor group is specific for NTF and they are probably receptors sensing nematode-derived pheromone.

Surprisingly, the expression of *gprC* was induced by *C. elegans.* The Δ*gprC*-deletion strain produced less traps than wild type. In comparison, the defects of of *gprB* and *gprD* deletions were weaker. The fact that none of the single deletions of any of the three receptors led to a complete loss of trap formation probably reflects some redundancy of the proteins. Double or a triple-deletion of the receptors has not yet been achieved.

GprC and the homologues are ascarosides-specific sensors of nematode-catching fungi, and the expression of *gprC* is induced by *C. elegans*. I hypothesized that GprC is a gene laterally transferred from nematodes. Ascarosides are secreted by nematodes and involved in many developmental processes (Jeong *et al*., 2005; Butcher *et al*., 2007; Pungaliya *et al*., 2009; Golden *et al*., 1982). Some receptors in *C. elegans* are identified above nerve cells to sense different types of ascarosides, and these receptors modulate roaming, dauer formation, lifespan and hermaphrodite repulsion (McGrath & Ruvinsky, 2019; Vidal *et al.*, 2018). Nematodes and nematode catching fungi share the same habitat and co-evolved together for millions of years by interacting. The insect-pathogenic fungus *Metarhizium* robertsii contains more than 100 genes gained from the insect hosts by HGT, and the locust specialist *Metaihizium acridum* gains a protease from an ancestor of broad host-range lineages to enable its host-range expansion (Zhang *et al*., 2019). It is possible that *gprC* is obtained by *A. flagrans* from the genome of its prey nematodes. The re-complementation experiment of the Δ*gprC*-deletion strain with chimeric proteins provides evidence for my hypothesis. Chimeric proteins were composed of the N-terminus of ascaroside-receptors from nematodes and the C-terminus of GprC. Successful re-complementation happens on chimeric receptors containing C-terminal GprC and N-terminal SRBC-64, SRBC-66 and Daf-38 individually. Normal trap morphogenesis in the Δ*gprC*-deletion strain is restored by each of these proteins. #2 and #3 ascarosides are sensed by receptors SRBC-64, SRBC-66 and Daf-38 of *C. elegans* by experimental confirmation and prediction (McGrath & Ruvinsky, 2019; Vidal *et al.*, 2018). Ascr #3 together with #1 and #7 have the greatest effect on trap induction of *A. oligospora* (Hsueh *et al.*, 2013). So GprC, which is essential for trap formation and the deletion strain of its encoding gene *gprC* can be re-complemented by these nematode receptors, might bind to specific ascarosides like #3.

In addition to HGT from other species, it could also be changes of receptors in ligand-specificity. A single base-pair change in an avirulent gene (a race-specific elicitor AVR4) causes virulence of the biotrophic fungus *Cladosporium fulvum* on tomato (Joosten *et al.*, 1994). The substitution or deletion of amino acids leads to gain of new functions or loss of original functions in *Schizophyllum commune* (Fowler *et al.*, 2001). In this fungus, new specificities are evolved by recombination and deletion, leading to differential responses to different pheromones in one receptor molecule (Kothe *et al.*, 2003). GprC might perform sensing roles in binding different types of ascarosides by making changes in an amino acid or a nucleotide level.

3.6 A conclusion of the G-protein signaling pathway in *A. flagrans*

To summurize the results above, here the entire pathway is indicated **(Fig. 28)**. Normally the fungus *A. flagrans* lives in soil saprotrophicly. The *artA* gene cluster expresses, and arthrosporols are synthesized by the fungus to inhibit trap formation. If the nutrient in environment is limited, hyphae secrete volatile compounds to lure approach of nematodes. When the concentration of ascarosides goes up to a

threshold, the G-protein coupled receptor GprC can sense ascarosides and passes the signal to G-alpha subunit. GasA turns down the expression level of the *artA*-gene cluster genes. The inhibitory effect of the *artA* cluster on trap formation is released so that the fungus produces traps. Another G-alpha subunit GasB performs a negative influence in the role of the *artA* cluster. The second messenger cAMP is generated by GasB to regulate this cluster. In addition to the suppressing mechanism of G-alpha subunits on the *artA* cluster, the transcriptional factor Ste12 performs helpful role on expression of this cluster. A little amount of arthrosporols synthesized from the low expression levels of *artA*-C keeps a proper numbers of traps. After the fungus consumes enough nematodes, hyphae will not secrete appealing substances to attract nematodes. Nematodes will swim away, ascarosides concentration drops down to a threshold, and G-proteins stops to suppress the expression of the *artA* cluster. Under the aid of Ste12, *artA*-C express highly again, leading to much production of arthrosporols. When the concentration of arthrosporols rises up to a threshold trap formation is inhibited. The fungus turns back to a saprotryphic lifestyle.

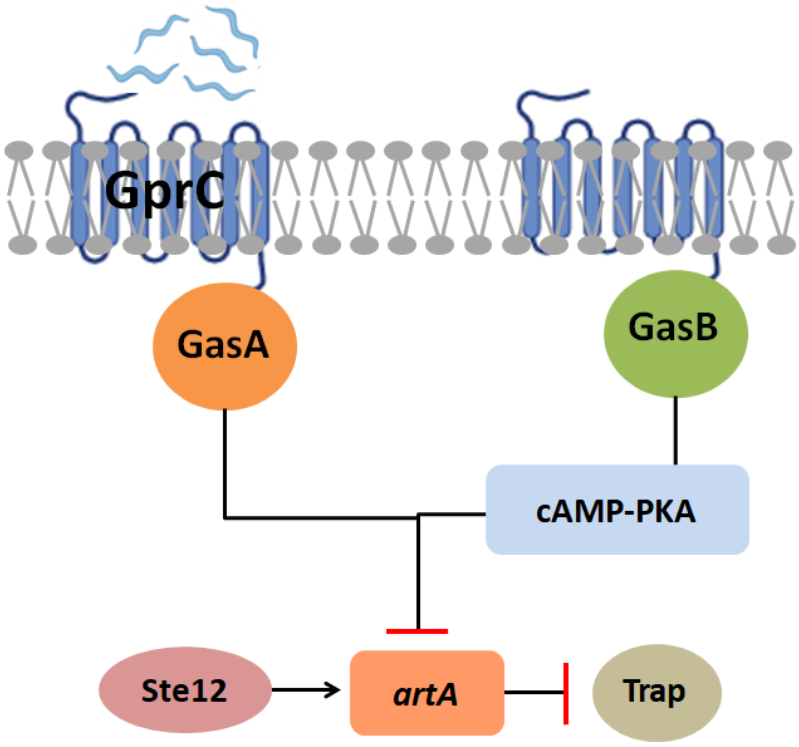

Fig. 28: Scheme of the regulation of trap formation by G-protein signaling pathways and GPCRs in *A. flagrans*. Ascarosides derived from the nematodes interact with GprC that activates GasA. GasB is activated probably by nutrients and generates the second messenger cAMP. Both Gas proteins aim to suppress the expression of the *artA*-gene cluster. Genes in this cluster encoding enzymes to synthesize the trap-inhibiting arthrosporols. The inhibitory effect is suppressed by signals from Gas proteins, and traps can be formed. At the mean time, the transcriptional factor Ste12 stimulates expression of the *artA*-gene cluster.

3.7 The characterization of the effector protein PefD

Pathogens secrete effector proteins to modulate defense responses and cell physiology of hosts (Owen *et al.*, 2007; Jashni *et al.*, 2015). In this work I characterized a small-secreted virulent factor in the predatory fungus *A. flagrans*. Exploration of its function reveals that it involves in the attack of fungus against nematodes. The fusion protein PefD-GFP localizes in infection site. This site is normally the first line of host defenses where many of the proteins are secreted. The access of penetration site is essential for attack against host. Microscopical pictures show the particular accumulation of fusion protein at this site, neither in the uninduced hyphae nor trophic hyphae that stretch inside the nematode body. This indicates that PefD is involved in the early step of infection. Proteins participating in initial steps of penetration normally accumulate at infection site and subsequently the infection bulb (Wernet *et al.*, 2021a). The enriched expression of PefD-GFP in fungus appeared the accumulation of fusion protein at the inner rim of empty traps. This is intriguing and it seems that the cell predicts the specific localization of the prey and recruits virulent proteins waiting there, until when a nematode is arrested and proteins are released. However the intelligently underlying mechanism remains unknown.

The signal peptide acts as a guide of secretion process. In the laccase assay, fusion protein PefD-LccC$^{\Delta SP}$ enabled the appearance of blue-green color indicating the successful secretion of the protein. The signal peptide in PefD leads to the secretion of the fusion protein. The deletion of signal peptide of PefD caused the cytoplasmic localization of PefD protein all over both vegetative hyphae and traps. It enforces the essential function of signal peptide for secretion. Normally the signal peptide is cleaved off in the ER, causing the localization of mature protein in ER. However the mature PefD protein was only observed in the cytoplasm, suggesting a novel secretion pathway of effectors. A specific secretion of the exocyst complex is characterized in *A. flagrans* (Wernet *et al.*, 2021a). In the Δ*exoA*-deletion strain, CyrA-mCherry protein is not capable to localize in the infection bulb as wild type, but at the inner rim of traps. This indicates that the exocyst complex is critical for the accurate localization of CyrA in the bulb and involves in the secretion of virulent factors. PefD is probably secreted as well by this novel pathway. The involvement in PefD secretion by exocyst complex needs further research.

The over-expressing strain of *pefD* gene displayed less nematicidal activity, showing it is responsible for killing captured nematodes. The Δ*cyrA*-deletion strain presents prolonged time during paralyzing while NipA seems to localize with components of the cytoskeleton and another virulence factor (Wernet *et al.*, 2021a; Menzner, 2020). And the localizations of different effectors (PefD, HinA, CyrA and NipA) showed varied localizations during infection. The diverse functions and varied localizations of virulent factors in the attacking process of *A. flagrans* against nematodes enforce the concept “Red Queen scenario”. It was termed in 1973 by Leigh Van Valen. Pathogens develop a variety of weapons to overcome defense responses of host and to perform

virulent roles. PefD harbors a propeptide. Normally protein precursors are preproproteins in which the propeptide is cleaved after translocation generating the mature protein and these peptides are considered to influence protein activities (Shinde & Inouye, 2000). However the open questions if the propeptide is cleaved off after penetration and the underlying role of PefD in nematodes remains currently unknown.

The propeptide of PefD might ensure the translocation and activity of the mature protein. The existence of a propeptide domain in a secretory protein ensures correct folding of proteins leaving the ER (Bauskin *et al.*, 2000). The translocation of effectors proteins from fungi into plant hosts are reviewed by Presti and Kahmann (2017). In the fungal and plant cells, there are multivesicular bodies (MVB) that release extracellular vesicles (EVs) of fungal or plant origin in order to shape biotrophic interfaces. The mature PefD protein without signal peptide and propeptide predictly localizes in nuclei. The underlying translocation mechanism and the involvement of the propeptide remain still unkown. The existence of a propeptide and the nuclear localization may be an indication for a toxic function. The effector protein SP7 secreted by the biotrophic fungus *Glomus intraradices* interacts with the pathogenesis-related transcription factor ERF19 in the plant nucleus (Kloppholz *et al.*, 2011). If the nucleus of nematodes is really the target of PefD, the protein might reprogram the genetic program of the prey. However, the nameode-killing process by the NTF is quite fast, there will be no time for differential gene expression. For another possibility, PefD might act on neurons, where it is further cleaved and release some neuropeptides-like proteins (NLPs). These peptides in nematodes have widespread and varied functions in nervous system (McVeigh *et al.*, 2006; Dash *et al.*, 2017). The interaction between PefD and NLPs needs to be explored.

4 Materials and methods

4.1 Chemicals and equipment used in this study

All restriction enzymes and PCR polymerases were obtained from New England Biolabs (NEB, Flankfurt). Chemicals used in this work were purchased from Roth (Karlsruhe), Merck (Darmstadt), Sigma (Taufkirchen), whereas the others are indicated in the text.
Antibiotics used in this work are listed as below:
Ampicillin stock solution: 100 mg/ml,
Hygromycin stock solution: 100 mg/ml,
Geneticin stock solution G480: 50 mg/ml.

Table 2: Equipment used in this work.

Equipment	Type	Manufacturer
PCR cycler	Labcycler	SensoQuest, Göttingen
Autoclave	3870ELV	Tuttnauer, Breda
Centrifuge with rotors	Eppendorf 5415R	Eppendorf, Hamburg
	AccuSpin Micro 17	Fisher Scientific, Schwerte
	Universal 320 R	Hettich, Tuttlingen
Heat block	Thermomixer 5436	Eppendorf, Hamburg
Hybridization oven	HB-1000 Hybridizer	UVP, Cambridge
Incubator	Mintron AL 72	Infors HAT, Bottmingen-Basel
	Heraeus 6000	Heraeus, Instruments Hanau
UV-cross linker	UV Stratalinker 2400	Stratagene, Heidelberg
pH meter	HHanna HI 208	Hanna, Romania
Magnetic stirrer	Heidolph MR3000	Heidolph, Germany
Gelscanner	SnapScan1236v	Agfa, Cologne
Microscope	Axio Imager Z1	Zeiss, Jena
	Eclips E200	Nikon, Japan
	Discovery.v12	Zeiss, Jena
UV/visible spectrophotometer	Nanodrop ND 1000	PeQlab, Erlangen
Vortex	Vortex-Genie2	Scientific Industry, Inc., New York

4.2 Organisms, plasmids and oligonucleotides

All *Escherichia coli* strains, *Saccharomyces cerevisiae* strains and *Arthrobotrys flagrans* strains are listed as below:

Table 3: *A. flagrans* used in this study.

Strain	Phenotype	Resistance	Source
D. flagrans CBS 349.94	Wild type (WT)	-	CBS-KNAW culture collection
A. oryzae	*Adenin⁻ Arginin⁻ Methionin⁻*	-	Russel J. Cox, Leibniz University
SXD01	*amyB(p)::artA::amyB(t) PXD1*	Ade	(Yu *et al*., 2021)
SXD05	*SXY05 x artA(p)::artA::artA(t) PXD6*	Amp, G418	(Yu *et al*., 2021)
SXD13	*oliC(p)::pefD-lccC$^{\Delta SP}$:: gluC(t) PXD19*	Amp, Hph	This work
SXD14	*pefD(p)::h2b:mCherry::tub(t) PXD17*	Amp, Hph	This work
SXD15	*oliC(p)::pefD$^{\Delta SP}$::GFP::gluC(t) PXD20*	Amp, Hph	This work
SXD24	*oliC(p)::pefD::GFP::gluC(t) PXD33*	Amp, Hph	This work
SXD26	*pefD(p)::pefD::GFP::gluC(t) PXD32*	Amp, Hph	This work
SXD27	*hinA(p)::hinA::GFP::gluC(t) PXD35*	Amp, Hph	This work
SXD28	*SNH30 x pefD(p)::pefD::GFP::gluC(t) PXD36*	Amp, G418	This work
SNH30	*cyrA(p)::cyrA::GFP::gluC(t) PNH32*	Amp, Hph	(Wernet *et al*., 2021a)
SXD30	*SXD26 x nipA(p)::nipA::mCherry PJM16,*	Amp, G418	This work
SXD33	*SXD27 x pefD(p)::pefD:: mCherry::gluC(t) PXD41*	Amp, G418	This work
SXD34	*SXD24 x oliC(p)::rab7:: mCherry::gluC(t) PXD51*	Amp, G418	This work
SXD35	*pefD(LB)::hph::pefD(RB) PXD42*	Amp, Hph	This work
SXD37	*oliC(p):: pefD ::gluC(t) PXD52*	Amp, Hph	This work
SXD38	*oliC(p):: pefD$^{\Delta Prop}$::gluC(t) PXD62*	Amp, Hph	This work
SXD39	*gasA(LB)::hph::gasA(RB) deletion cassette PXD66*	Amp, Hph	This work
SXD40	*gasB(LB)::hph::gasB(RB) deletion cassette PXD64*	Amp, Hph	This work
SXD41	*SNH14 x oliC(p)::pefD$^{\Delta SP\Delta Prop}$:: mCherry::gluC(t) PXD47*	Amp, G418	This work
SNH14	*h2b(p)::h2b::GFP*	Amp, Hph	(Wernet *et al*., 2021a)
SXD42	*SXD39 x gasA(p)::gasA::gasA(t) PXD71*	Amp, G418	This work
SXD43	*SXD40 x gasB(p)::gasB::gasB(t) PXD72*	Amp, G418	This work
SXD44	*SXD39 x artA(p)::h2b:mCherry PXD73*	Amp, G418	This work
SXD45	*SXD40 x artA(p)::h2b:mCherry PXD73*	Amp, G418	This work
SXD46	*oliC(p)::gasA::gluC(t) PXD76*	Amp, Hph	This work
SXD48	*oliC(p)::GFP::dfl_001239::gluC(t) PXD80*	Amp, Hph	This work
SXD50	*SXD40 x artA(LB)::G418::artA(RB) deletion cassette PXD75*	Amp, G418	This work
SXD53	*artA::GFP::trpC(p)::hph::trpC(t)::artA(t) PXD88; artB::mCherry::trpC(p)::hph::trpC(t)*	Amp, Hph	(Yu *et al*., 2021)

	::artB(t) PXD89		
SXD54	*gasA(LB)::hph::gasA(RB) deletion cassette PXD66, artA::GFP::trpC(p)::hph::trpC(t)::artA(t) PXD88*	Amp, Hph	This work
SXD55	*gasB(LB)::hph::gasB(RB) deletion cassette PXD64, artA::GFP::trpC(p)::hph::trpC(t)::artA(t) PXD88*	Amp, Hph	This work
SXD56	*ste12(LB)::hph::ste12(RB) deletion cassette PXD102*	Amp, Hph	This work
SXD57	*gprC(LB)::hph::gprC(RB) deletion cassette PXD103*	Amp, Hph	This work
SXD60	*tpr(LB)::hph::tpr(RB) deletion cassette PXD104*	Amp, Hph	This work
SXD62	*SXD57 x gprC(p)::gprC::gprC(t) PXD106*	Amp, G418	This work
SXD63	*SXD56 x ste12(p)::ste12::ste12(t) PXD107*	Amp, G418	This work
SXD82	*gprC(p)::daf-37(N)::gprC(C)::gprC(t) PXD128*	Amp, G418	This work
SXD83	*gprC(p)::srbc-64(N) ::gprC(C)::gprC(t) PXD127*	Amp, G418	This work
SXD84	*gprC(p)::daf-38(N)::gprC(C)::gprC(t) PXD133*	Amp, G418	This work
SXD85	*gprC(p)::octr-1(N)::gprC(C)::gprC(t) PXD134*	Amp, G418	This work
SXD86	*oliC(p)::rgs1::gluC(t) PXD77*	Amp, Hph	This work
SXD87	*oliC(p)::rgs2::gluC(t) PXD78*	Amp, Hph	This work
SXD88	*oliC(p)::rgs3::gluC(t) PXD86*	Amp, Hph	This work
SXD89	*oliC(p)::rgs4::gluC(t) PXD87*	Amp, Hph	This work
SXD90	*oliC(p)::mapkB::gfp::gluC(t) PXD85*	Amp, Hph	This work
SXD91	*gasC(LB)::hph::gasC(RB) deletion cassette PXD65*	Amp, Hph	This work
SXD92	Δ*plc1 PXD112*	Amp, Hph	This work
SXD93	Δ*plc2 PXD110*	Amp, Hph	This work
SXD94	Δ*gpb1 PXD111*	Amp, Hph	This work
SXD95	*oliC(p)::gasA^{G42R}::gluC(t) PXD108*	Amp, Hph	This work
SXD96	*oliC(p)::gasB^{G45R}::gluC(t) PXD109*	Amp, Hph	This work
SXD97	*oliC(p)::gasA^{Q204L}::gluC(t) PXD114*	Amp, Hph	This work
SXD98	*oliC(p)::gasB^{Q208L}::gluC(t) PXD113*	Amp, Hph	This work
SXD99	*gprC(p)::srbc-66(N)::gprC(C)::gprC(t) PXD127*	Amp, G418	This work
SXY05	Δ*artA PXY09*	Amp, Hph	(Yu *et al*., 2021)
SXY14	Δ*artC PXY15*	Amp, Hph	(Yu *et al*., 2021)
SXY15	Δ*artB PXY16*	Amp, Hph	(Yu *et al*., 2021)
SXY16	Δ*artD PXY17*	Amp, Hph	(Yu *et al*., 2021)
SXY17	*artA(p)::h2b:mCherry PXY18*	Amp, Hph	(Yu *et al*., 2021)

SXY20	*artB(p)::h2b:mCherry PXY21*	Amp, Hph	(Yu *et al*., 2021)
SXY19	*artC(p)::h2b:mCherry PXY20*	Amp, Hph	(Yu *et al*., 2021)

Table 4: *E. coli* used in this study.

Strain	Phenotype	Source
Top10	*F−mcrA_(mrr-hsdRMSmcrBC) _80lacZ_M15 _lacX74 recA1 araD139 _(ara-leu)7697 galU galK rpsL (StrR) endA1 nupG*	Invitrogen, Karlsruhe
OP50	*ura-*	Institut für Biologie, Bioinformatik und Molekulargenetik, Freiburg
WXD2	*Myo-2(p)::tdTomoto, hsp-16.48(p)::GFP::unc-54UTR PXD45*	
WXD3	*Myo-2(p)::tdTomoto, hsp-16.48(p)::pefD::GFP::unc-54UTR PXD46*	

Table 5: *S. cerevisiae* used in this study.

Strain	Phenotype	Source
Y187	*MATα; ura3-52; his3-200; ade2-101; trp1-901; leu2- 3; 112; gal4Δ; met-; gal80Δ; URA3::GAL1UAS-GAL1TATAlacZ*	(Harper *et al*., 1993)
AH109	*MATa; trp1-901; leu2-3, 112; ura3-52; his3-200; gal4Δ; gal80Δ; LYS2::GAL1UAS-GAL1TATA-HIS3; GAL2UAS-GAL2TATA-ADE2; URA3::MEL1UAS-MEL1TATA-lacZ*	(James *et al*., 1996)
Positive control	*AH109 x pGADT7-T and pGBKT7-53*	(Gao *et al*., 2021)
Negative control	*AH109 x pGADT7-T and pGBKT7- Lam*	(Gao *et al*., 2021)
SXD64	*Y187 x PXD125 AD-A*	This work
SXD65	*Y187 x PXD126 AD-B*	This work
SXD66	*Y187 x PXD123 AD-3*	This work
SXD67	*Y187 x PXD124 AD-4*	This work
SXD68	*AH109 x PXD121 BD-A*	This work
SXD69	*AH109 x PXD122 BD-B*	This work
SXD70	*AH109 x PXD119 BD-3*	This work
SXD71	*AH109 x PXD120 BD-4*	This work
SXD72	*SXD68 x SXD66 A+3*	This work
SXD73	*SXD68 x SXD67 A+4*	This work
SXD74	*SXD69 x SXD66 B+3*	This work
SXD75	*SXD69 x SXD67 B+4*	This work
SXD76	*SXD70 x SXD64 3+A*	This work
SXD77	*SXD70 x SXD65 3+B*	This work
SXD78	*SXD67 x SXD64 4+A*	This work

SXD79	*SXD67 x SXD65 4+B*	This work

Table 6: Plasmids used in this work.

Strain	Phenotype	Resistance	Source
pJET1.2	-	Amp	Thermo Fisher
PXD01	*amyB(p)::artA::amyB(t)*	Amp, Ade	(Yu *et al*., 2021)
PXD06	*artA(p)::artA::artA(t)*	Amp, G418	(Yu *et al*., 2021)
PXD17	*pefD(p)::h2b:mCherry*	Amp, Hph	This work
PXD19	*oliC(p)::pefD-lccC$^{\Delta SP}$:: gluC(t)*	Amp, Hph	This work
PXD20	*oliC(p):: pefD$^{\Delta SP}$:: GFP::gluC(t)*	Amp, Hph	This work
PNH32	*cyrA(p)::cyrA::GFP::gluC(t)*	Amp, Hph	(Wernet *et al*., 2021a)
PXD32	*pefD(p)::pefD::GFP::gluC(t)*	Amp, Hph	This work
PXD33	*oliC(p):: pefD::GFP::gluC(t)*	Amp, Hph	This work
PXD35	*hinA(p)::hinA::GFP::gluC(t)*	Amp, Hph	This work
PXD41	*pefD(p)::pefD::mCherry::tub(t)*	Amp, G418	This work
PXD42	*pefD(LB)::hph::pefD(RB)*	Amp, Hph	This work
PXD45	*hsp-16.48(p)::GFP::unc-54UTR*	-	This work
PXD46	*hsp-16.48(p)::pefD::GFP::unc-54UTR*	-	This work
PXD47	*oliC(p)::pefD$^{\Delta SP\Delta Prop}$:: mCherry::gluC(t)*	Amp, G418	This work
PXD51	*oliC(p)::rab7::mCherry::gluC(t)*	Amp, G418	This work
PXD52	*oliC(p)::pefD::gluC(t)*	Amp, Hph	This work
PJM16	*nipA (p)::nipA::mCherry*	Amp, Hph	(Menzner, 2020)
PXD62	*oliC(p):: pefD$^{\Delta Prop}$::gluC(t)*	Amp, Hph	This work
PXD64	Δ*gasB*	Amp, Hph	This work
PXD65	Δ*gasC*	Amp, Hph	This work
PXD66	Δ*gasA*	Amp, Hph	This work
PXD71	*gasA(p)::gasA::gasA(t)*	Amp, G418	This work
PXD72	*gasB(p)::gasB::gasB(t)*	Amp, G418	This work
PXD73	*artA(p)::h2b:mCherry*	Amp, G418	This work
PXD75	Δ*artA*	Amp, G418	This work
PXD76	*oliC(p)::gasA::gluC(t)*	Amp, Hph	This work
PXD77	*oliC(p)::rgs1::gluC(t)*	Amp, Hph	This work
PXD78	*oliC(p)::rgs2::gluC(t)*	Amp, Hph	This work
PXD79	*oliC(p)::GFP::dfl_001239::gluC(t)*	Amp, Hph	This work
PXD85	*oliC(p)::mapkB::GFP::gluC(t)*	Amp, Hph	This work
PXD86	*oliC(p)::rgs3::gluC(t)*	Amp, Hph	This work
PXD87	*oliC(p)::rgs4::gluC(t)*	Amp, Hph	This work
PXD88	*artA::GFP::trpC(p)::hph::trpC(t)::artA(t)*	Amp, Hph	(Yu *et al*., 2021)
PXD89	*artB::mCherry::trpC(p)::hph::trpC(t) ::artB(t)*	Amp, Hph	(Yu *et al*., 2021)
PXD102	Δ*ste12*	Amp, Hph	This work
PXD103	Δ*gprC*	Amp, Hph	This work
PXD104	Δ*tprA*	Amp, Hph	This work

PXD106	*gprC(p)::gprC::gprC(t)*	Amp, G418	This work
PXD107	*ste12(p)::ste12::ste12(t)*	Amp, G418	This work
PXD108	*oliC(p)::gasA^{G42R}::gluC(t)*	Amp, Hph	This work
PXD109	*oliC(p)::gasB^{G45R}::gluC(t)*	Amp, Hph	This work
PXD110	Δ*plc2*	Amp, Hph	This work
PXD111	Δ*gpb1*	Amp, Hph	This work
PXD112	Δ*plc1*	Amp, Hph	This work
PXD113	*oliC(p)::gasB^{Q208L}::gluC(t)*	Amp, Hph	This work
PXD114	*oliC(p)::gasA^{Q204L}::gluC(t)*	Amp, Hph	This work
PXD117	Δ*gprC*	Amp, G418	This work
PXD118	Δ*gprD*	Amp, G418	This work
PXD119	*pGBKT-7 with GprC inner loop 3 cDNA*	Kan, Trp	This work
PXD120	*pGBKT-7 with GprC inner loop 4 cDNA*	Kan, Trp	This work
PXD121	*pGBKT-7 with gasA cDNA*	Kan, Trp	This work
PXD122	*pGBKT-7 with gasB cDNA*	Kan, Trp	This work
PXD123	*pGADT-7 with GprC inner loop 3 cDNA*	Amp, Leu	This work
PXD124	*pGADT-7 with GprC inner loop 4 cDNA*	Amp, Leu	This work
PXD125	*pGADT-7 with gasA cDNA*	Amp, Leu	This work
PXD126	*pGADT-7 with gasB cDNA*	Amp, Leu	This work
PXD127	*gprC(p)::srbc-64(N)::gprC(C)::gprC(t)*	Amp, G418	This work
PXD128	*gprC(p)::daf-37(N)::gprC(C)::gprC(t)*	Amp, G418	This work
pGADT7	*Gal4 DNA-activation domain*	Amp, Leu	Clontech
pGBKT7	*Gal4 DNA-binding domain*	Kan, Trp	Clontech
PXY09	Δ*artA*	Amp, Hph	(Yu *et al*., 2021)
PXY15	Δ*artC*	Amp, Hph	(Yu *et al*., 2021)
PXY16	Δ*artB*	Amp, Hph	(Yu *et al*., 2021)
PXY17	Δ*artD*	Amp, Hph	(Yu *et al*., 2021)
PXY18	*artA(p)::h2b::mCherry::tub(t)*	Amp, Hph	(Yu *et al*., 2021)
PXY20	*artC(p)::h2b::mCherry::tub(t)*	Amp, Hph	(Yu *et al*., 2021)
PXY21	*artB(p)::h2b::mCherry::tub(t)*	Amp, Hph	(Yu *et al*., 2021)
PNH30	*gpdA(p)::mCherry::tub(t)*	Amp, Hph	(Yu *et al*., 2021)

Table 7: Oligonucleotides used in this study.

Name	Sequence
***gasA* deletion**	
GasALB-pjet-ol-for	GATGGCTCGAGTTTTTCAGCAAGATACCTTCGTCATCATCAGATCA
GasALB-H-ol-rev	GTTGACCTCCACTAGCATTACACTTTTTGACGGTGTTTCTTTAGAAAAA
GasARB-H-ol-for	ATGCTCTTTCCCTAAACTCCCCCCAACGAGTTCCCGACCAATGA
GasARB-pjet-ol-rev	ATTGTAGGAGATCTTCTAGAAAGATAATACATGAACACACACCAGG
H-GasALB-ol-for	TTTTTTCTAAAGAAACACCGTCAAAAAGTGTAATGCTAGTGGAGGT

H-GasARB-ol-rev	TGTTGGTCATTGGTCGGGAACTCGTTGGGGGGAGTTTAGGGAAA
GasAko_up_for	CCTGCAAGAGGGGAGCAAA
GasAko_down_rev	CCTCGATTACAATTGTTTGGAG
GasA_LB_for	ACCTTCGTCATCATCAGATCA
GasA_LB_rev	AAAAATGCCAGCGGCAGAG
GasA_RB_rev	AATACATGAACACACACCAGG
GasA_ORF_for	ATGGGTTGCAGCATGTCTAC
GasA_ORF_rev	TTATATCAGACCGCAGTTTCTG
***gasB* deletion**	
GasBLB_pjet_ol_for	GATGGCTCGAGTTTTTCAGCAAGATCACCACTGCAGTAACCTCTA
GasBLB-H-ol-rev	GTTGACCTCCACTAGCATTACACTTTTTGGCTGACTTGCAATCTC
GasBRB-H-ol-for	ATGCTCTTTCCCTAAACTCCCCCCACCGACTAAAAATACCAACATCC
GasBRB-pjet-ol-rev	ATTGTAGGAGATCTTCTAGAAAGATTCCGAGATAGCGGTGTTCA
H-GasBLB-ol-for	TCGGTGAGATTGCAAGTCAGCCAAAAAGTGTAATGCTAGTGGAGGT
H-GasBRB-ol-rev	GTCGGATGTTGGTATTTTTAGTCGGTGGGGGGAGTTTAGGGAAA
GasB_KO_up_for_n	TGACTAGTAGCCCAAATGAAC
GasB_KO_down_rev_n	TAGACGGGCTGCATTTTGG
GasB_LB_for	CACCACTGCAGTAACCTCTA
GasB_RB_for	CCGACTAAAAATACCAACATCC
GasB_RB_rev	TCCGAGATAGCGGTGTTCA
GasB_ORF_for	ATGGGTGGCTGCATGTCG
GasB_ORF_rev	TTATAAGATACCAGAGTCCTTGA
***gasC* deletion**	
GasCLB-pjet-ol-for	GATGGCTCGAGTTTTTCAGCAAGATATCTTGTCGTCAGTCAGCCA
GasCLB-H-ol-rev	GTTGACCTCCACTAGCATTACACTTTTCGAGGAATGACCCGAAGA
GasCRB-H-ol-for	ATGCTCTTTCCCTAAACTCCCCCCATCAACCAATTTTCCATCTAGCT
GasCRB-pjet-ol-rev	ATTGTAGGAGATCTTCTAGAAAGATCGAGGCTGGCCTATACATA
H-GasCLB-ol-for	TCCGCTCTTCGGGTCATTCCTCGAAAAGTGTAATGCTAGTGGAGGT
H-GasCRB-ol-rev	ACGAGCTAGATGGAAAATTGGTTGATGGGGGGAGTTTAGGGAAA
GasCko_up_for	GGCCACTCTCGAGACTTTT
GasCko_down_rev	GGCTGATAAGCTATAAAGGCC
GasC_LB_for	ATCTTGTCGTCAGTCAGCCA
GasC_RB_rev	CGAGGCTGGCCTATACATA
GasC_ORF_for	ATGTGCATGGGTGGAGATG

GasC_ORF_rev	TTATAGGATCAATTGGTGGAGG
Recomplementation	
BB_TrpC P_for	AAGTGTAATGCTAGTGGAGGT
BB_Pjet_rev	ATCTTGCTGAAAAACTCGAGC
GasALB_recomp_ol_for	GATGGCTCGAGTTTTTCAGCAAGATCGTAACGACGCCGATTGAAT
GasARB_recomp_ol_rev	GTTGACCTCCACTAGCATTACACTTCCTCGATTACAATTGTTTGGAG
GasBLB_recomp_ol_for	GATGGCTCGAGTTTTTCAGCAAGATGGAGGGGTTGTTAAGGATGT
GasBRB_recomp_ol_rev	GTTGACCTCCACTAGCATTACACTTTCCGAGATAGCGGTGTTCA
pksA(p)::h2b::mCherry::G418	
BB_pksA_h2bmcherry_for	CTCTTTCCCTAAACTCCCC
BB_pksA_h2bmcherry_rev	ggatccATCTTGCTGAAAAAC
Hph_pksAh2bmcherry_ol_for	TCGAGTTTTTCAGCAAGATggatccAAGTGTAATGCTAGTGGAGGT
Hph_ pksAh2bmcherry_ol_rev	AGGTGGGGGGAGTTTAGGGAAAGAGTGGGGGGAGTTTAGGGAAA
TrpC_ter_seq_for	AAAGTGACAGGCGCCCTTAA
***artA* deletion**	
artA_LB_for	TCTCTGTAGCCTATCTGTAAG
artA _RB_rev	CAGTATCACCAATTCTCATCTG
artALB_pjet_ol_for	GATGGCTCGAGTTTTTCAGCAAGATTCTCTGTAGCCTATCTGTAAG
artALB_hph_ol_rev	GTTGACCTCCACTAGCATTACACTTGGCAGGCCAAAGAAGTCAA
artARB_hph_ol_for	ATGCTCTTTCCCTAAACTCCCCCCAGGGAAGTGTTGGTATGGGTT
artARB_pjet_ol_rev	ATTGTAGGAGATCTTCTAGAAAGATCAGTATCACCAATTCTCATCTG
H-artALB-ol-for	TTTGACTTGACTTCTTTGGCCTGCCAAGTGTAATGCTAGTGGAGGT
H-artARB-ol-rev	AGAAAAACCCATACCAACACTTCCCTGGGGGGAGTTTAGGGAAA
artAKO_up_for	GCAATGATGTTGATGAGGATC
artAKO_down_rev	GCCTATCTATACCGACTTCC
artAKO_nearup_for	GGGTTCCTCGTACCAATCT
artAKO_neardown_rev	AAGGGAAGGACAAACAGATAG
GasA overexpression	
GasA_OE_ol_for	TCACAATCGATCCAACCggcgcgccATGGGTTGCAGCATGTCTAC
GasA_OE_ ol_rev	TAATCATACATCTTATCTACATACGTTATATCAGACCGCAGTTTCTG
BB_Tgluc_for	CGTATGTAGATAAGATGTATGATT
BB_Polic_Asc1_rev	ggcgcgccGGTTGGAT
RGS q-PCR	

RGS1_q_for	GAATTGTCGATAACTCCGGCA
RGS1_q_rev	GCTTTCAGTGGGAGTTGACTT
RGS2_q_for	ACCATTGCCTCGAGACTTTAG
RGS2_q_rev	ACATCTTGACGTATTGGCACG
RGS3_q_for	GATCTCCACAGCACACCGT
RGS3_q_rev	CTTCATCGAAGACCTCCGGA
RGS4_q_for	GGACTAGCTCTGATAGAAACG
RGS4_q_rev	CCTCGCTTGGTAGTATTGGAA
RGS Overexpression	
RGS1_OE_ol_for	TCACAATCGATCCAACCggcgcgccATGCCTGATACGACTGTCCT
RGS1_OE_ol_rev	TAATCATACATCTTATCTACATACGCTATTTTGCATGTTGCTGTACA
RGS2_OE_ol_for	TCACAATCGATCCAACCggcgcgccATGTCTGCGCGGAATTATAGA
RGS2_OE_ol_rev	TAATCATACATCTTATCTACATACGTCATTGGTAAGGATCGCTCG
RGS3_OE_ol_for	TCACAATCGATCCAACCggcgcgccATGGCCAGAAATACCGATAG
RGS3_OE_ol_rev	TAATCATACATCTTATCTACATACGTTACAATCTCCTCCCAGGTA
RGS4_OE_ol_for	CACAATCGATCCAACCggcgcgccATGTCGACCACAGGCAGC
RGS4_OE_ol_rev	TAATCATACATCTTATCTACATACGTTACTGTCTCAGCTCTGGAAA
BB_Tgluc_for	CGTATGTAGATAAGATGTATGATT
BB_Polic_Asc1_rev	ggcgcgccGGTTGGAT
Ste12(DFL_001239) q-PCR	
Ste12_q_for	ACTGCTGCTGGTATGTACGG 60.5
Ste12_q_rev	GGTGTAGCAGAAAACGCAGC 60.5
oliC(p)::GFP::dfl_1239::gluC(t)	
1239_Ngfp_for	TaggcgcgccATGTATTCACACAACGCTCTC
1239_Ngfp_rev	CGttaattaaTTACATCTGGGGTATCAGTTG
oliC(p)::mapkB::GFP::gluC(t)	
MapkB_Asc1_for	CCggcgcgccATGTCTCGCCAGAACTCGA
MapkB_Pac1_rev	cttaattaaCCGCATGATTTCCTCAAAGAT
***ste12* deletion**	
Ste12LB_pjet_ol_for	GATGGCTCGAGTTTTTCAGCAAGATCTATCAAAGGCTTCGTTGCTT
Ste12LB_H_ol_rev	GTTGACCTCCACTAGCATTACACTTATTTGTGTGTGAGTGTGCGA
H_ste12LB_ol_for	GGGGTCGCACACTCACACACAAATAAGTGTAATGCTAGTGGAGGT
H_ste12RB_ol_rev	TTTCTTTTCCCTGGTTAGATTTGCTTGGGGGGAGTTTAGGGAAA
Ste12RB_H_ol_for	ATGCTCTTTCCCTAAACTCCCCCCAAGCAAATCTAACCAGGGAAAAG
Ste12RB_pjet_ol_rev	ATTGTAGGAGATCTTCTAGAAAGATTTCGATGGCTGGAGCCTATT
Ste12LB_for	CTATCAAAGGCTTCGTTGCTT
Ste12RB_rev	TTCGATGGCTGGAGCCTATT
Ste12ko_up_for	TCGTCTGTAGTCGTCTTCGT
Ste12ko_down_rev	TCGGAGGATACGTTTGCTGT
Ste12ORFin_for	ATGTATTCACACAACGCTCTC

Ste12ORFin_rev	TGAGGGTTCATCTGAGGCAT
Hph_rev	TGGGGGGAGTTTAGGGAAA
Hph_for	AAGTGTAATGCTAGTGGAGGT
***gprC* deletion**	
GprCLB_pjet_ol_for	GATGGCTCGAGTTTTTCAGCAAGATCCTTGTTTCGCCATGACATG
GprCLB_H_ol_rev	GTTGACCTCCACTAGCATTACACTTGGTTGCGTCAGTGTATTATCA
GprCRB_H_ol_for	ATGCTCTTTCCCTAAACTCCCCCCACCGCGAAGAGAGTAATGAAC
GprCRB_pjet_ol_rev	ATTGTAGGAGATCTTCTAGAAAGATCACTGATCCCCTGTATATTGA
H_GprCLB_ol_for	CGGATGATAATACACTGACGCAACCAAGTGTAATGCTAGTGGAGGT
H_GprCRB_ol_rev	TTCTAGTTCATTACTCTCTTCGCGGTGGGGGGAGTTTAGGGAAA
GprCLB_for	CCTTGTTTCGCCATGACATG
GprCRB_rev	CACTGATCCCCTGTATATTGA
GprCORF_for	ATGGCCTTCACGACACTTTC
GprCORFin_rev	TGTTTCCGAAATCCAGACTTC
GprCko_up_for	AAAAGCAAATGGAATGGACCC
GprCko_down_rev	ACTCCCTATTAGCTTTCATGG
***artR* deletion**	
TPRLB_pjet_ol_for	GATGGCTCGAGTTTTTCAGCAAGATGGACACCGCAAAGAACACTT
TPRLB_H_ol_rev	GTTGACCTCCACTAGCATTACACTTTTGCTTATTGGTTCACCTGGA
H_TPRLB_ol_for	CCGATCCAGGTGAACCAATAAGCAAAAGTGTAATGCTAGTGGAGGT
H_TPRRB_ol_rev	CAAACTGGTAGAGCGGACTGGGTACTGGGGGGAGTTTAGGGAAA
TPRRB_H_ol_for	ATGCTCTTTCCCTAAACTCCCCCCAGTACCCAGTCCGCTCTAC
TPRRB_pjet_ol_rev	ATTGTAGGAGATCTTCTAGAAAGATGAATTAAGAGCAGAAGCAGCT
TPRLB_for	GGACACCGCAAAGAACACTT
TPRRB_rev	GAATTAAGAGCAGAAGCAGCT
TPR-OPF_for	ATGGACCCTGGTAACAGAGA
TPR-OPFin_rev	AGGTGAAGAAATTCTGGTCGA
TPRko_up_for	TTCAAAGAATCGGGTTAACGG
TPRko_down_rev	GCGAGAACTGTAGGTACTGT
gprC/ ste12 recomplementation	
3rre_ol_for	GATGGCTCGAGTTTTTCAGCAAGATCCCAAATCCATGGTGAACCA
3rre_ol_rev	GTTGACCTCCACTAGCATTACACTTACTCCCTATTAGCTTTCATGG

Ste12re_ol_for	GATGGCTCGAGTTTTTCAGCAAGATATGCTGGGCTAGTGGTAATAT
Ste12re_ol_rev	GTTGACCTCCACTAGCATTACACTTTCGGAGGATACGTTTGCTGT
Chimeric protein of GprC	
SRBC64_3rLB_ol_for	CGGATGATAATACACTGACGCAACCATGCCTGAAATAGTAATAATCTTG
SRBC64N_3rC_ol_rev	CAGCCATGTGTCATCACATATCGAATTGAATTTGGTCTCTTGAGAC
3r_C_for	TTCGATATGTGATGACACATGG
3r_LB_rev	GGTTGCGTCAGTGTATTATCA
Daf37_3rLB_ol_for-n	CGGATGATAATACACTGACGCAACCATGGATGTCATTGGGAACAT
Daf37N_3rC_ol_rev-n	CAGCCATGTGTCATCACATATCGAAAGAATATACCTGCTGATAAATAG
SRX43_3rLB_ol_for	CGGATGATAATACACTGACGCAACCATGGTGCTCCGAAATCTGAC
SRX43N_3rC_ol_rev	CAGCCATGTGTCATCACATATCGAACGAATAGAGGCTCAGCAGA
SRG36_3rLB_ol_for	CGGATGATAATACACTGACGCAACCATGACGCTGGCAAGCTTG
SRG36N_3rC_ol_rev	CAGCCATGTGTCATCACATATCGAAGCGTTTTATTGTGGTATCTAG
SRBC66_3rLB_ol_for	CGGATGATAATACACTGACGCAACCATGTCAGCCATTACTATAACTTG
SRBC66N_3rC_ol_rev	**CAGCCATGTGTCATCACATATCGAATTGAACCTGGTCTCGTAACG**
SRX44_3rLB_ol_for	CGGATGATAATACACTGACGCAACCATGGTAACAACATTTCGAAACGA
SRX44N_3rC_ol_rev	**CAGCCATGTGTCATCACATATCGAAGCTTAACAGTAGAAGTTTTGCT**
octr_3rLB_ol_for	CGGATGATAATACACTGACGCAACCATGTGGAACCTTAACTGCAGT
octrN_3rC_ol_rev	**CAGCCATGTGTCATCACATATCGAAATCAGTGCTAACGGAGCACT**
Daf38_3rLB_ol_for	CGGATGATAATACACTGACGCAACCATGCTTCTCCCTTCAAACTTG
Daf38N_3rC_ol_rev	**CAGCCATGTGTCATCACATATCGAACCAGAACTCGGCGTCAAA**
SRG37_3rLB_ol_for	CGGATGATAATACACTGACGCAACCATGAATCGAAATGTACTGGAATC
SRG37N_3rC_ol_rev	AGCCATGTGTCATCACATATCGAAAATTATCGCTTTAAATGTGGATAAAA
Site mutation GTT---AGA	
Pjet_for	ATCTTTCTAGAAGATCTCCTACA
Hyg_rev	TGGGGGGAGTTTAGGGAAA
GasALB_hyg_for	ATGCTCTTTCCCTAAACTCCCCCCACGTAACGACGCCGATTGAAT

GasA_G42R_ol_rev	ATCTGTTTTAAGATTGTGGACTTTCCGGATTCtctAGCACCTGT
GasA_G42R_ol_for	CCAACCGCTAAACTTGGGTCCGATCACAGGTGCTagaGAATCCG
GasARB_pjet_rev	ATTGTAGGAGATCTTCTAGAAAGATCCTCGATTACAATTGTTTGGAG
GasA_G42R_for	ACAGGTGCTAGAGAATCCG
GasA_G42R_rev	CGGATTCTCTAGCACCTGT
GasBLB_hyg_for	ATGCTCTTTCCCTAAACTCCCCCCAGGAGGGGTTGTTAAGGATGT
GasB_G45R_rev	CACTCTCTCTGGATCCTGT
GasB_G45R_for	ACAGGATCCAGAGAGAGTG
GasBRB_pjet_rev	ATTGTAGGAGATCTTCTAGAAAGATTCCGAGATAGCGGTGTTCA
GasA_mutate_seq_for	TTGCTATTGGGTACGTTCCG
GasB_mutate_seq_for	CTTTCTACGGCTCCTGAGAT
***plc1* deletion**	
PLC1LB_pjet_ol_for	GATGGCTCGAGTTTTTCAGCAAGATTTGTCGACTGTGCATCGTGA
PLC1LB_H_ol_rev	GTTGACCTCCACTAGCATTACACTTGGTGGGATATCCACCTCG
PLC1RB_H_ol_for	ATGCTCTTTCCCTAAACTCCCCCCACATGTTGAGCGTGGGATGAA
PLC1RB_pjet_ol_rev	ATTGTAGGAGATCTTCTAGAAAGATAACTGCTTCCAACTACCACG
H_PLC1LB_ol_for	GAACGTGCGAGGTGGATATCCCACCAAGTGTAATGCTAGTGGAGGT
H_PLC1RB_ol_rev	GACATTTCATCCCACGCTCAACATGTGGGGGGAGTTTAGGGAAA
PLC1LB_for	TTGTCGACTGTGCATCGTGA
PLC1RB_rev	AACTGCTTCCAACTACCACG
PLC1_ORFin_for	ATCGTAGATCCAGCAGCCTA
PLC1_ORFin_rev	CGTTCCACGACCGTTTAACA
PLC1ko_up_for	TGACTGTGACGAGCTTAGCT
PLC1ko_down_rev	GTGTTTGCTGAACAGATTGCT
***plc2* deletion**	
PLC2LB_pjet_ol_for	GATGGCTCGAGTTTTTCAGCAAGATATGGCAGTGTATGAGGAGCA
PLC2LB_H_ol_rev	GTTGACCTCCACTAGCATTACACTTGGTTTTCTAGGCTACTTGGTA
PLC2RB_H_ol_for	ATGCTCTTTCCCTAAACTCCCCCCAGTGTGATACATACGGGACTAT
PLC2RB_pjet_ol_rev	ATTGTAGGAGATCTTCTAGAAAGATTGTCTCGTCACCAGACTTCA
H_PLC2LB_ol_for	GTATTACCAAGTAGCCTAGAAAACCAAGTGTAATGCTAGTGGAGGT
H_PLC2RB_ol_rev	GTGAATAGTCCCGTATGTATCACACTGGGGGGAGTTTAGGGAAA

PLC2LB_for	ATGGCAGTGTATGAGGAGCA
PLC2RB_rev	TGTCTCGTCACCAGACTTCA
PLC2_ORFin_for	TCCGAAGCCTTCACCCAAT
PLC2_ORFin_rev	GGTGGTGAGTTCTTGGATC
PLC2ko_up_for	GGATGTTCCGAAAGAGTTGAA
PLC2ko_down_rev	GCTCTTGAGGCAAAGGTTATT
***gbsA* deletion**	
gbsALB_pjet_ol_for	GATGGCTCGAGTTTTTCAGCAAGATCGCTGCTCAACACATTTCCA
gbsALB_H_ol_rev	GTTGACCTCCACTAGCATTACACTTTCGGGAGGTTAGAGTACGAT
gbsARB_H_ol_for	ATGCTCTTTCCCTAAACTCCCCCCATCTCGCCCAGCTCACTAAAA
gbsARB_pjet_ol_rev	ATTGTAGGAGATCTTCTAGAAAGATTAGGGTAGACAGGCAAGGT
H_ gbsALB_ol_for	ATTTGATCGTACTCTAACCTCCCGAAAGTGTAATGCTAGTGGAGGT
H_ gbsARB_ol_rev	ATCACTTTTAGTGAGCTGGGCGAGATGGGGGGAGTTTAGGGAAA
gbsALB_for	CGCTGCTCAACACATTTCCA
gbsARB_rev	TAGGGTAGACAGGCAAGGT
gbsA_ORFin_for	CCGATGCTGATTGTGAGTTC
gbsA_ORFin_rev	CGGATCCAGTACCAAATGCA
gbsAko_up_for	TGGTTGTGGTGGTGCATTGT
gbsAko_down_rev	TGGTTCGTACATTAACACCGA
Site mutation	
Pjet_for	ATCTTTCTAGAAGATCTCCTACA
Hyg_rev	TGGGGGGAGTTTAGGGAAA
GasALB_hyg_for	ATGCTCTTTCCCTAAACTCCCCCCACGTAACGACGCCGATTGAAT
GasA_Q204L_rev	GAACGcaaACCACCAACG
GasA_Q204L_for	CGTTGGTGGTttgCGTTC
GasARB_pjet_rev	ATTGTAGGAGATCTTCTAGAAAGATCCTCGATTACAATTGTTTGGAG
GasBLB_hyg_for	ATGCTCTTTCCCTAAACTCCCCCCAGGAGGGGTTGTTAAGGATGT
GasB_Q208L_rev	TTTCGCTTCTaagACCACC
GasB_Q208L_for	GGTGGTcttAGAAGCGAAA
GasBRB_pjet_rev	ATTGTAGGAGATCTTCTAGAAAGATTCCGAGATAGCGGTGTTCA
GasA_mutate_seq_for	TTGCTATTGGGTACGTTCCG
GasB_mutate_seq_for	CTTTCTACGGCTCCTGAGAT
***gprC* deletion**	
GprCLB_pjet_ol_for	GATGGCTCGAGTTTTTCAGCAAGATGACAAATTGCAACTTCCGGC
GprCLB_H_ol_rev	GTTGACCTCCACTAGCATTACACTTCTTAAAGACTTCATTTGGGAGG

H_GprCLB_ol_for	CCCCCTCCCAAATGAAGTCTTTAAGAAGTGTAATGCTAGTGGAGGT
H_GprCRB_ol_rev	ATAACTCCGAAATGCAATTCTAAGGTGGGGGGAGTTTAGGGAAA
GprCRB_H_ol_for	GCTCTTTCCCTAAACTCCCCCCACCTTAGAATTGCATTTCGGAG
GprCRB_pjet_ol_rev	ATTGTAGGAGATCTTCTAGAAAGATAGTTTCCGGAGAAGAAGCC
GprCLB_for	GACAAATTGCAACTTCCGGC
GprCRB_rev	AGTTTCCGGAGAAGAAGCC
GprCLB_for-n	TCAATCCAAAAGCTTCAGTGG
GprCRB_rev-n	GAGGAGTGAATCTTGATAGCT
GprC_ORFin_for	GGTTCCCAGTTTTATCCTCC
GprC_ORFin_rev	AAGCGCAGTGATGGATACCA
GprCko_up_for	GGCACGGTTGAGTTTAGCTT
GprCko_down_rev	GCATCGGTGTTGTAAAACGTA
***gprD* deletion**	
GprDLB_pjet_ol_for	GATGGCTCGAGTTTTTCAGCAAGATAGTATCCAAGGGAGTCCTAG
GprDLB_H_ol_rev	GTTGACCTCCACTAGCATTACACTTCTCCGGCTAAATGTCACCA
H_GprDLB_ol_for	GGGCGCTGGTGACATTTAGCCGGAGAAGTGTAATGCTAGTGGAGGT
H_GprDRB_ol_rev	AAAAGCAAAGCAAGCTGGTATCTAATGGGGGGAGTTTAGGGAAA
GprDRB_H_ol_for	ATGCTCTTTCCCTAAACTCCCCCCATTAGATACCAGCTTGCTTTGC
GprDRB_pjet_ol_rev	ATTGTAGGAGATCTTCTAGAAAGATATTCGACCGCGATGCAATAC
GprDLB_for	AGTATCCAAGGGAGTCCTAG
GprDRB_rev	ATTCGACCGCGATGCAATAC
GprDLB_for-n	GCGGGAAGAGATGTCTAAATT
GprDRB_rev-n	CAAAAGACCCTGCCGTATG
GprD_ORF_for	ATGACGCAACTCCCGTACTT
GprD_ORFin_rev	GCCGCCTGTTAATTAAAGAGA
GprDko_up_for	CCACTTTGATCCCTCAAGCT
GprDko_down_rev	ACACCGCAAGCCGAGAATAT
Y2H	
BD-GasA-for	ATATGGCCATGGAGGCCGAATTCCCATGGGTTGCAGCATGTCTAC
BD-GasA-rev	GGCCGCTGCAGGTCGACGGATCCCCTTATATCAGACCGCAGTTTCTG
AD-GasA-for	CAACGCAGAGTGGCCATTATGGCCCATGGGTTGCAGCATGTCTAC
AD-GasA-rev	CGAGGCGGCCGACATGTTTTTTCCCTTATATCAGACCGCAGTTTCTG
BD-GasB-for	ATATGGCCATGGAGGCCGAATTCCCATGGGTGGCTGCATGTCG

BD-GasB-rev	GGCCGCTGCAGGTCGACGGATCCCCTAAGATACCAGAGTCCTTGAG
AD-GasB-for	CAACGCAGAGTGGCCATTATGGCCCATGGGTGGCTGCATGTCG
AD-GasB-rev	CGAGGCGGCCGACATGTTTTTTCCCTAAGATACCAGAGTCCTTGAG
BD-GprC3-for	ATATGGCCATGGAGGCCGAATTCCCCGAAAACGGTTCGGTGCG
BD-GprC3-rev	GGCCGCTGCAGGTCGACGGATCCCCAATTCTCCTAACCCTTCTCGA
AD-GprC3-for	CAACGCAGAGTGGCCATTATGGCCCCGAAAACGGTTCGGTGCG
AD-GprC3-rev	CGAGGCGGCCGACATGTTTTTTCCCAATTCTCCTAACCCTTCTCGA
BD-GprC4-for	ATATGGCCATGGAGGCCGAATTCCCAACGAAAGAGTCTGGAGACAA
BD-GprC4-rev	GGCCGCTGCAGGTCGACGGATCCCCTTACTCTCTTCGCGGTCC
AD-GprC4-for	CAACGCAGAGTGGCCATTATGGCCCAACGAAAGAGTCTGGAGACAA
AD-GprC4-rev	CGAGGCGGCCGACATGTTTTTTCCCTTACTCTCTTCGCGGTCC
PefD reporer assay	
P5559_h2b_ol_for	TTGTAAAACGACGGCCAGTGAATTCCGAAGACCTTTGCTGTTCTC
P5559_h2b_ol_rev	TCGGCGGCGGCTTTTGGTGGCATTTTGATAGTATGAAAGTTTATATGGTT
PefD laccase assay	
5559_gpd_for	caggcgcgccATGAAGATCTCATTCGTTTTCG
5559_LA_rev	gaaccggtGTTCTTCTTGCAGTGCTCCT
PefD no SP localization	
5559wosp_cGFP_Asc1_for	CCggcgcgccATGGTAGCAATTCCCTCTACT
5559_cGFP_Pac1_rev	cttaattaaGTTCTTCTTGCAGTGCTCCT
pefD(p)::pefD::GFP::gluC(t)	
5559_LB_ol_for	TTTCCCTAAACTCCCCCCActgcagCGAAGACCTTTGCTGTTCTC
5559_cGFP_ol_Pac1_rev	CACCCTTGGAAACCATcttaattaaGTTCTTCTTGCAGTGCTCCT
BB_cGFP_Pac1_for	ttaattaagATGGTTTCCAAGGGT
BB_LB_PefC_rev	ctgcagTGGGGGGAGTTT
oliC(p)::pefD::GFP::gluC(t)	
5559_cGFP_Asc1_for	CCggcgcgccATGAAGATCTCATTCGTTTTCGC
5559_cGFP_Pac1_rev	cttaattaaGTTCTTCTTGCAGTGCTCCT
hinA(p)::hinA::GFP::gluC(t)	
8101_LB_ol_for_n	TTTCCCTAAACTCCCCCCActgcagCAAGTATCAAATATGCATGCCT
8101_cGFP_ol_Pac1_rev	CACCCTTGGAAACCATcttaattaaGTTCTTCAAGCCAGCATACTT
BB_cGFP_Pac1_for	ttaattaagATGGTTTCCAAGGGT
BB_LB_PefC_rev	ctgcagTGGGGGGAGTTT
pefD(p)::pefD:: mCherry::gluC(t)	
5559_LB_ol_fo	TTTCCCTAAACTCCCCCCActgcagCGAAGACCTTTGCTGTTCTC

5559_mcherry_ol_Pac1_rev	CCTCGCCCTTGCTTACcttaattaaGTTCTTCTTGCAGTGCTCCT
BB_mcherry_Pac1_for	ttaattaagGTAAGCAAGGGCG
BB_LB_PefC_rev	ctgcagTGGGGGGAGTTT
***pefD* deletion**	
5559LB-pjet-ol-for-n	GATGGCTCGAGTTTTTCAGCAAGATAACCTGCGTTAGTCGCGATT
5559LB-H-ol-rev	TGACCTCCACTAGCATTACACTTTTTGATAGTATGAAAGTTTATATGGTT
5559RB-H-ol-for	ATGCTCTTTCCCTAAACTCCCCCCAGATACAGATTTTGTTAAACTGCG
5559RB-pjet-ol-rev-n	ATTGTAGGAGATCTTCTAGAAAGATTTAGAAGGCAGTCTTGACGG
H-5559LB-ol-for	CCATATAAACTTTCATACTATCAAAAAGTGTAATGCTAGTGGAGGT
H-5559RB-ol-rev	TCCGCAGTTTAACAAAATCTGTATCTGGGGGGAGTTTAGGGAAA
5559ko_up_for_n	CTACCAAACTTCGAAGAAGG
5559ko_down_rev_nn	GAGCCCTCAATATTTCTGTAC
oliC(p)::rab7:: mCherry::gluC(t)	
Rab7_Polic_ol_for	TCACAATCGATCCAACCggcgcgccATGTCCTCGAGAAAGAAGGTC
Rab7_mcherry_ol_rev	CCTCGCCCTTGCTTACcttaattaaACAAGCGCACCCATCTCTG
BB_mcherry_Pac1_for	ttaattaagGTAAGCAAGGGCG
BB_Polic_Asc1_rev	ggcgcgccGGTTGGAT
***pefD* over-expression**	
5559_Polic_Asc1_ol_for	TCACAATCGATCCAACCggcgcgccATGAAGATCTCATTCGTTTTCG
5559ATG_Tgluc_ol_rev	TAATCATACATCTTATCTACATACGTTAGTTCTTCTTGCAGTGCTC
BB_Tgluc_for	CGTATGTAGATAAGATGTATGATT
BB_Polic_Asc1_rev	ggcgcgccGGTTGGAT
oliC(p)::pefD$^{\Delta SP\Delta Prop}$:: mCherry::gluC(t)	
Mcherry_Pac1_5559_ol_for	GCACTGCAAGAAGAACttaattaagGTAAGCAAGGGCGAGGTAA
Mcherry_ATG_Tgluc_ol_rev	TCATACATCTTATCTACATACGCTAAGCGGCCGCTTTGTAGAG
BB_TAG_Tgluc_for	TAGCGTATGTAGATAAGATGTATG
BB_Pac1_5559_rev	cttaattaaGTTCTTCTTGCAGTG
oliC(p)::pefD$^{\Delta Prop}$:::gluC(t)	
5559noProp_SP_ol_for	CTTCCTCCTCGCTACTGCTCAGGCTGCAGATATTGACTGCGAAAAG
5559ATG_Tgluc_ol_rev	TAATCATACATCTTATCTACATACGTTAGTTCTTCTTGCAGTGCTC
BB_Tgluc_fof	CGTATGTAGATAAGATGTATGATT
BB_5559SP_rev	AGCCTGAGCAGTAGCGAG
hsp-16.48(p)::GFP::unc-54UTR	

Phsp_ppf37_ol_for	AGATATCCTGCAGGAATTCCTCGAGGCTGGACGGAAATAGTGGT A
Phsp_GFP_ol_rev	CTGAGCCTCCAGATCCACCTGACATttcttgaagtttagagaatgaacag
BB_ppf37GFP_for	ATGTCAGGTGGATCTGGAG
BB_MCS_rev	CTCGAGGAATTCCTGCAGG
hsp-16.48(p)::pefD::GFP ::unc-54UTR	
5559_Phsp_ol_for	ctgttcattctctaaacttcaagaaATGAAGATCTCATTCGTTTTCG
5559_ppf37_ol_rev	AAACTGAGCCTCCAGATCCACCTGAGTTCTTCTTGCAGTGCTCC T
BB_ppf37_for	TCAGGTGGATCTGGAGGCT
BB_Phsp_rev	ttcttgaagtttagagaatgaacag

4.3 Microbiological methods

All the microbes were autoclaved before being thrown. All the microorganisms used in this work were autoclaved at 121° C for 20 min. The heat sensitive stuff was sterilized with the membrane filter (Pore size 0.22 µm; Merck, Darmstadt).

4.3.1 Microbiological methods of *E. coli*

For the cultivation, *E. coli* was kept on the solid LB agar or liquid LB at 37° C for overnight. For selection 100 µg/ml Ampicillin was added. For the permanent stock, 1 ml of overnight culture was mixed with 1 ml 50 % Glycerol and mixed well, kept in -80° C.
For the transformation into the competent cell of *E. coli* Top10, 100-1000 ng plasmid DNA or 10 µl of the Gibson Assembly product was added and incubated for 15-20 min on ice. After the heat shock at 42° C for 90 s, the cell was incubated on ice for 2-3 min. Afterwards it was spread evenly with the sterile triangle spreader on the LB plate including Ampicillin for the incubation for overnight at 37° C.

Table 8: The medium and solution used for *E. coli.*

Solution	**Composition**
LB (Lysogeny Broth)	10 g Trypton 5 g Yeast extract 5 g NaCl 15 g Agar pH 7.0
Ampicillin (1000 x)	5 g Ampicillin 25 ml ddH_2O 25 ml 100 % Ethanol Kept in -20° C

4.3.2 Microbiological methods of *S. cerevisae*

Preparation of competent yeast cells — LiAc Method

Before starting, the starting strain AH109 or Y187 was streaked on a YPDA agar plate with a small portion of frozen yeast stock and incubated at 30° C for 3 days.

For preparation of the competent cells, one big colony was picked and well suspended in a 250 ml flask containing 50 ml YPDA for overnight at 220 rpm 30° C until the OD600 reaching 0.15-0.3. Then estimated volume of the overnight culture was transferred into a 250 ml flask containing 50 ml 2 x YPDA at 220 rpm 30° C for 3 h until the OD600 between 0.4-0.7. Afterwards the culture was centrifuged at 2000 rpm for 5 min and the supernatant was discarded. The cell pellet was re-suspended in 50 ml sterile ddH_2O for the second time of centrifuge. After the supernatant was discarded, the cells were re-suspended in 1.5 ml of 1.1 x TE/LiAc Solution.

Note: Competent cells should be used for transformation immediately following preparation; however, if necessary they can be stored at room temperature for a few hours without significantly affecting the competency.

Small-scale yeast transformation

The stuff was added as the following order.

Component	1 (µl)	2 (µl)	3 (µl)	4 (µl)
pGADT7- GasA	1	-	-	-
pGADT7- GasB	-	1	-	-
pGBKT7- loop3	-	-	1	-
pGBKT7- loop4	-	-	-	1
Herring Testes Carrier DNA (10 mg/ml), denatured*	5	5	5	5
AH109 competent yeast cells	-	-	50	50
Y187 competent yeast cells	50	50	-	-
PEG/LiAc Solution	500	500	500	500
SD plate	-Leu	-Leu	-Trp	-Trp

* heated at 95°C for 10 min and immediately chilled in an ice bath for 1 min.

The mixture was vortexed thoroughly and incubated for 30 min at 220 rpm 30° C. Then 70 μl of DMSO (Sigma) was added and mixed well by vortexing for heat shock at 42° C for 15 min with gentle shaking, at the mean time being inverted every 5 min. Afterwards the cells were chilled on ice for 1-2 min. For the recovery the cells were collected by being centrifuged at 14000 rpm 5 s and mixed with 0.5 ml 2 x YPDA by pipetting and shaking for 1.5 h at 220 rpm 30° C. Afterwards the cells were collected by centrifuged for 5 s at 14000 rpm and re-suspended in 0.5 ml of 1 x TE buffer. 200 μl of the suspended cells was spread on SD plate (-Leu or -Trp) with glass beads and incubated at 30° C for 2-4 days. When the transformants appeared, one of the

biggest colonies was picked and streaked on the same selection medium.

Small-scale yeast mating

One colony of each type (an AH109 with a Y187) was picked, suspended and incubated in the glass tube containing 0.5 ml of 2 x YPDA medium for overnight at 70 rpm 30° C. The cells were spread on SD minimal media with sterile 5 mm glass beads to promote even spreading of the cells and incubated at 30°C for 3-5 days to allow diploid cells to form visible colonies. One of the biggest colonies was picked and streaked on a fresh SD medium lacking in Trp and Leu (SD-LW). The Mating scheme was performed as below:

AD GasA x BD loop 3
AD GasB x BD loop 3
AD GasA x BD loop 4
AD GasB x BD loop 4
AD loop 3 x BD GasA
AD loop 3 x BD GasA
AD loop 4 x BD GasB
AD loop 4 x BD GasB

Yeast growth assay

A 5 ml overnight culture of diploid was prepared at 220 rpm 30° C. On the second day, the same concentration of the cells was prepared and they were diluted for 1:10, 1:100 and 1:1000. 5 µl of each suspension was dropped onto one SD-LW, TDO (SD-LWH) and QDO (SD-LWHA) plate respectively including the positive (sRM49: pGADT7-T x pGBKT7-p53) and negative (sRM50: pGADT7-T x pGBKT7-Lam) control.

Table 9: The media and solutions used for yeast.

Solution	Composition
PEG/LiAc Solution	8 ml 35 % PEG4000 1 ml 10 x TE Buffer 1 ml 1 M LiAc (10 x)
1.1X TE/LiAc Solution	1.1 ml 10 x TE 1.1 ml 1 M LiAc (10 x) To 10 ml with ddH_2O
YPDA medium	20 g/L Peptone 10 g/L Yeast extract 20 g/L Agar 0.03 % Adenine hemisulfate

	Add ddH_2O to 950 ml
	Adjust the pH to 6.5
	Autoclaved
	50 ml 40 % dextrose (glucose) (2 %)
SD medium	6.7 g Yeast nitrogen base without amino acids
	20 g Agar
	20 g Glucose
	Appropriate amino acids lack specific nutrients

4.3.3 Microbiological methods of *A. flagrans*

Cultivation of *A. flagrans*

A. flagrans was cultivated in Petri dishes with PDA at 28°C for 5-10 days. For selection, 100 µg/ml Hygromycin or 150 µg/ml Geneticin was added. For the maintenance, mycelia and spores were scraped off a 7-day-old-plate culture and suspended in 2 ml 25 % glycerol.

A. flagrans transformation

The mycelia and spores from a 7-day-old-plate culture of *A. flagrans* were collected and inoculated in 100 ml of PDB and incubated at 28 ° C and 180 rpm for 24 hours. The mycelium was filtered through sterile one layer Miracloth and washed with MN buffer. The wet mycelia were transferred to 5 ml of MN buffer with 25 mg kitalase and 100 mg Glucanx (Novozyme) and incubated at 28 ° C 70 rpm for 2-3 hours. The amount of protoplast was checked microscopically. Then the protoplast was collected by being filtered through two layers of Miracloth to separate undigested mycelium. The filtrate was filled to 50 ml with MN buffer and centrifuged for 15 minutes at 2500 rpm. The supernatant was removed and the protoplast washed again with 50 ml KTC buffer. The protoplast pellet was re-suspended in 0.5-1 ml of KTC and then kept on ice or in -4° C. The concentration was calculated by the Hemocytometer.

For the transformation, 100 µl of protoplasts (the number is about 20 x 10^6) are mixed with 3 µg plasmid DNA and incubated for 2 minutes on ice. Next, 1 ml PTC6000 solution was added to the falcon, carefully mixed and incubated for 20 minutes at room temperature. Thereafter, the falcon is filled to 10 ml with hand-warm-PDASS melted with microwave. After a short inverting the mixture was applied to a Petri dish with PDA containing Hygromycin or Geneticin and incubated for 7 days at 28 ° C until the colonies appearing.

Trap induction and slide preparation

For the trap induction, a solid, thin LNA agar was prepared firstly. For this, a slide was put between two slides wrapped with adhesive tape. And another slide was placed on two wrapped slides perpendicularly as a bridge, leading to the formation of gap

between the bridge slide and the middle slide. Then the gap was filled with 0.5 ml melted LNA until the agar solidifying. Mycelia of *A. flagrans* were picked with a toothpick, and rolled on the thin agar block letting the spores in the mycelia left. The slide was put on two 1 ml pipette tips in a sterile Petri dish with a little water. After the incubation at 28° C for hours, the spores would be germinated, and the nematodes were rinsed off the original NGM plate and added on the slide. The next day, the sample was examined by the microscope.

The application of 8'-Bromo-cAMP

8'-Bromo-cAMP (Darmstadt, Sigma) was used as the analog of cAMP. 1mg of it was dissolved into 20 µl 1 M Ammonia as the stock solution of 50 mg/ml (122.52mM) and the working concentration is 5mM after being suspended in the melted medium which was cooled down to the proper temperature.

Preparation of spore suspension

The mycelia and spores were scraped off a 7-day-old-plate culture of *A. flagrans* with an inoculation shovel and transferred into a 50 ml falcon. It was filled to 50 ml with sterile water and vortex of the suspension of spores. Afterwards the suspension was filtered with 2 layers of Miracloth into a new falcon. The filtered spores were centrifuged at 13,000 rpm for 5 min and the supernatant was discarded. Then the spores were re-suspended with 1 ml water. The concentration was checked and calculated by the Hemocytometer. The counted area is 0.0025 mm^2 and the depth 0.02 mm, leading to the volume of 0.0025 x 0.02 mm^3. 1ml equals to 1000 mm^3.

The number of spores/ml = $\frac{\text{the number of spores counted x } 1000}{0.0025 \text{ x } 0.02}$

Table 10: The media and buffers used for *A. flagrans.*

Solution/L	Composition
Potato Dextrose agar	24 g Potato Dextrose Broth
	Set pH to 6.6 with NaOH
	15 g Agar
PDASS top agar	24 g Potato Dextrose Broth
	205 g Sucrose
	0.3 g Yeast extract
	0.3 g Pepton
	Set pH to 6.6 with NaOH
	7.5 g Agar
Low nutrient agar (LNA)	1 g KCl
	0.2 g $MgSO_4 \cdot 7\ H_2O$
	0.4 mg $MnSO_4 \cdot 4\ H_2O$
	0.88 mg $ZnSO_4 \cdot 7\ H_2O$

	3 mg $FeCl_3 \cdot 6\ H_2O$ Set pH to 5.5 with 0.1 M HCl 10 g Agar
MN buffer	75.8 g $MgSO_4 \cdot 7H_2O$ 17.54 g NaCl
KTC buffer	89.46 g KCl 7.4 g $CaCl_2$ 10 ml Tris-HCl (1 M)

4.3.4 Microbiological methods of *C. elegans*

Methods used for *C.elegans* mostly were according to the NematodeBook (Stiernagle, 2006).

Cultivation of *C. elegans*

Nematode Growth Medium was melted by microwave, and after being added the sterile additional solutions, it was poured on Petri dishes and dried out in the clean bench. *E. coli OP50*, cultivated by shaking at 37 ° C 180 rpm overnight, was added on the NGM plates, approximately 300 µl on the 6 cm and 500 µl on the 9.2 cm Ø Petri dishes until it dried out.

For the cultivation of *C. elegans*, a circa 0.5 cm large agar block of a 5-day-old *C. elegans* culture plate was cut out and transferred to a fresh NGM agar plate on the grass of bacterial. The culture took place for 4-7 days.

***C. elegans* rinse**

To rinse the nematodes from the agar plate, it was washed with 1 ml of sterile water into an eppi tube. The nematode suspension was centrifuged in 2000 rpm for 2 min and discarded the supernatant to get rid of the bacteria. Then the washing step was repeated until the supernatant was clear. The nematode suspension was ready to be used after discarding the supernatant.

Ascarosides extraction

The extraction of a blend of ascarosides was followed generally a reported protocol (Zhang *et al*, 2013). 90,000 nematodes were inoculated into the culture medium of 150 ml and incubated at 20 °C for 9 days for being shaken at 225 rpm. Then the culture was cooled on ice for 1 h before the nematodes were precipitated by centrifugation of 10,000 rpm, 30 min. The supernatant liquid was freeze-dried, and the dried material was suspended in the solution of 20 ml chloroform: methanol (3:1). After evaporation of the supernatant, the residual part was dissolved in 1000 µl ddH2O and centrifuged to remove insoluble solid material, and then the solvent was freeze-dried again. The final compound was redissolved in 500 µl ddH2O and filtered

through a membrane (22 µm pore Ø). The isolated ascaroside blend was added to the targeted samples.

Generation of transgenic *C. elegans* strains

Plasmids harboring the *pefD* fusion constructs were injected at a concentration of 5 ng/µl into wildtype nematodes (N2) with a pharyngeal co-injection marker (*myo-2p::tdTomato*) 5 ng/µl and 1 kb ladder (Eurofins) as filler DNA. Co-injection marker positive transformants were selected.

Table 11: The media and buffers used for *C. elegans.*

Solution/L	Composition
M9 Buffer	3 g KH_2PO_4
	6 g Na_2HPO_4
	5 g NaCl
	1 ml $MgSO_4$ (1 M)
Nematode Growth Medium (NGM)	3 g NaCl
	2.5 g Pepton
	1 ml Cholesterol (5mg/ml in Ethanol)
	17 g Agar
	Autoclaved
	1 ml $CaCl_2$ (1M)
	1 ml $MgSO_4$ (1M)
	25 ml KPO_4 Buffer
	(10.83 g KH_2PO_4, 3.56 g K_2HPO_4)

4.4 Molecular biological methods

4.4.1 Polymerase chain reaction (PCR)

The PCR was performed with Phusion - DNA - Polymerase or Q5 High - Fidelity DNA - Polymerase (NEB) as the manufacturer protocols. Oligonucleotides were synthesized by Eurofins Genomics Germany GmbH (Ebersberg, Germany), and a 10 mM concentration of the diluted primer was used for the PCR. The reaction was carried out with the PCR cycler. The reaction system and program are listed as below:

Reaction system:	
Template	1 µl (gDNA 100-300 ng, plasmid 30-50 ng)
Forwad primer	2.5 µl
Reverse primer	2.5 µl
Q5 buffer	10 µl
Q5 polymerase	2.5 U
ddH_2O	To 50 µl

PCR program:

Temperature	Duration	Cycle
95° C	5 min	
95° C	1 min	32 cycles
50-80° C	1 min	
72° C	30 s/kb	
72° C	10 min	

Note: The annealing temperature depends on the oligonucleotides.

4.4.2 DNA agarose gel electrophoresis and gel recovery

The PCR product and other DNA samples were separated and identified by a running agarose gel. The agarose was normally made in a 0.8-2 % concentration with 0.5 x TAE buffer. The melting agarose was mixed with 2 µl 1:10 diluted Midori Green Advance (Biozym) and poured into a gel chamber with corresponding comb. Until solidification the PCR product or DNA samples were combined with 6 x loading dye and pipetted into the gel hole. At the mean time 1 kb DNA ladder (New England Biolabs) was added as the reference. Then the gel was run for 15 min - 1 h at 100 V in the gel chamber and the duration depends on the length of DNA. After running the DNA band was visualized in the gel at 302 nm UV light. The camera (INTAS, Goetting) connecting to the video printer was used to take a photo.

The corresponding DNA bands were cut out under UV light with the protection of glasses and put into an eppi tube. The PCR product was recovered from an agarose gel with the Zymoclean Gel DNA Recovery Kit (Zymo Research).

Table 12: Solutions used for the molecular biological methods.

Solution	Composition
50 x TAE buffer (pH 8.0)	40 mM Tris-HCl 2 mM EDTA 20 mM NaAc
DNA loading dye (6 x)	0.25 g Bromophenol blue 3 ml glycerol 7 ml ddH_2O

4.4.3 DNA digestion and ligation

The genomic DNA or plasmid was digested with restriction endonucleases using appropriate reaction buffers from New England Biolabs.

	gDNA digestion	Plasmid digestion for ligation	Plasmid digestion for confirmation
DNA	25 µl of pure	5 µl of midi	2 µl of mini

	extraction product	preparation product	preparation product
Restriction enzyme	2 µl	2 µl	1 µl
Buffer(10 x)	5 µl	5 µl	1 µl
ddH_2O	To 50 µl	To 50 µl	To 10 µl
Duration	Overnight	2 h - overnight	20 min
Temperature	37° C	37° C	37° C

The DNA ligation was carried out with T4 ligase (1 U/µl; NEB) for 1 h at room temperature in a volume of 20 µl. The ratio of vector to insert was 1:3 respectively for ligation.

4.4.4 Cloning with Gibson-Assembly

Cloning was performed with Gibson-Assembly by ligating insert and vector. Both of them were amplified with PCR and the primers for insert carried 25 bp overlap for ligation. The ratio of vector to insert was 1:2 and they were combined with 15 µl Gibson Assembly enzyme mix, bringing the total volume into 20 µl. The reaction was incubated for 30 min at 50° C and then 10 µl of it was transformed into *E. coli*.

Table 13: The composition of Gibson-Assembly-Enzyme-Mix.

Reagent	Concentration
Iso-Buffer (5 x)	26.6 % v/v
T5-Exonuclease (10 u/µl)	5.3 um/ml
Q5-Polymerase (2 u/µl)	33.3 u/ml
Taq Ligase (40 u/µl)	5333.3 u/ml
ddH_2O	58.3 % v/v

4.4.5 Mini-preparation of plasmid DNA from *E. coli* by alkaline lysis method

Plasmid DNA was isolated from *E. coli* transformants by means of alkaline lesis. For this purpose, 1.5 ml of an overnight culture was pelleted for 1 min at 13,000 rpm. After discarding the supernatant, the pellet was dissolved in 200 µl re-suspension buffer. Afterwards 200 µl lysis buffer was added and mixed well by inverting 5 times. Macromolecules were precipitated by adding 200 µl of a 1.5 M KAc (pH 4.8), incubated for 10 min on ice and centrifuged for 5 min at 4° C and 13,000 rpm. Then the supernatant was transferred in reaction vessels with 500 µl 100 % isopropanol and incubated for 10 min on ice. The plasmid DNA was then pelleted at 4° C and 13,000 rpm for 5 min. Then the pellet was washed with 500 µl 70 % ethanol, subsequently tried at 58° C and dissolved in 20 µl ddH_2O.

Table 14: The solutions for mini-preparation of the plasmid DNA.

Buffer	Composition
Re-suspension buffer	50 mM Tris-HCl (pH 7.5) 10 mM Na_2EDTA 100 µg/ml RNase A
Lysis buffer	0.2 M NaOH
KAc	1 % SDS 1.5 M KAc (pH 4.8)

4.4.6 Midi-preparation of plasmid DNA from *E. coli* with the kit and DNA sequence

The plasmid DNA isolated from mini-preparation was verified with restriction enzyme. Then the *E. coli* strain was cultured in a flask with 50 ml LB containing ampicillin. The culture was used for the midi-preparation with NucleoSpin Plasmid EasyPure Kit (Macherey Nagel).

4 ml of the overnight culture was pelleted and the supernatant was discarded. The pellet was resuspended in 150 µl A1 buffer by vortex. Then 250 µl A2 buffer was added and inverted for 5 times. After incubation for 2min at room temperature, 350 µl A3 buffer was added and inverted until the lysate became white then centrifuged for 3 min at 4° C and 13,000 rpm. A column was put in a collecting tube and 700 µl of the supernatant was transferred into it. The flow was discarded after centrifugation for 30 s at 2000 x g. Then 450 µl AQ buffer was pipette inside the column and centrifuged for 1min at 4° C and 13,000 rpm. The centrifugation was repeated again to make the filter in the column tried. A new eppi tube was prepared and the column was put on it. They were centrifuged for 1 min at 13,000 rpm for collecting the DNA. At last the concentration of plasmid DNA was measured with the Nanodrop.

For sequencing, 50-100 ng/µl of the plasmid DNA was mixed with the primer and sent to Eurofins MWG as the final step of confirmation when it is needed.

4.4.7 Preparation of genomic DNA of *A. flagrans*

For the isolation of gDNA from the 2-3 day-colonies of transformants, a small block of agar with fungus was picked into an eppi tube, crushed and sunk inside 750 µl of lysis buffer 1. The eppi tube was incubated for 60 minutes at 65° C on a shaking thermo heater. Afterwards 350 µl KAc buffer 1 was added and incubated on ice for 15 min. Cell debris and agar were centrifuged for 30 min at 13,000 rpm, 4° C and 700 µl of the supernatant was then transferred to a new reaction vessel with 800 µl of 100 % isopropanol, inverted several times and incubated for 20 min at -20° C. Subsequently the DNA pellet was collected by centrifuging for 15 min and washed again with 70 % ethanol. After drying for 3 min on 68° C, the pellet was dissolved in 50 µl of TE buffer with 50 µg/ml RNase A by shaking at 68° C.

For a pure genomic DNA extraction, the mycelia and spores were scraped out of a 7-day-old culture and spread into a 6 cm Ø Petri dish with PDB and incubated at 28 °

C for 2 days around. Then the mycelia were rubbed in a mortar with the help of liquid nitrogen. The mycelium powder was spread into a 1.5 ml eppi tube with 700 µl of lysis buffer 2 and incubated for 60 min at 65° C on a shaking thermo heater. By adding 200 µl of 3M KAc buffer 2 and inverting 10 times, proteins were precipitated on ice for 30 min. Afterwards the eppi was centrifuged for 15 min at 13,000 rpm, 4° C and 500 µl of the supernatant was transferred into a new eppi tube and incubated in -20° C for 20 min. After centrifuging 15 min at 13,000 rpm, 4° C, the DNA pellet was washed with 70 % ethanol by centrifuging for 5 min. Subsequently DNA was dried and dissolved in 50 µl of TE buffer with 50 µg/ml RNase A by shaking at 68° C.

Table 15: Buffers for the isolation of genomic DNA of *A. flagrans.*

Buffer	Composition
Lysis Buffer 1	0.2 % SDS 50 mM Na_2EDTA, pH 8.0
KAc Buffer 1	1.5 M KAc, pH 4.8
Lysis Buffer 2	1 % SDS 50 mM Tris-HCL, pH 7.5 50 mM Na_2EDTA, pH 8.0
KAc Buffer 2	1.5 M KAc, pH 4.8
TE Buffer (10 x)	100 mM Tris-HCL, pH 7.9 10 mM Na_2EDTA

4.4.8 Isolation of RNA of *A. flagrans*, Synthesis of cDNA from RNA and qRT PCR

For the preparation of fungus for the RNA isolation, the mycelia scraped from a 7-day-old culture were grown in PDB for 2 days at. For the expression analysis of induced mycelia, 1 x 10^6 spores were evenly spread on the autoclaved cellophane on top of the LNA plate at 28° C. After 24 h, nematodes rinsed from 5 of the 9 cm 7-day-old NGM plate were added between the mycelia and incubated for another 24 h at 28° C. On the third day, trap production was checked under a microscope.

For the isolation of RNA from *A. flagrans*, the E.Z.N.A. Fungal RNA Mini Kit (Omega, Bio-Tek) was used as the manufacturer protocol. Some of frozen gound fungal tissue ground with liquid nitrogen was added to a 1.5 ml microcentrifuge tube and immediately 500 µl RB buffer mixed with 2-mercaptoethanol was pipette in and vortexed vigorously to make sure that all of the clumps have dispersed. A homogenizer Mni Column was put into a 2 ml Collection tube and the lysate was transferred to the Homogenizer Mini Column for centrifuging 5 min at 13,000 x g at room temperature. Carefully 450 µl of the supernatant of the filtrate was transferred to a new 1.5 ml microcentrifuge tube and 225 µl 100 % ethanol was added and mixed thoroughly by vortex. A HiBind RNA Mini Column was inserted in to a 2 ml Collection Tube and all the liquids including any precipitates from the centrifuge tube were transferred into the HiBind Column. After centrifuging at 10000 x g for 30 sec at room temperature, the filtrate was discarded and the collection tube was reused. 500 µl of

the RNA Wash Buffer I was added in the HiBind Column and centrifuged at 10000 x g for 30 sec at room temperature. After discarding the filtrate and the collection tube, the HiBind RNA Column was transferred into a new collection tube and 500 µl RNA Wash Buffer II was added and centrifuged at 10000 x g at 30 sec at room temperature. Then the filtrate was discarded and the wash step with RNA Wash Buffer II was repeated again. Subsequently the tube and column were centrifuged at 13,000 rpm for 2 min at room temperature for complete drying of the HiBind RNA Mini Column. The dried Column was transferred to a clean 1.5 ml microcentrifuge tube and the RNA was collected by centrifuging for 1min at top speed after adding 50 µl Nuclease-free Water.

For the synthesis of coding DNA, the SuperScript Double-Stranded cDNA Synthesis Kit (Thermo Fisher Scientific) was used as the manufacturer protocol.

For the gene expression analysis with quantitative Real Time RT-PCR, the LuNA Universal One-Step RT-QPCR Kit (NEB) was used by manufacturer's instructions and the reaction in the ICCLER IQ (Bio-Rad) was performed. The RNA was previously treated with the DNase Turbo DNA Free Kit (Invitrogen by Thermo Fischer). The putative gamma actin gene *dfl_002353* was used as a reference for quantification of relative expression. The expression was calculated with the formula $2^{-(\Delta\Delta Ct)}$.

4.4.9 Southern blot

The pure genomic DNA was isolated as **4.4.7**, and a gel was run to check the quality and quantity of gDNA. Then the gDNA was digested overnight with corresponding restriction enzyme. The probe was prepared by PCR amplification with DIG Probe Synthesis Kit as manufacturer's instructions. It is recovered from a gel by being frozen in -80° C for 10 min and squeezed into a centrifuged tube. As a comparison, the band with DIG ran slowly than it without DIG.

On the second day a small gel was run to check the gDNA digested thoroughly. Afterwards the gDNA was precipitated by being mixed with 2-3 x 100 % ethonal and 1/10 3 M NaAc, inverted several times and incubated for 20 min at -20° C, washed with 70 % ethonal, dried out on thermol heater and dissolved with 30 µl ddH_2O. Then a big 0.8 % gel was run with 30 µl gDNA and 6 µl loading dye for 1 h (depends on the lengths of bands, enough for differentiation). After taking a picture, a tip was used to make holes on the ladder and a knife was used for cutting off the borders and margins. Then the gel was washed in 0.25 M HCl solution for 20 min in slow speed. After the band of loading dye becoming yellow for at least 5 min, the gel was rinsed shortly in sterile ddH_2O and also in DENAT solution for 20 min till color turns back and rinse again. The last step is still washing in RENAT solution for 20 min. When the gel was ready for membrane transferring, 20 x SSC buffer was poured in a flat bowl and a glass slide on top, then the whatman paper on the glass and its borders soaked in the buffer as a bridge. The gel was put on the bridge upside-down without any air bubble. The Nylon membran (Roti-Nylon plus, Roth) in the same size with the

gel was put on top of gel without any air bubble. Afterwards three same sized whatman papers were put on the membrane and then a stack of paper towels on it. On the very top some weight was put.

After transferring overnight, the gel and membrane were downside-up, and the marker was marked with a tip. A gel scanner was used to make sure the gel is empty of any band. The membrane marked of the ladder was dried on whatman paper for 5 min. Then the DNA on whatman paper was fixed under a UV Cross linker. Afterwards the membrane was pre-hybridized at 65° C for 40 min - 1 h with 40 ml Southern-Hybridization Buffer which was preheated. Spatenously the probe was re-suspended in 1ml of Southern Hybridization Buffer and denatured at 95° C for 5-10 min on a thermol heater. The pre-hybridization buffer was discarded and the membrane was incubated with the probe and 15-20 ml Southern Hybridization Buffer for at least 6 h.

On the following day, the probe was poured into a falcon and kept in -20° C incase for reuse. The membrane was washed three times independently with 2 x SSPE + 0.1 % SDS buffer, 1 x SSPE + 0.1 % SDS buffer and 0.1 x SSPE + 0.1 % SDS buffer at 65° C for 15 min. Then the following steps were carried out at 25° C. The membrane was washed with 20 ml DIG Wash buffer at 25° C for 5 min and then all liquid was removed with pipette. After being incubated in 25 ml DIG2 for 30 min, the membrane was again incubated with 25 ml Anti-DIG antibody solution for 30 min (longer incubation may cause background). Afterwards the membrane was washed with 50 ml DIG Wash buffer for two times of 15 min. Then the membrane was incubated in 40 ml DIG3 for 5 min. For the development, the membrane was put in a plastic bag soaked in 1 ml CDP Star solution. Then the membrane was watched with Chemi Smart Chemi luminescence (PEQLAB).

If it was needed, the membrane was washed with ddH_2O for 1 min, with stripping buffer at 37° C for two times of 15 min and with 2 x SSC for 5 min. Then it was ready for pre-hybridization or stored between two layers of whatman paper until needed.

Table 16: Solutions and buffers for the Southern blot of *A. flagrans.*

Buffer	Composition
0.25 M HCl/L	32 % HCl 28.4 ml ddH_2O 972 ml (HCl into water)
DENAT/L	NaCl 87.6 g (1.5 M) Filled with ddH_2O NaOH 16 g (0.4 M).
RENAT/L	87.6 g NaCl (1.5 M) 44.4 gTris-HCl (282 mM) 26.5 g Tris-Base (218 mM) Filled with ddH_2O.
20 x SSC/2 L	350.6 g NaCl (3 M) 176.4 g NaCitrate · $2H_2O$ (0.3 M)·

	set pH to 7.0 with HCl
Southern Hybridization Buffer/L	500 ml 1 M Na-phosphate buffer 70 g SDS (7 %) Autoclaved
1M Na-phosphate buffer	Pour solution 2 into 1 until pH 7.0 is reached Solution 1/L: 177.99 g $Na_2HPO_4 \cdot 2H_2O$ (1 M) Solution 2/L : 156.01 g $NaH_2PO_4 \cdot 2H_2O$ (1 M)
20 x SSPE/L	175.3 g NaCl (3 mM) 27.6 g $Na_2HPO_4 \cdot 2H_2O$ (227 mM) 7.4 g $Na_2EDTA \cdot 2H_2O$ (20 mM) set pH to 7.4 with NaOH (about 4 cookies)
DIG1 (1 x)/L	11.61 g Maleic acid (0.1 M) 8.77 g NaCl (0.15 M) set pH to 7.5 with 5 M NaOH, autoclave
DIG WASH (1 x)/a membrane	450 µL Tween 20 150 ml DIG1 Prepare freshly
DIG2 (1 x)/a membrane	2.5 g milk powder Filled to 50 ml with DIG1 Prepare freshly
Anti-DIG antibody solution /a membrane	20 ml DIG2 2 µL antibody (1:10000-1:20000) (Centrifuged for 5 min at 13,000 rpm 4° C, pipetted carefully from the surface)
DIG3 (1 x)/L	5.84 g NaCl (0.1 M) 10.17 g$MgCl_2 \cdot 6H_2O$ (0.05 M) set pH to 9.5 with Tris-HCl autoclave
CDP-Star solution/a membrane	2 µL CDP (1:500) DIG3 1 ml Stored at 4° C max. 1 week, reused for 5 times
Stripping Buffer/L	8 g NaOH 10 ml 10 % SDS

4.4.10 Targeted deletion of genes by homologous recombination

For the targeted deletion of genes with the means of homologous recombination, a deletion cassette was created. For this purpose, the Hygromycin Resistance Cassette (Hph) was flanked by about 1 kb regions of upstream and downstream from the putative open reading frame (ORF) in *A. flagrans* genome. The fragments were cloned into the PJET1.2 vector with Gibson Assembly. *E. coli* was transformed with the vector; the plasmid DNA was isolated and confirmed by restriction digestion and sequencing. 1.5 µg of the deletion cassette (*gasA(p)::trpC(p)::hph::trpC(t)::gasA(t)*) amplified by PCR was used for the transformation of *A. flagrans*.

4.5 Image formation and data process

4.5.1 Light and fluorescence microscopy

For microscopic observation, a ZEISS Axioimager Z.1 and the Zen Blue Software (2012) were used including the lenses: Plan Apochromat 63 x/1.4 Oilmerization, EC Plan - Neofluor 40 x/0.75, 20 x/0.50, EC Plan Neofluar 10 x/0.30. The detection was done with the help of a MRM camera.

For work with *C. elegans*, a ZEISS stereo discovery.v12 was used.

For quantification of spores and protoplasts, a NIKON Eclips E200 was manipulated.

To dye the nucleus, the fluorescent dye DAPI (LINARIS, Dossenheim) was used and examined with an Excitation maximum of 350 nm and one Emission maximum of 440 nm. A drop was added to the sample for the incubation for 10 min in the dark before microscopy.

4.5.2 Data analysis and image processing

The software Fiji/ImageJ (Version 2.0) was used for image editing. Data diagrams and statistical analysis were made with the software GraphPad Prism 8.0 and IBM SPSS Statistics 19. DNA sequences and circular plasmid DNA map were visualized with the APE Plasmid Editor, Jalview and DNAMAN v6. The phylogenetic analysis was performed with the software and program of megaX 10.2.5 and EvolView2.

The experiments were carried out in the biological and technical triple. For statistical analyzes, an unpaired T test was performed (* p-value < 0.05, ** p-value < 0.01, *** p-value < 0.001).

5 References

Alspaugh, J. A., Pukkila-Worley, R., Harashima, T., Cavallo, L. M., Funnell, D., Cox, G. M., Perfect, J. R., Kronstad, J. W. & Heitman, J. (2002). Adenylyl cyclase functions downstream of the Gα protein Gpa1 and controls mating and pathogenicity of *Cryptococcus neoformans*. *Eukaryot Cell* **1(1)**, 75–84.

Andersson, J. O., Sjogren, A. M., Davis, L. A. M., Embley, T. M. & Roger, A. J. (2003). Phylogenetic analyses of diplomonad genes reveal frequent lateral gene transfers affecting eukaryotes. *Curr Biol* **13**, 94–104.

Ansari, K., Martin, S., Farkasovsky, M., Ehbrecht, I. M. & Kuntzel, H. (1999). Phospholipase C binds to the receptor-like GPR1 protein and controls pseudohyphal differentiation in *Saccharomyces cerevisiae*. *J Biol Chem* **274**, 30052–30058.

Bardwell, L. (2005). A walk-through of the yeast mating pheromone response pathway. *Peptides* **26**, 339–350.

Bauskin, A. R., Zhang, H. P., Fairlie, W. D., He, X. Y., Russell, P. K., Moore, A. G., Brown, D. A., Stanley, K. K. & Breit, S. N. (2000). The propeptide of macrophage inhibitory cytokine (MIC-1), a TGF-beta superfamily member, acts as a quality control determinant for correctly folded MIC-1. *EMBO J* **19(10)**, 2212–20.

Beiko, R. G., Harlow, T. J. & Ragan, M.A. (2005). Highways of gene sharing in prokaryotes. *Proc Natl Acad Sci U S A* **102**, 14332–14337.

Bayram, Ö., Bayram, Ö. S., Ahmed, Y. L., Maruyama, J., Valerius, O., Rizzoli, S. O., Ficner, R. & Irniger, S. (2012). The *Aspergillus nidulans* MAPK module AnSte11-Ste50-Ste7-Fus3 controls development and secondary metabolism. *PLoS Genet* **8(7)**, e1002816.

Borkovich, K. A., Alex, L. A., Yarden, O., Freitag, M., Turner, G. E., Read, N. D., Seiler, S., Bell-Pedersen, D., Paietta, J., Plesofsky, N., Plamann, M., Goodrich-Tanrikulu, M., Schulte, U., Mannhaupt, G., Nargang, F. E., Radford, A., Selitrennikoff, C., Galagan, J. E., Dunlap, J. C., Loros, J. J., Catcheside, D., Inoue, H., Aramayo, R., Polymenis, M., Selker, E. U., Sachs, M. S., Marzluf, G. A., Paulsen, I., Davis, R., Ebbole, D. J., Zelter, A., Kalkman, E. R., O'Rourke, R., Bowring, F., Yeadon, J., Ishii, C., Suzuki, K., Sakai, W. & Pratt, R. (2004). Lessons from the genome sequence of *Neurospora crassa*: tracing the path from genomic blueprint to multicellular organism. *Microbiol Mol Biol Rev* **68(1)**, 1–108.

Bouwmeester, H., Schuurink, R. C., Bleeker, P. M. & Schiestl, F. (2019). The role of volatiles in plant communication. *Plant J* **100**, 892–907.

Brown, N. A., Schrevens, S., Van Dijck, P. & Goldman, G. H. (2018). Fungal G-protein-coupled receptors: mediators of pathogenesis and targets for disease control. *Nat Microbiol* **3(4)**, 402–414.

Bucci, C., Thomsen, P., Nicoziani, P., McCarthy, J. & van Deurs, B. (**2000**). Rab7: A key to lysosome biogenesis. *Mol Biol Cell* **11**, 467–480.

Burke, J. M. & Miller, J. E. (2020). Sustainable approaches to parasite control in ruminant livestock. *Vet Clin North Am Food Anim Pract* **36(1)**, 89–107.

Burke, J. M., Miller, J. E., Larsen, M. & Terrill, T. H. (2005). Interaction between copper oxide wire particles and *Duddingtonia flagrans* in lambs. *Vet parasitol* **134(1-2)**, 141–146.

Butcher, R. A., Fujita, M., Schroeder, F. C. & Clardy, J. (2007). Small-molecule pheromones that control dauer development in *Caenorhabditis elegans*. *Nat Chem Biol* **3**, 420–422.

Chen, S. A., Lin, H. C., Schroeder, F. C. & Hsueh, Y. P. (2021). Prey sensing and response in a nematode-trapping fungus is governed by the MAPK pheromone response pathway. *Genetics* **217(2)**, iyaa008.

Chen, T. H., Hsu, C. S., Tsai, Ho, Y. F. & Lin, N. S. (2001). Heterotrimeric G-protein and signal transduction in the nematode-trapping fungus *Arthrobotrys dactyloides*. *Planta* **212(5)**, 858–863.

Chen, Y. H., Liu, X., Dai, R., Ou, X., Xu, Z. F., Zhang, K. Q. & Niu, X. M. (2020). Novel polyketide-terpenoid hybrid metabolites and increased fungal nematocidal ability by disruption of genes 277 and 279 in nematode-trapping fungus *Arthrobotrys oligospora*. *J Agric Food Chem* **68(30)**, 7870–7879.

Choi, Y. H., Lee, N. Y., Kim, S. S., Park, H. S & Shin, K. S. (2020). Comparative characterization of G-protein α subunits in *Aspergillus fumigatus*. *Pathogens* **9(4)**, 272.

Clavijo McCormick, A., Unsicker, S. B. & Gershenzon, J. (2012). The specificity of herbivore-induced plant volatiles in attracting herbivore enemies. *Trends Plant Sci* **17**, 303–310.

Colombo, S., Ma, P., Cauwenberg, L., Winderickx, J., Crauwels, M., Teunissen, A., Nauwelaers, D., de Winde, J. H., Gorwa, M. F., Colavizza, D. & Thevelein, J. M. (1998). Involvement of distinct G-proteins, Gpa2 and Ras, in glucose-and intracellular acidification-induced cAMP signalling in the yeast *Saccharomyces cerevisiae*. *The EMBO J* **17(12)**, 3326–3341.

Cooke, R. G. (1969). Two nematode-trapping hyphomycetes, *Duddingtonia flagrans* gen. et comb. nov. and *Monagrosporium mutabilis* sp. nov. *Trans Br Mycol Soc* **53(2)**, 315–319.

Corda, A. G. J. (1839). Pracht-Flora europaischer Schimmelbildungen. vol 43. Leipzig.

Dos Reis, T. F., Mellado, L., Lohmar, J. M., Silva, L. P., Zhou, J. J., Calvo, A. M., Goldman, G. H. & Brown, N. A. (2019). GPCR-mediated glucose sensing system regulates light-dependent fungal development and mycotoxin production. *PLoS Genet* **15(10)**, e1008419.

Dash, M., Dutta, T. K., Phani, V., Papolu, P. K., Shivakumara, T. N. & Rao, U. (2017). RNAi-mediated disruption of neuropeptide genes, nlp-3 and nlp-12, cause multiple behavioral defects in *Meloidogyne incognita*. *Biochem Biophys Res Commun* **490(3)**, 933–940.

Delgado-Jarana, J., Martínez-Rocha, A. L., Roldán-Rodriguez, R., Roncero, M. I. & Di Pietro, A. (2005). *Fusarium oxysporum* G-protein β subunit Fgb1 regulates hyphal growth, development, and virulence through multiple signalling pathways. *Fungal Genet and Biol* **42(1)**, 61–72.

DeZwaan, T. M., Carroll, A. M., Valent, B. & Sweigard, J. A. (1999). *Magnaporthe*

grisea Pth11p is a novel plasma membrane protein that mediates appressorium differentiation in response to inductive substrate cues. *Plant Cell* **11**, 2013–2030.

Di Giusto, B., Bessière, JM., Guéroult, M., Lim, L. B. L., Marshall, D. J., Hossaert-McKey, M. & Gaume, L. (2010). Flower-scent mimicry masks a deadly trap in the carnivorous plant *Nepenthes rafflesiana*. *J Ecol* **98**, 845–856.

Doehlemann, G., Berndt, P. & Hahn, M. (2006). Different signalling pathways involving a Gα protein, cAMP and a MAP kinase control germination of *Botrytis cinerea* conidia. *Mol Microbiol* **59(3)**, 821–835.

Dos Reis, T. F., Mellado, L., Lohmar, J. M., Silva, L. P., Zhou, J. J., Calvo, A. M., Goldman, G. H. & Brown, N. A. (2019). GPCR-mediated glucose sensing system regulates light-dependent fungal development and mycotoxin production. PLoS *Genet* **15(10)**, e1008419.

Dohlman, H. G. & Thorner, J. W. (2001). Regulation of G-protein-initiated signal transduction in yeast: paradigms and principles. *Annu Rev Biochem* **70**, 703–754.

Doolittle, W. F. (1999). Lateral genomics. *Trends Cell Biol* **9**, M5–M8.

Duddington, C. L. (1949). A new predacious species of *Trichothecium*. *Trans Br Mycol Soc* **32(3–4)**, 284–287.

Dugassa, J., Hussein, A., Kebede, A. & Mohammed, C. (2018). Prevalence and associated risk factors of gastrointestinal nematodes of sheep and goats in Ziway Dugda District, Eastern Arsi Zone of Oromia regional state, Ethiopia. *Multidiscipl Adv Vet Sci* 2301–310.

D'Souza, C. A., Alspaugh, J. A., Yue, C., Harashima, T., Cox, G. M., Perfect, J. R. & Heitman, J. (2001). Cyclic AMP-dependent protein kinase controls virulence of the fungal pathogen *Cryptococcus neoformans*. *Mol Cellu Biol* **21(9)**, 3179–3191.

Eglen, R. M., Bosse, R. & Reisine, T. (2007). Emerging concepts of guanine nucleotide-bindinG-protein-coupled receptor (GPCR) function and implications for high throughput screening. *Assay Drug Dev Technol* **5(3)**, 425–452.

Escudero N, Ferreira S R, Lopez-Moya F, Escudero, N., Ferreira, S. R., Lopez-Moya, F., Naranjo-Ortiz, M. A., Marin-Ortiz, A. I., Thornton, C. R &, Lopez-Llorca, L. V. (2016). Chitosan enhances parasitism of *Meloidogyne javanica* eggs by the nematophagous fungus *Pochonia chlamydosporia*. *Fungal Biol* **120(4)**, 572–585.

Fan, Y., Zhang, W., Chen, Y., Xiang, M. & Liu, X. (2021). DdaSTE12 is involved in trap formation, ring inflation, conidiation, and vegetative growth in the nematode-trapping fungus *Drechslerella dactyloides*. *Appl Microbiol Biotechnol* **105(19),** 7379–7393.

Fitzpatrick D A. (2012).Horizontal gene transfer in fungi. *FEMS Microbiol Lett* **329(1)**, 1–8.

Flach, A., Marsaioli, A. J., Singer, R. B., Amaral, M. C., Menezes, C., Kerr, W. E., Batista-Pereira, L. G. &, Corrêa, A. G. (2006). Pollination by sexual mimicry in *Mormolyca ringens*: a floral chemistry that remarkably matches the pheromones of virgin queens of *Scaptotrigona* sp. *J Chem Ecol* **32**, 59–70.

Fowler, T. J., Mitton, M. F., Vaillancourt, L. J. & Raper, C. A. (2001). Changes in mate recognition through alterations of pheromones and receptors in the multisexual mushroom fungus *Schizophyllum commune*. *Genetics* **158(4)**, 1491–503.

Fresenius G. (1852). Beitraege zur Mykologie. *Heft* **1–2**, 1–80.

Fu, Y. & Galan, J. E. (1999). A salmonella protein antagonizes Rac-1 and Cdc42 to mediate host-cell recovery after bacterial invasion. *Nature* **401**, 293–297.

Gao, X., Herrero, S., Wernet, V., Erhardt, S., Valerius, O., Braus, G. H. & Fischer, R. (2021). The role of *Aspergillus nidulans* polo-like kinase PlkA in microtubule-organizing center control. *J Cell Sci* **134(16)**, jcs256537.

Golden, J. W. & Riddle, D. L. (1982). A pheromone influences larval development in the nematode *Caenorhabditis elegans*. *Science* **218**, 578–580.

Gust, A. A., Pruitt, R. & Nurnberger, T. (2017). Sensing danger: key to activating plant immunity. *Trends Plant Sci* **22**, 779–91.

Haegeman, A., Jones, J. T. & Danchin, E. G. (2011). Horizontal gene transfer in nematodes: a catalyst for plant parasitism? *Mol Plant Microbe Interact* **24(8)**, 879–887.

Han, K. H., Seo, J. A. & Yu, J. H. (2004). Regulators of G‐protein signalling in *Aspergillus nidulans*: RgsA downregulates stress response and stimulates asexual sporulation through attenuation of GanB (Gα) signalling. *Mol Microbial* **53(2)**, 529–540.

Haj Hammadeh, H., Serrano, A., Wernet, V., Stomberg, N., Hellmeier, D., Weichert, M., Brandt, U., Sieg, B., Kanofsky, K., Hehl, R., Fischer, R. & Fleißner, A. (2022). A dialogue-like cell communication mechanism is conserved in filamentous ascomycete fungi and mediates interspecies interactions. *Proc Natl Acad Sci U S A* **119(12)**, e2112518119.

Hamel, L. P., Nicole, M. C., Duplessis, S & Ellis, B. E. (2012). Mitogen-activated protein kinase signaling in plant-interacting fungi: distinct messages from conserved messengers. *Plant Cell* **24(4)**, 1327–1351.

Harashima, T. & Heitman, J. (2004). Nutrient control of dimorphic growth in *Saccharomyces cerevisiae*. In: Nutrient Induced Responses in Eukaryotic Cells, Vol. 7, ed. J. Winderickx and P.M. Taylor, Berlin, Germany: Springer-Verlag, 131–169.

Hardt, W. D., Chen, L. M., Schuebel, K. E., Bustelo, X. R. & Galan, J. E. (1998). *S. typhimurium* encodes an activator of Rho GTPases that induces membrane ruffling and nuclear responses in host cells. *Cell* **93**, 815–826.

Harper, J. W., Adami, G. R., Wei, N., Keyomarsi, K. & Elledge, S. J. (1993). The p21 Cdk-interactinG-protein Cip1 is a potent inhibitor of G1 cyclin-dependent kinases. *Cell* **75**, 805–816.

Haynes, K. F., Gemeno, C., Yeargan, K. V., Millar, J. G. & Johnson, K. M. (2002). Aggressive chemical mimicry of moth pheromones by a bolas spider: how does this specialist predator attract more than one species of prey? *Chemoecology* **12**, 99–105.

He, Z. Q., Wang, L. J., Wang, Y. J., Chen, Y. H., Wen, Y., Zhang, K. Q. & Niu, X. M. (2021). Polyketide Synthase–Terpenoid Synthase Hybrid Pathway Regulation of Trap Formation through Ammonia Metabolism Controls Soil Colonization of Predominant Nematode-Trapping Fungus. *J Agric Food Chem* **69(15)**, 4464–4479.

Hill, C., Goddard, A., Davey, J. & Ladds, G. (2006). Investigating RGS proteins in yeast. *Semin Cell Dev Biol* **17**, 352–62.

Hsueh, Y. P., Gronquist, M. R., Schwarz, E. M., Nath, R. D., Lee, C. H., Gharib, S., Schroeder, F. C & Sternberg, P. W. (2017). Nematophagous fungus *Arthrobotrys oligospora* mimics olfactory cues of sex and food to lure its nematode prey. *Elife* **6**, e20023.

Hsueh, Y. P., Mahanti, P., Schroeder, F. C. & Sternberg, P. W. (2013). Nematodetrapping fungi eavesdrop on nematode pheromones. *Curr Biol* **23**, 83–86.

Hsueh, Y. P., Xue, C. & Heitman, J. (2007). G-protein signaling governing cell fate decisions involves opposing Gα subunits in *Cryptococcus neoformans*. *Mol Biol Cell* **18(9)**, 3237–3249.

Hu, Y., Hao, X., Chen, L., Akhberdi, O., Yu, X., Liu, Y. & Zhu, X. (2018). Gα-cAMP/PKA pathway positively regulates pigmentation, chaetoglobosin A biosynthesis and sexual development in *Chaetomium globosum*. *PLoS One* **13(4)**, e0195553.

Hyde, K. D., Swe, A. & Zhang, K. Q. (2014). Nematode-trapping fungi, p 1–12. In Zhang, K. Q., Hyde, K. D. (ed), Nematode-Trapping Fungi. Springer, Dordrecht, The Netherlands.

Ilangopathy, M., Palavesam, A., Amaresan, S. S. P. & Muthusamy, R. (2019). Economic impact of gastrointestinal nematodes on meat production from sheep. *Int J Livest Res* **9**, 44–48.

James, P., Haliaday, J. & Craig, E. A. (1996). Genomic libraries and a host strain designed for highly efficient two-hybrid selection in yeast. *Genetics* **144**, 1425–1436.

Jansson, H. B. (1994). Adhesion of conidia of *Drechmeria coniospora* to *Caenorhabditis elegans* wild type and mutants. *J Nematol* **26(4)**, 430.

Jashni, M. K., Dols, I. H. M., Iida, Y., Boeren, S., Beenen, H. G., Mehrabi, R., Collemare, J. & de Wit, P. J. G. M. (2015). Synergistic action of a metalloprotease and a serine protease from *Fusarium oxysporum* f. sp. *lycopersici* cleaves chitin-binding tomato chitinases, reduces their antifungal activity, and enhances fungal virulence. *Mol Plant Microbe Interact* **28**, 996–1008.

Jeong, P. Y., Jung, M., Yim, Y. H., Kim, H., Park, M., Hong, E., Lee, W., Kim, Y. H., Kim, K. & Paik, Y.K. (2005). Chemical structure and biological activity of the *Caenorhabditis elegans* dauer-inducing pheromone. *Nature* **433**, 541–545.

Ji, X., Li, H., Zhang, W., Wang, J., Liang, L., Zou, C., Yu, Z., Liu, S. & Zhang, K. Q. (2020). The lifestyle transition of *Arthrobotrys oligospora* is mediated by microRNA-like RNAs. *Sci China Life Sci* **63(4)**, 543–551.

Jiang, L., Zhang, Y., Xu, J., Zhang, K. Q. & Zhang, Y. (2018). The complete mitochondrial genomes of the nematode-trapping fungus *Arthrobotrys oligospora*. *Mitochondrial DNA B Resour* **3(2)**, 966–967.

Jones, J. D. G., Vance, R. E. & Dangl, J. L. (2016). Intracellular innate immune surveillance devices in plants and animals. *Science* **354(6316)**, aaf6395.

Jones, J. T., Furlanetto, C. & Kikuchi, T. (2005). Horizontal gene transfer from bacteria and fungi as a driving force in the evolution of plant parasitism in nematodes. *Nematology* **7(5)**, 641–646.

Joosten, M. H., Cozijnsen, T. J. & De Wit, P. J. (1994). Host resistance to a fungal

tomato pathogen lost by a single base-pair change in an avirulence gene. *Nature* **367(6461)**, 384–6.

Juergens, A., El-Sayed, A. M. & Suckling, D. M. (2009). Do carnivorous plants use volatiles for attracting prey insects? *Funct Ecol* **23**, 875–887.

Jung, M. G., Kim, S. S., Yu, J. H. & Shin, K. S. (2016). Characterization of gprK encoding a putative hybrid G-protein-coupled receptor in *Aspergillus fumigatus*. *PLoS One* **11(9)**, e0161312.

Kelley, L. A., Mezulis, S., Yates, C. M., Wass, M. N. & Sternberg, M. J. E. (2015). The Phyre2 web portal for protein modeling, prediction and analysis. *Nat Protoc* **10**, 845–858.

Kim, D. W., Lenzen, G., Page, A. L., Legrain, P., Sansonetti, P. J. & Parsot, C. (2005). The *Shigella flexneri* effector OspG interferes with innate immune responses by targeting ubiquitin conjugating enzymes. *Proc Natl Acad Sci U S A* **102**:14046–14051.

Klessig, D. F., Manohar, M., Baby, S., Koch, A., Danquah, W. B., Lina, E., Park, H. J., Kloppholz, S., Kuhn, H. & Requena, N. A secreted fungal effector of *Glomus intraradices* promotes symbiotic biotrophy. *Curr Biol* **21(14)**, 1204–9.

Kolkman, J. M., Turgeon, B. G., Nelson, R., Leach, J. E., Williamson, V. M., Kogel, K. H., Kachroo, A. & Schroeder, F. C. (2019). Nematode ascaroside enhances resistance in a broad spectrum of plant-pathogen systems. *J. Phytopathol.* **167**, 265–72

Kothe, E., Gola, S. & Wendland, J. (2003). Evolution of multispecific mating-type alleles for pheromone perception in the homobasidiomycete fungi. *Curr Genet* **42(5)**, 268–75.

Kou, Y., Tan, Y. H., Ramanujam, R. & Naqvi, N. I. (2017). Structure–function analyses of the Pth11 receptor reveal an important role for CFEM motif and redox regulation in rice blast. *New Phytol* **214(1)**, 330–342.

Kraakman, L., Lemaire, K., Ma, P., Teunissen, A. W., Donaton, M. C., Van Dijck, P., Winderickx, J., de Winde, J. H. & Thevelein, J. M. (1999). A *Saccharomyces cerevisiae* G-protein coupled receptor, Gpr1, is specifically required for glucose activation of the cAMP pathway during the transition to growth on glucose. *Mol Microbiol* **32(5)**, 1002–12.

Kuo, C. Y., Chen, S. A. & Hsueh, Y. P. (2020). The high osmolarity glycerol (HOG) pathway functions in osmosensing, trap morphogenesis and conidiation of the nematode-trapping fungus *Arthrobotrys oligospora*. *J Fungi* **6(4)**, 191.

Kraakman, L., Lemaire, K., Ma, P., Teunissen, A. W., Donaton, M. C., Van Dijck, P., Winderickx, J., de Winde, J. H. & Thevelein, J.M. (1999). A *Saccharomyces cerevisiae* G-protein coupled receptor, Gpr1, is specifically required for glucose activation of the cAMP pathway during the transition to growth on glucose. *Mol Microbiol* **32(5)**, 1002–1012.

Kwon-Chung, K. J. & Rhodes, J. C. (1986). Encapsulation and melanin formation as indicators of virulence in *Cryptococcus neoformans*. *Infect Immun* **51**, 218–223.

Kwon-Chung, K. J., Polacheck, I. & Popkin, T. J. (1982). Melaninlacking mutants of *Cryptococcus neoformans* and their virulence for mice. *J Bacteriol* **150**,

1414–1421.

Lafon, A., Han, K. H., Seo, J. A., Yu, J. H. & d'Enfert, C. (2006). G-protein and cAMP-mediated signaling in aspergilli: a genomic perspective. *Fungal Genet Biol* **43(7)**, 490–502.

Lafon, A., Seo, J. A., Han, K. H., Yu, J. H. & d'Enfert, C. (2005). The heterotrimeric G-protein GanB(alpha)-SfaD(beta)-GpgA(gamma) is a carbon source sensor involved in early cAMP-dependent germination in *Aspergillus nidulans*. *Genetics* **171(1)**, 71–80.

Lawton, J. R. (1957). The formation of constricting rings in nematode-catching *Hyphomycetes* grown in pure culture. *J Exp Bot* **8(1)**, 50–54.

Leberer, E., Harcus, D., Dignard, D., Johnson, L., Ushinsky, S., Thomas, D. Y. & Schröppel, K. (2001). Ras links cellular morphogenesis to virulence by regulation of the MAP kinase and cAMP signalling pathways in the pathogenic fungus *Candida albicans. Mol Microbiol* **42(3)**, 673–87.

Lee, B. N. & Adams, T. H. (1994). Overexpression of flbA, an early regulator of *Aspergillus* asexual sporulation, leads to activation of brlA and premature initiation of development. *Mol Microbiol* **14**, 323–34.

Lee, C. H., Chang, H. W., Yang, C. T., Wali, N., Shie, J. J. & Hsueh, Y. P. (2020). Sensory cilia as the Achilles heel of nematodes when attacked by carnivorous mushrooms. *Proc Natl Acad Sci U S A* **117(11)**, 6014–6022.

Lengeler, K. B., Davidson, R. C., D'Souza, C., Harashima, T., Shen, W. C., Wang, P., Pan, X., Waugh, M. & Heitman, J. (2000). Signal transduction cascades regulating fungal development and virulence. *Microbiol Mol Biol Rev* **64**, 746–785.

Li, J., Wu, R., Wang, M., Borneman, J., Yang, J. & Zhang, K. Q. (2019). The pH sensing receptor AopalH plays important roles in the nematophagous fungus *Arthrobotrys oligospora*. *Fungal Biol* **123(7)**, 547–554.

Li, J., Zou, C., Xu, J., Ji, X., Niu, X., Yang, J., Huang, X. & Zhang, K. Q. (2015). Molecular mechanisms of nematode-nematophagous microbe interactions: basis for biological control of plant-parasitic nematodes. *Annu Rev Phytopathol* **53**, 67–95.

Li, L., Wright, S. J., Krystofova, S., Park, G. & Borkovich, K. A. (2007). Heterotrimeric G-protein signaling in filamentous fungi. *Annu Rev Microbiol* **61**, 423–452.

Li, L., Yang, M., Luo, J., Qu, Q., Chen, Y., Liang, L. & Zhang, K. (2016). Nematode-trapping fungi and fungus-associated bacteria interactions: the role of bacterial diketopiperazines and biofilms on *Arthrobotrys oligospora* surface in hyphal morphogenesis. *Environ Microbiol* **18(11)**, 3827–3839.

Li, X., Kang, Y. Q., Luo, Y. L., Zhang, K. Q., Zou, C. G. & Liang, L. M. (2017). The NADPH oxidase AoNoxA in *Arthrobotrys oligospora* functions as an initial factor in the infection of *Caenorhabditis elegans*. *J Microbiol* **55(11)**, 885–891.

Liang, L., Gao, H., Li, J., Liu, L., Liu, Z. & Zhang, K. Q. (2017). The Woronin body in the nematophagous fungus *Arthrobotrys oligospora* is essential for trap formation and efficient pathogenesis. *Fungal Biol* **121(1)**, 11–20.

Liang, L., Liu, Z., Liu, L., Li, J., Gao, H., Yang, J. & Zhang, K. Q. (2016). The nitrate assimilation pathway is involved in the trap formation of *Arthrobotrys oligospora*, a nematode-trapping fungus. *Fungal Genet Biol* **92**, 33–39.

Liang, M., Du, S., Dong, W., Fu, J., Lim Z., Qiao, Y., Yin, X., Nie, F., Uang, X. & Wang, R. (2019). iTRAQ-based quantitative proteomic analysis of mycelium in different predation periods in nematode trapping fungus *Duddingtonia flagrans*. *Biol Control* **134**, 63–71.

Liebmann, B., Müller, M., Braun, A. & Brakhage, A. A. (2004). The cyclic AMP-dependent protein kinase a network regulates development and virulence in *Aspergillus fumigatus*. *Infect Immun* **72(9)**, 5193–5203.

Liu, K., Tian, J., Xiang, M. & Liu, X. (2012). How carnivorous fungi use three-celled constricting rings to trap nematodes. *Protein Cell* **3(5)**, 325–328.

Liu, T., Huang, Y., Chen, X. X., Long, X., Yang, Y. H., Zhu, M. L., Mo, M. H. & Zhang, K. Q. (2020). Comparative transcriptomics reveals features and possible mechanisms of glucose-mediated soil fungistasis relief in *Arthrobotrys oligospora*. *Front Microbiol* **10**, 3143.

Liu, Y., Yang, K., Qin, Q., Lin, G., Hu, T., Xu, Z. & Wang, S. (2018). G-protein α subunit GpaB is required for asexual development, aflatoxin biosynthesis and pathogenicity by regulating cAMP signaling in *Aspergillus flavus*. *Toxins* **10(3)**, 117.

Lo Presti, L. & Kahmann, R. (2017). How filamentous plant pathogen effectors are translocated to host cells. *Curr Opin Plant Biol* **38**, 19–24.

Lolle, S., Stevens, D. & Coaker, G. (2020). Plant NLR-triggered immunity: from receptor activation to downstream signaling. *Curr Opin Immunol* **62**, 99–105.

Ma, N., Zhao, Y., Wang, Y., Yang, L., Li, D., Yang, J., Jiang, K., Zhang, K. Q. & Yang, J. (2021). Functional analysis of seven regulators of G-protein signaling (RGSs) in the nematode-trapping fungus *Arthrobotrys oligospora*. *Virulence* **12(1)**, 1825–1840.

Maller, J. L. (2003). Signal transduction. Fishing at the cell surface. *Science* **300**, 594–595.

Mander, G. J., Wang, H., Bodie, E., Wagner, J., Vienken, K., Vinuesa, C., Foster, C. & Martín, J. F. (2017). Key role of LaeA and velvet complex proteins on expression of β-lactam and PR-toxin genes in *Penicillium chrysogenum*: cross-talk regulation of secondary metabolite pathways. *J Ind Microbiol Biotechnol* **44(4-5)**, 525–535.

Menzner Jennifer (2020). Etablierung eines optogenetischen Systems in *C. elegans* und Untersuchung eines Virulenzfaktors in *D. flagrans*. Masterarbeit, KIT. Karlsruhe.

McVeigh, P., Leech, S., Marks, N. J., Geary, T. G. & Maule, A. G. (2006). Gene expression and pharmacology of nematode NLP-12 neuropeptides. *Int J Parasitol* **36(6)**, 633–40.

Leeder, A. C., Allen, G., Hamill, V., Janssen, G. G., Dunn-Coleman, N., Karos, M., Lemaire, H. G., Subkowski, T., Bollschweiler, C., Turner, G., Nüsslein, B. & Fischer, R. (2006). Use of laccase as a novel, versatile reporter gene for filamentous fungi. *Appl Environ Microbiol* **72(7)**, 5020–5026.

Manfiolli, A. O., Siqueira, F. S., Dos Reis, T. F., Van Dijck, P., Schrevens, S., Hoefgen, S., Föge, M., Straßburger, M., de Assis, L. J., Heinekamp, T., Rocha, M. C., Janevska, S., Brakhage, A. A., Malavazi, I., Goldman, G. H. & Valiante, V. (2019). Mitogen-activated protein kinase cross-talk interaction modulates the production of melanins in *Aspergillus fumigatus*. *Mbio* **10(2)**, e00215–19.

Manohar, M., Tenjo-Castano, F., Chen, S., Zhang, Y. K., Kumari, A., Williamson, V. M., Wang, X., Klessig, D. F. & Schroeder, F. C. (2020). Plant metabolism of nematode pheromones mediates plant-nematode interactions. *Nat Commun* **11(1)**, 1–11.

Manosalva, P., Manohar, M., Von Reuss, S. H., Chen, S., Koch, A., Kaplan, F., Choe, A., Micikas, R. J., Wang, X., Kogel, K. H., Sternberg, P. W., Williamson, V. M., Schroeder, F. C. & Klessig, D. F. (2015). Conserved nematode signalling molecules elicit plant defenses and pathogen resistance. *Nat Commun* **6**(1), 1–8.

Mitiku, M. (2018). Plant-parasitic nematodes and their management: A review. *Agric Res Technol* **8**, 30–38.

Mitreva, M., Smant, G. & Helder, J. (2009). Role of horizontal gene transfer in the evolution of plant parasitism among nematodes. *Methods Mol Biol* 517–535.

McGrath, P. T. & Ruvinsky, I. (2019). A primer on pheromone signaling in *Caenorhabditis elegans* for systems biologists. *Curr Opin Syst Biol* **13**, 23–30.

Mukherjee, S., Keitany, G., Li, Y., Wang, Y., Ball, H. L., Goldsmith, E. J. & Orth, K. (2006). *Yersinia* YopJ acetylates and inhibits kinase activation by blocking phosphorylation. *Science* **312**, 1211–1214.

Neves, S. R., Ram, P. T. & Iyengar, R. (2002). G-protein pathways. *Science* 296, 1636–39.

Orth, K., Xu, Z., Mudgett, M. B., Bao, Z. Q., Palmer, L. E., Bliska, J. B., Mangel, W. F., Staskawicz, B. & Dixon, J. E. (2000). Disruption of signaling by *Yersinia* effector YopJ, a ubiquitin-like protein protease. *Science* **90**, 1594–1597.

Ottmann, C., Luberacki, B., Kufner, I., Koch, W., Brunner, F., Weyand, M., Mattinen, L., Pirhonen, M., Anderluh, G., Seitz, H. U., Nurnberger, T. & Oecking, C. (2009). A common toxin fold mediates microbial attack and plant defense. *Proc Natl Acad Sci U S A* **106**, 10359–10364.

Owen, K. A., Thomas, K. S. & Bouton, A. H. (2007). The differential expression of *Yersinia pseudotuberculosis* adhesins determines the requirement for FAK and/or Pyk2 during bacterial phagocytosis by macrophages. *Cell Microbiol* **9**, 596–609.

Pramer, D. & Stoll, N. R. (1959). Nemin: a morphogenic substance causing trap formation by predaceous fungi. *Science* **129(3354)**, 966–967.

Pukkila-Worley, R. & Alspaugh, J, A. (2004). Cyclic AMP signaling in *Cryptococcus neoformans*. *FEMS Yeast Res* **4(4–5)**, 361–367.

Pungaliya, C., Srinivasan, J., Fox, B. W., Malik, R. U., Ludewig, A. H., Sternberg, P. W. & Schroeder, F. C. (2009). A shortcut to identifying small molecule signals that regulate behavior and development in *Caenorhabditis elegans*. *Proc Natl Acad Sci U S A* **106**, 7708–7713.

Rebecchi, M. J. & Pentyala, S. N. (2000) Structure, function, and control of phosphoinositide-specific Phospholipase C. *Physiol Rev* **80**, 1291–1335.

Regenfelder, E., Spellig, T., Hartmann, A., Lauenstein, S., Bölker, M. & Kahmann, R. (1997). G-proteins in *Ustilago maydis*: transmission of multiple signals? *EMBO J* **16(8)**, 1934–1942.

Richardson, A. O. & Palmer, J. D. (2007). Horizontal gene transfer in plants. *J Exp Bot* **58**, 1–9.

Scholler, M. & Rubner, A. (1994). Predacious activity of the nematode-destroying

fungus *Arthrobotrys oligospora* in dependence of the medium composition. *Microbiol Res* **149(2)**, 145–149.

Schroeder, F. C. (2015). Modular assembly of primary metabolic building blocks: a chemical language in *C. elegans*. *Chem Biol* **22(1)**, 7–16.

Schumacher, J., Viaud, M., Simon, A. & Tudzynski, B. (2008). The Gα subunit BCG1, the phospholipase C (BcPLC1) and the calcineurin phosphatase co-ordinately regulate gene expression in the grey mould fungus *Botrytis cinerea*. *Mol Microbiol* **67(5)**, 1027–1050.

Shimizu, K. & Keller, N. P. (2001). Genetic involvement of a cAMP-dependent protein kinase in a G-protein signaling pathway regulating morphological and chemical transitions in *Aspergillus nidulans*. *Genetics* **157(2)**, 591–600.

Shinde, U. & M. Inouye. (2000). Intramolecular chaperones: polypeptide extensions that modulate protein folding. *Semin Cell Dev Biol* **11**, 35–44.

Shirasu, M., Fujioka, K., Kakishima, S., Nagai, S., Tomizawa, Y., Tsukaya, H., Murata, J., Manome, Y. & Touhara, K. (2010). Chemical identity of a rotting animal-like odor emitted from the inflorescence of the titan arum (*Amorphophallus titanum*). *Biosci Biotechnol Biochem* **74**, 2550–2554.

Siddique, S., Coomer, A., Baum, T. & Williamson, V. M. (2022). Recognition and Response in Plant–Nematode Interactions. *Annu Rev of Phytopathol* **60**.

Song, D., Dolan, J. W., Yuan, Y. L. & Fields, S. (1991). Pheromone-dependent phosphorylation of the yeast STE12 protein correlates with transcriptional activation. *Genes Dev* **5(5)**, 741–50.

Sperschneider, J., Dodds, P. N., Gardiner, D. M., Singh, K. B. & Taylor, J. M. (2018). Improved prediction of fungal effector proteins from secretomes with EffectorP 2.0. *Mol Plant Pathol* **19(9)**, 2094–2110.

Srinivasan, J. Kaplan, F., Ajredini, R., Zachariah, C., Alborn, H. T., Teal, P. E., Malik, R. U., Edison, A. S., Sternberg, P. W. & Schroeder, F. C. (2008). A blend of small molecules regulates both mating and development in *Caenorhabditis elegans*. *Nature* **454**, 1115–1118.

Stensmyr, M. C., Urru, I., Collu, I., Celander, M., Hansson, B. S. & Angioy, A. M. (2002). Pollination: Rotting smell of deadhorse arum florets. *Nature* **420**, 625–626.

Stiernagle, T. (2006). Maintenance of *C. elegans*. 1551-8507 WormBook.
http://www.nematodebook.org.

Su, H. N., Xu, Y. Y., Wang, X., Zhang, K. Q. & Li, G. H. (2016). Induction of trap formation in nematode-trapping fungi by bacteria-released ammonia. *Lett Appl Microbiol* **62(4)**, 349–353.

Tag, A., Hicks, J., Garifullina, G., Ake C, Jr., Phillips, T. D., Beremand, M. & Keller, N. (2000). G-protein signalling mediates differential production of toxic secondary metabolites. *Mol Microbiol* **38(3)**, 658–665.

Thaminy, S., Miller, J. & Stagljar, I. (2004). The split-ubiquitin membrane-based yeast two-hybrid system. *Methods Mol Biol* **261**,297–312.

Thevelein, J. M. & de Winde, J. H. (1999). Novel sensing mechanisms and targets for the cAMP-protein kinase A pathway in the yeast *Saccharomyces cerevisiae*. *Mol Microbiol* **33**, 904–918.

Tolkacheva, T., McNamara, T. P., Piekarz, E. & Courchesne, W. (1994). Cloning of a *Cryptococcus neoformans* gene, GPA1, encoding a G-protein K-subunit homolog. *Infect Immun* **62**, 2849–2856.

Tong, Y., Wu, H., Liu, Z., Wang, Z. & Huang, B. (2020). G-protein subunit Gαi in mitochondria, MrGPA1, affects conidiation, stress resistance, and virulence of entomopathogenic fungus *Metarhizium robertsii*. *Front Microbiol* **11**, 1251.

Valetin Wernet (2022). Untersuchung der Fallenbildung und Anwendung des Nematoden-fangenden Pilzes *Duddingtonia flagrans* Doktorarbeit, KIT. Karlsruhe.

Valle-Maldonado, M. I., Patiño-Medina, J. A., Pérez-Arques, C., Reyes-Mares, N. Y., Jácome-Galarza, I. E., Ortíz-Alvarado, R., Vellanki, S., Ramírez-Díaz, M. I., Lee, S. C., Garre, V. & Meza-Carmen, V. (2020). The heterotrimeric G-protein beta subunit Gpb1 controls hyphal growth under low oxygen conditions through the protein kinase A pathway and is essential for virulence in the fungus *Mucor circinelloides*. *Cell Microbiol* **22(10)**, e13236.

Vidal, B., Aghayeva, U., Sun, H., Wang, C., Glenwinkel, L., Bayer, E. A. & Hobert, O. (2018). An atlas of *Caenorhabditis elegans* chemoreceptor expression. *PLoS biology* **16(1)**, e2004218.

Wacker, D., Stevens, R. C. & Roth, B. L. (2017). How ligands illuminate GPCR molecular pharmacology. *Cell* **170(3)**, 414–427.

Wang H, Sun S, Ge W, Zhao, L., Hou, B., Wang, K., Lyu, Z., Chen, L., Xu, S., Guo, J., Li, M., Su, P., Li, X., Wang, G., Bo, C., Fang, X., Zhuang, W., Cheng, X., Wu, J., Dong, L., Chen, W., Li, W., Xiao, G., Zhao, J., Hao, Y., Xu, Y., Gao, Y., Liu, W., Liu, Y., Yin, H., Li, J., Li, X., Zhao, Y., Wang, X., Ni, F., Ma, X., Li, A., Xu, S. S., Bai, G., Nevo, E., Gao, C., Ohm, H. & Kong, L. (2020). Horizontal gene transfer of Fhb7 from fungus underlies *Fusarium* head blight resistance in wheat. *Science* **368(6493)**, eaba5435.

Mai Wang (2022). Analysis of G-protein coupled receptors in *A. flagrans*. Master thesis, KIT. Karlsruhe.

Wang, R. B., Yang, J. K., Lin, C., Zhang, Y. & Zhang, K. Q. (2006). Purification and characterization of an extracellular serine protease from the nematode-trapping fungus *Dactylella shizishanna*. *Lett Appl Microbiol* **42(6)**, 589–594.

Wang, X., Li, G. H., Zou, C. G., Ji, X. L., Liu, T., Zhao, P. J., Liang, L. M., Xu, J. P., An, Z. Q., Zheng, X., Qin, Y. K., Tian, M. Q., Xu, Y. Y., Ma, Y. C., Yu, Z. F., Huang, X. W., Liu, S. Q., Niu, X. M., Yang, J. K., Huang, Y. & Zhang, K. Q. (2014). Bacteria can mobilize nematode-trapping fungi to kill nematodes. *Nat Commun* **5(1)**, 1–9.

Wernet, N., Wernet, V. & Fischer, R. (2021a). The small-secreted cysteine-rich protein CyrA is a virulence factor participating in the attack of *Caenorhabditis elegans* by *Duddingtonia flagrans*. *PLoS Pathog* **17(11)**, e1010028.

Wernet, V., Herrero, S. & Fischer, R. (2021b). Soft but Not Too Soft—How a Rigid Tube Expands without Breaking. *Mbio* **12(3)**, e00501–21.

Wernet, V., Wäckerle, J. & Fischer, R. (2022). The STRIPAK component SipC is involved in morphology and cell-fate determination in the nematode-trapping fungus *Duddingtonia flagrans*. *Genetics* **220(1)**, iyab153.

Wibisono, S., Wibisono, P. & Sun, J. (2021). Neural G-protein-coupled receptor OCTR-1 mediates temperature effects on longevity by regulating immune

response genes in *C. elegans*. bioRxiv.

Xie, M., Bai, N., Yang, J., Jiang, K., Zhou, D., Zhao, Y., Li, D., Niu, X., Zhang, K. Q. & Yang, J. (2020). Protein kinase Ime2 is required for mycelial growth, conidiation, osmoregulation, and pathogenicity in nematode-trapping fungus *Arthrobotrys oligospora*. *Front Microbiol* **10**, 3065.

Xie, M., Ma, N., Bai, N., Zhu, M., Zhang, K. Q. & Yang, J. (2022). Phospholipase C (AoPLC2) regulates mycelial development, trap morphogenesis, and pathogenicity of the nematode-trapping fungus *Arthrobotrys oligospora*. *J Appl Microbiol* **132(3)**, 2144–2156.

Xie, M., Wang, Y., Tang, L., Yang, L., Zhou, D., Li, Q., Niu, X., Zhang, K. Q. & Yang, J. (2019). AoStuA, an APSES transcription factor, regulates the conidiation, trap formation, stress resistance and pathogenicity of the nematode-trapping fungus *Arthrobotrys oligospora*. *Environ Microbiol* **21(12)**, 4648–4661.

Xu, Z. F., Chen, Y. H., Song, T. Y., Zeng, Z. J., Yan, N., Zhang, K. Q. & Niu, X. M. (2016). Nematicidal key precursors for the biosynthesis of morphological regulatory arthrosporols in the nematode-trapping fungus *Arthrobotrys oligospora*. *J Agric Food Chem* **64(42)**, 7949–7956.

Xu, Z. F., Wang, B. L., Sun, H. K., Yan, N., Zeng, Z. J., Zhang, K. Q. & Niu, X. M. (2015). High trap formation and low metabolite production by disruption of the polyketide synthase gene involved in the biosynthesis of arthrosporols from nematode-trapping fungus *Arthrobotrys oligospora*. *J Agric Food Chem* **63(41)**, 9076–9082.

Xue, C., Bahn, Y. S., Cox, G. M. & Heitman, J. (2006). G-protein-coupled receptor Gpr4 senses amino acids and activates the cAMP-PKA pathway in *Cryptococcus neoformans*. *Mol Biol Cell* **17(2)**, 667–679.

Xue, C., Hsueh, Y. P. & Heitman, J. (2008). Magnificent seven: roles of G-protein-coupled receptors in extracellular sensing in fungi. *FEMS Microbiol Rev* **32(6)**, 1010–1032.

Xue, Y., Batlle, M. & Hirsch, J. P. (1998). GPR1 encodes a putative G-protein-coupled receptor that associates with the Gpa2p Galpha subunit and functions in a Ras-independent pathway. *EMBO J* **17(7)**, 1996–2007.

Yang, C. T., de Ulzurrun, G. V. D., Gonçaces, A. P., Lin, H. C., Chang, C. W., Huang, T. Y., Chen, S. A., Lai, C. K., Tsai, I. J., Schroeder, F. C., Stajich, J. E. & Hsueh, Y. P. (2020). Natural diversity in the predatory behavior facilitates the establishment of a robust model strain for nematode-trapping fungi. *Proc Natl Acad Sci U S A* **117(12)**, 6762–6770.

Yang, J., Liang, L., Zhang, Y., Li, J., Zhan,g L., Ye, F., Gan, Z. & Zhang, K. Q. (2007). Purification and cloning of a novel serine protease from the nematode-trapping fungus *Dactylellina varietas* and its potential roles in infection against nematodes. *Appl Microbiol Biotechnol* **75(3)**, 557–565.

Yang, J., Wang, L., Ji, X., Feng, Y., Li, X., Zou, C., Xu, J., Ren, Y., Mi, Q., Wu, J., Liu, S., Liu, Y., Huang, X., Wang, H., Niu, X., Li, J., Liang, L., Luo, Y., Ji, K., Zhou, W., Yu, Z., Li, G., Liu, Y., Li, L., Qiao, M., Feng, L. & Zhang, K. Q. (2011). Genomic and proteomic analyses of the fungus *Arthrobotrys oligospora* provide insights into

nematode-trap formation. *PLoS Pathog* **7(9)**, e1002179.

Yang, K., Qin, Q., Liu, Y., Zhang, L., Liang, L., Lan, H., Chen, C., You, Y., Zhang, F. & Yang, L., Li, X., Bai, N., Yang, X., Zhang, K. Q. & Yang, J. (2022). Transcriptomic Analysis Reveals That Rho GTPases Regulate Trap Development and Lifestyle Transition of the Nematode-Trapping Fungus *Arthrobotrys oligospora*. *Microbiol Spectr* **10(1)**, e01759–21.

Youssar, L., Wernet, V., Hensel, N., Yu, X., Hildebrand, H. G., Schreckenberger, B., Kriegler, M., Hetzer, B., Frankino, P., Dillin, A. & Fischer, R. (2019). Intercellular communication is required for trap formation in the nematode-trapping fungus *Duddingtonia flagrans*. *PLoS Genet* **15(3)**, e1008029.

Yu, H., Duan, J., Wang, B. & Jiang, X. (2012). The function of snodprot in the cerato-platanin family from *Dactylellina cionopaga* in nematophagous fungi. *Biosci Biotechnol Biochem* **76(10)**, 1835–1842.

Yu, J. H. (2006). Heterotrimeric G-protein signaling and RGSs in *Aspergillus nidulans*. *J Microbiol* **44(2)**, 145–154.

Yu, J. H., Wieser, J. & Adams, T. H. (1996). The Aspergillus FlbA RGS domain protein antagonizes G-protein signaling to block proliferation and allow development. *EMBO J* **15**, 5184–90

Yu, R., Shen, X., Liu, M., Yin, Z., Li, X., Feng, W., Hu, J., Zhang, H., Zheng, X., Wang, P. & Zhang, Z. (2021). The rice blast fungus MoRgs1 functioning in cAMP signaling and pathogenicity is regulated by casein kinase MoCk2 phosphorylation and modulated by membrane protein MoEmc2. *PLoS Pathog* **17(6)**, e1009657.

Yu, X., Hu, X., Mirza, M., Kirschhöfer, F., Brenner-Weiß, G., Schäfer, J., Bunzel, M. & Fischer, R. (2021). Fatal attraction of *Caenorhabditis elegans* to predatory fungi through 6-methyl salicylic acid. *Nat Commun* **12**, 5462.

Yu, X., Liu, H., Niu, X., Akhberdi, O., Wei, D., Wang, D. & Zhu, X. (2017). The Gα1-cAMP signaling pathway controls conidiation, development and secondary metabolism in the taxol-producing fungus *Pestalotiopsis microspora*. *Microbiol Res* **203**, 29–39.

Yun, C. W., Tamaki, H., Nakayama, R., Yamamoto, K. & Kumagai, H. (1997). G-protein coupled receptor from yeast *Saccharomyces cerevisiae*. *Biochem Biophys Res Commun* **240**, 287–292.

Zhang, D., Zhu, X., Sun, F., Zhang, K., Niu, S. & Huang, X. (2017). The roles of actin cytoskeleton and actin-associated protein Crn1p in trap formation of *Arthrobotrys oligospora*. *Res Microbiol* **168(7)**, 655–663.

Zhang, G., Zheng, Y., Ma, Y., Yang, L., Xie, M., Zhou, D., Niu, X., Zhang, K. Q. & Yang, J. (2019). The velvet proteins VosA and VelB play different roles in conidiation, trap formation, and pathogenicity in the nematode-trapping fungus *Arthrobotrys oligospora*. *Frontiers Microbiol* 1917.

Zhang, Q., Chen, X., Xu, C., Zhao, H., Zhang, X., Zeng, G., Qian, Y., Liu, R., Guo, N., Mi, W., Meng, Y., Leger, R. J. S. & Fang, W. (2019). Horizontal gene transfer allowed the emergence of broad host range entomopathogens. *Proc Natl Acad Sci U S A* **116(16)**, 7982–7989.

Zhang, W., Hu, C., Hussain, M., Chen, J., Xiang, M. & Liu, X. (2019). Role of

low-affinity calcium system member Fig1 homologous proteins in conidiation and trap-formation of nematode-trapping fungus *Arthrobotrys oligospora*. *Sci Rep* **9(1)**, 1–9.

Zhang, W., Liu, D., Yu, Z., Hou, B., Fan, Y., Li, Z., Shang, S., Qiao, Y., Fu, J., Niu, J., Li, B., Duan, K., Yang, X. & Wang, R. (2020). Comparative genome and transcriptome analysis of the nematode-trapping fungus *Duddingtonia flagrans* reveals high pathogenicity during nematode infection. *Biol Control* **143**, 104159.

Zhang, X., Noguez, J. H., Zhou, Y. & Butcher, R. A. (2013) Analysis of ascarosides from *Caenorhabditis elegans* using mass spectrometry and NMR spectroscopy. *Methods Mol Biol* **1068**, 71–92

Zhang, Y. Q. & Yu, Z. F. (2019). The complete mitochondrial genomes of the nematode-trapping fungus *Arthrobotrys musiformis*. *Mitochondrial DNA Part B* **4(1)**, 979–980.

Zhen, Z., Xing, X., Xie, M., Yang, L., Yang, X., Zheng, Y., Chen, Y., Ma, N., Li, Q., Zhang, K. Q. & Yang, J. (2018). MAP kinase Slt2 orthologs play similar roles in conidiation, trap formation, and pathogenicity in two nematode-trapping fungi. *Fungal Genet Biol* **116**, 42–50.

Zhen Z, Zhang G, Yang L, Ma, N., Li, Q., Ma, Y., Niu, X., Zhang, K. Q. & Yang, J. (2019). Characterization and functional analysis of calcium/calmodulin-dependent protein kinases (CaMKs) in the nematode-trapping fungus *Arthrobotrys oligospora*. *Appl Microbiol Biotechnol* **103(2)**, 819–832.

Zhou, D., Xie, M., Bai, N., Yang, L., Zhang, K. Q. & Yang, J. (2020). The autophagy-related gene Aolatg4 regulates hyphal growth, sporulation, autophagosome formation, and pathogenicity in *Arthrobotrys oligospora*. *Front Microbiol* **2939**.

Zhou, D., Zhang, Y., Xu, J., Jiang, L., Zhang, K. Q. & Zhang, Y. (2018). The complete mitochondrial genome of the nematode-trapping fungus *Dactylellina haptotyla*. *Mitochondrial DNA Part B* **3(2)**, 964–965.

Zopf, W. (1888). Zur Kenntnis der Infektions-Krankheiten neiderer Thiere. *Nova Acta Leop Acad Naturf Halle* **52**, 7.

Zuber, S., Hynes, M. J. & Andrianopoulos, A. (2002). G-protein signaling mediates asexual development at 25 C but has no effect on yeast-like growth at 37 C in the dimorphic fungus *Penicillium marneffei*. *Eukaryot Cell* **1(3)**, 440–447.

Acknowlegement

Every PhD student looks forward to the day when they graduate from their PhD, and I am no exception. But I never thought that four years would pass in a flash. When the day came, I looked back and was filled with sadness. I can still remember the days when I first entered the lab, when I was still very young. Facing an unfamiliar country, unfamiliar people, and a completely unknown field, I was at a loss. As I started to try to talk with my mentors and colleagues, and slowly explore my new topic, the tricky things smoothed out one by one. I put my sweat into it, my time into it, and my heart into interactions with people. Looking back now, I am full of rewards.

I am grateful to my mentor, Reinhard Fischer, for his hard work in training me, his encouragement, and his generosity and generosity to me. He was the one who guided me when I was standing outside the door of scientific research; he was the one who pulled me out when I was deep in a scientific problem; he was the one who made me laugh when I was embarrassed by the mistakes I made. I believe that after many years, his voice, smile and magnificent figure will still be in front of my eyes, and his influence on me will always be with me. I would also like to thank Prof. Dr. Jörg Kämper and Prof. Dr. Natalia Requena for their careful guidance and kindness during the days.

I would like to thank all my colleagues in the lab. Thanks to Dr. Xi Yu for helping me with my project, for teaching me to have a scientific mind, and I am very happy to work with her. Thanks to Dr. Xiaolei Gao and Dr. Zhenzhong Yu for their help and sincere advice. Thanks to Jia Gao for your company and professional research advice all the way. Thanks to my master's student, Mai Wang, for her help in my G-protein project and in my life. Thanks to Meihang Du for being with me for several years and for enlightening me when I was troubled. Thanks to Elke for helping me to inject worms and for her tolerance and help. Thanks to Mr. and Mrs. Wernet for your help and guidance on my topic, your professionalism has been my motivation to move forward. Thanks to Jenny and Maria for your usual help and happy communication. Thanks to Satur for your guidance and help on my topic. Thanks to colleagues for helping to revise my PhD thesis. Thanks to the namtode group, it was a pleasure to discuss related topics with you and to chat with you guys in the daily life. I also thank the secondary metabolism group, the light group, the polarization growth group, trainees, Fabienne, Tamara and Elisabeth for being with me day and night and making progress together. I really enjoyed having lunch with all of you and celebrating birthdays, holidays and successes of our group together. Spending time together when things were difficult and laughing together when things went well were the four fulfilling years I spent here.

Last but not least, I am especially grateful to my husband and my daughter. My husband is my mentor in life, so that I am not confused or lost in life, and he also takes the responsibility of being the chef of our family, so that our family can eat the

most authentic Chinese delicacies even abroad, which is also my source of happiness every day; my lovely daughter is the sun of my life, and her existence is the best motivation for all my efforts. You are the ones who fill the gaps in my life, fill my life with sunshine and make my days less monotonous and boring. I'm sure you enjoy the time we spend together as much as I do. I am also very grateful to our parents for their moral support and financial support. Your encouragement and help are the best support for our little family in Germany. With you waiting for us in China, we have more goals and motivation to work hard in Germany.

In the near future, I will return to China and start a new work and life. The years I lived in Karlsruhe will be the most precious memories of my life. I hope we can keep working together and communicating in our lives.